

Diplomarbeit

conducted at:

Prof. Dr.-Ing U. Wiesmann

Technische Universität Berlin, Institut für Verfahrenstechnik

and

Prof. Dr. M.K. Stenstrom

University of California Los Angeles, Civil and Environmental Engineering

Treatment of Water Contaminated with the High Explosive RDX Activated Carbon Adsorption and Regeneration Using Alkaline Hydrolysis in a Fixed-Bed Reactor

by

Uwe Büsgen

Matr.Nr. 127 044

TU Berlin

Fachbereich 6

Umwelttechnik

Berlin 1996

Professor Dr.-Ing. U. Wiesmann
Institut für Verfahrenstechnik
Technische Universität Berlin

Diplomaufgabe

für

Herrn Uwe Büsgen, Matr.-Nr. 127 044

Aufgabe: Treatment of Water Contaminated with the High Explosive RDX by Activated Carbon Adsorption and Regeneration Using Alkaline Hydrolysis

Erläuterung: RDX (Hexahydro-1,3,5-Trinitro-1,3,5-Triazine) wurde in den USA seit dem 2. Weltkrieg als einer der wichtigsten Sprengstoffe in großen Mengen produziert. Lange Zeit ging man sehr sorglos mit dem Prozeßwasser und den Reststoffen um, so daß einige stehende Gewässer aber auch das Grundwasser in der unmittelbaren Nähe der Munitionsfabriken z. T. hochgradig kontaminiert sind. In der Arbeitsgruppe von Prof. Stenstrom vom Department of Environmental Engineering der University of California in Los Angeles (UCLA) werden Arbeiten zur Entwicklung von Verfahren, zur Reinigung dieser Oberflächen- und Grundwässer durchgeführt. Da über den biologischen Abbau von RDX noch keine Informationen vorliegen, wird derzeit eine physikalisch/chemische Abtrennung von RDX und eine chemische Umwandlung in unschädliche Produkte als aussichtsreich angesehen.

Ihre Aufgabe ist

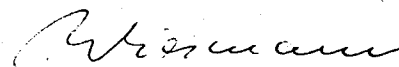
- a) die Untersuchungen der Kinetik der Adsorption von RDX auf Aktivkoks in Batch-Adsorbern,
- b) die Messung von Durchbruchkurven bei der Adsorption im Rohrsorber
- c) und die Messung der Regeneration des Aktivkoks durch alkalische Hydrolyse im Rohrsorber.

Die experimentellen Ergebnisse der Teilaufgaben a) und b) sind mit theoretischen Ergebnissen und, soweit möglich, dem Meßergebnis von Herrn H. Heilmann zu vergleichen.

Tag der Ausgabe: 2.7.96

Tag der Abgabe:

Betreuer: Professor Dr. Stenstrom (UCLA)



Professor Dr.-Ing. U. Wiesmann

Abstract

With the end of the cold war many nations including the US are destroying large stock piles of weapons and munitions. Both nuclear and non-nuclear weapons are being destroyed. Most of these munitions, including nuclear weapons, contain high explosives (HE) such as RDX (Hexahydro-1,3,5-trinitro-1,3,5-triazine), HMX (1,3,5,7-tetranitro-1,3,5,7-tetrazine) or TNT (2,4,6-trinitrotoluene), which are difficult to destroy in an environmentally acceptable fashion. Previously high explosives have been destroyed by detonations or controlled open burning. Both methods are no longer viable because they may cause air pollution or release other material to the environment.

HE disposal has been investigated at the University of California Los Angeles (UCLA), Department of Civil and Environmental Engineering, for three years using several techniques. The alkaline hydrolysis method described herein is potentially useful for destroying bulk HE as well as low concentrations in wastewater. For wastewater applications the HE-laden wastewaters are first treated with activated carbon adsorption, which reduces the volume of material to be exposed to alkaline hydrolysis. The laden-activated carbon is next regenerated with sodium hydroxide solutions at pH's ranging from 10 to 12 and temperatures from 70°C to 80°C.

In this thesis, the novel treatment scheme using activated carbon columns is described. The RDX adsorption kinetics were investigated and the surface diffusion coefficient for RDX adsorption onto granular activated carbon (Filtrisorb-400) was found to be $9.11 \cdot 10^{-10} \text{cm}^2/\text{s}$, which correspond well with Heilmann's (1996) findings.

RDX adsorption experiments were successfully conducted using virgin and regenerated activated carbon fixed-beds. In order to regenerate laden columns, a sodium hydroxide solution with a pH ranging between 11 and 12 and a temperature ranging between 70°C and 80°C was used. Results show that activated carbon in fixed-bed adsorbers can be regenerated in 300 to 400 minutes at pH 12 and 80°C without producing hazardous by-products. The column adsorption capacity decreases slightly with each adsorption/regeneration cycle.

CONTENTS

1. INTRODUCTION.....	4
2. LITERATURE REVIEW	6
2.1. ADSORPTION.....	6
2.2. ACTIVATED CARBON.....	7
2.3. PRODUCTION OF ACTIVATED CARBON.....	8
2.4. ADSORPTION ISOTHERMS	9
2.5. ADSORPTION KINETICS.....	10
2.6. CONTACTORS.....	12
2.7. MASS TRANSFER ZONE AND BREAKTHROUGH CURVE.....	14
2.8. REGENERATION OF EXHAUSTED ACTIVATED CARBON.....	16
2.9. ALKALINE HYDROLYSIS OF RDX.....	17
3. MATERIALS AND METHODS	20
3.1. ANALYTICAL.....	20
3.1.1. <i>High Performance Liquid Chromatography</i>	20
3.1.2. <i>Ion Chromatography</i>	20
3.1.3. <i>Miscellaneous Analytical Methods</i>	21
3.2. MATERIALS.....	21
3.2.1. <i>Activated Carbon</i>	21
3.2.2. <i>Activated Carbon Pretreatment</i>	22
3.2.3. <i>RDX</i>	22
3.2.4. <i>Preparation of the synthetic RDX-solution</i>	23
3.2.5. <i>Glass Columns</i>	23
3.2.6. <i>Miscellaneous Materials</i>	24
3.3. EXPERIMENTS.....	24
3.3.1. <i>Kinetic Batch Experiments of RDX-Adsorption onto Activated Carbon</i>	24
3.3.2. <i>Fixed-Bed Experiments</i>	25
3.3.3. <i>Regeneration Experiments of Exhausted Activated Carbon Columns</i>	27

3.3.4. <i>Multipoint BET-Surface Area Measurements</i>	28
4. HOMOGENEOUS SURFACE DIFFUSION MODEL	30
4.1. ASSUMPTIONS	30
4.2. EXPERIMENTAL PROCEDURE	31
4.3. CALCULATIONS	32
5. RESULTS AND DISCUSSION	33
5.1. HOMOGENEOUS SURFACE DIFFUSION MODEL	33
5.1.1. <i>Stirrer Speed Experiment</i>	33
5.1.2. <i>Kinetic Experiment</i>	34
5.1.3. <i>Findings</i>	36
5.2. ADSORPTION OF RDX ONTO ACTIVATED CARBON IN FIXED-BED COLUMNS	37
5.2.1. <i>Results</i>	37
5.2.1.1. Flow Rate	37
5.2.1.2. Effect of Different Numbers of Regenerations	39
5.2.1.3. Complete Breakthrough Curves	41
5.2.2. <i>Discussion</i>	42
5.2.2.1. Errors	42
5.2.2.2. Findings	43
5.3. REGENERATION EXPERIMENTS OF EXHAUSTED ACTIVATED CARBON COLUMNS	44
5.3.1. <i>Results</i>	45
5.3.1.1. Flow Rate	45
5.3.1.2. Comparison of Regeneration's With Equal Parameters	47
5.3.1.3. pH and Temperature Effects	48
5.3.1.4. Regeneration of Three Exhausted Columns Using One Liter Regeneration Liquid	50
5.3.1.5. OH- consumption	51
5.3.1.6. Comparison of the Regeneration Experiments	55
5.3.2. <i>Discussion</i>	57
5.3.2.1. Errors	57
5.3.2.2. Findings	57

5.4. ADDITIONAL EXPERIMENTS.....	59
5.4.1. <i>Results</i>	59
5.4.1.1. Total Organic Carbon.....	59
5.4.1.2. Multipoint BET-Surface Area.....	60
5.4.2. <i>Discussion</i>	60
5.4.2.1. Errors.....	60
5.4.2.2. Findings.....	61
6. CONCLUSIONS.....	62
7. ZUSAMMENFASSUNG.....	64

APPENDIX

Appendix I:	References
Appendix II:	Table of Abbreviations
Appendix III:	Table of Tables
Appendix IV:	Table of Figures
Appendix V:	Tables
Appendix VI:	Figures
Appendix VII:	Derivation of Homogeneous Surface Diffusion Model (HSDM) equations
Appendix VIII:	Symbols

1. Introduction

High explosives (HE) contaminated waters occur at contaminated sites and during weapon production and dismantling (Wujcik *et al.*, 1992). Contaminated sites can be found all over the world at weapon production sites, dismantling sites, and stockpiles of weapons. With the tightening of environmental regulations and grown public concern about contaminated military sites in the US and Germany, proper treatment has become very important.

Additionally, both the Intermediate-Range Nuclear Forces Treaty (INF) and the Strategic Arms Reduction Treaties (START I and II) require reduction in weapons inventory. Therefore, weapons dismantling efforts in East and West will produce large amounts of waste HE, such as RDX (Hexahydro-1,3,5-Trinitro-1,3,5-Triazine, CAS 121-82-4), HMX (Octahydro-1,3,5,7-Tetranitro-1,3,5,7-Tetrazocine, CAS 2691-41-0) and TNT (Trinitrotoluene). For example, the U.S. Department of Energy (DOE) will generate 50,000 kg of excess high quality maincharge explosives per year from dismantling nuclear weapons (Almanda and Flory, 1993).

It is difficult to treat HE-laden water in an environmentally acceptable fashion. Traditionally, HE-laden waters were treated by adsorption on activated carbon fixed-beds (Patterson *et al.*, 1976). The exhausted carbon was either burned or disposed. This method of treatment is now banned and can no longer be used (Almanda and Flory, 1993). Furthermore, conventional thermal regeneration is not suitable due to safety problems when the explosive in the carbon exceeds 8% (w/w) (Andern *et al.*, 1975). In Germany, open burning is not used anymore since the Bundeswehr took charge over the East German Military sites (Entsorga, 1991). Nevertheless, the contaminated ground and process waters have to be treated in order to meet legislative standards for protecting both the environment and public health. Furthermore, advanced treatment technologies have to be economical.

Research of HE-laden water treatment is currently being conducted and sponsored by DOE and the Department of Defence (DOD) at their national laboratories and in universities. Research has been underway in the UCLA Civil and Environmental Engineering Department in order to develop biological treatment processes for HE contaminated wastewaters (Ro and Stenstrom, 1991; Wilkie, 1994) and the aqueous alkaline hydrolysis (Heilmann, 1994, 1996 and 1996a) for over 3 years.

Heilmann's (1996) objective was to combine the alkaline hydrolysis with activated carbon treatment for RDX and HMX contaminated water treatment. RDX and HMX are sparingly soluble in water (50 mg/L and 5 mg/L at 25°C, respectively) (Gibbs and Popolato, 1980). When hydrolyzed directly, without pre-concentration, large amounts of water have to be heated and a lot of NaOH has to be added in order to reach the necessary temperature and pH. Therefore, the treatment of the original water volume with alkaline hydrolysis is uneconomical.

Alternatively, the contaminants can be adsorbed onto activated carbon, thereby purifying the water and concentrating the HE on the activated carbon. The exhausted carbon can be regenerated using alkaline hydrolysis and reused to treat another charge of contaminated water. This process leads to a significant reduction in the volume of waste to be treated with base hydrolysis, and does not produce large quantities of HE-contaminated by-products.

Heilmann (1996) showed in batch experiments that RDX-laden activated carbon can be regenerated using alkaline hydrolysis. The adsorbed RDX is desorbed and mineralized by hydrolysis at elevated temperatures. The regeneration liquid contains the end-products of the RDX hydrolysis which are: N_2 , NH_3 , N_2O , CH_2O , H_2 , NO_2^- , $HCOO^-$, and CH_3COO^- . This liquid can be degraded in regular wastewater treatment plants with nitrification and denitrification stages (Heilmann, 1996). This process is both economical and effective as an environmental cleanup process because hazardous waste storage is not required.

RDX has been a major compound in nuclear and conventional weapons and is the most important explosive in the U.S. It was part of high performance explosive compositions, such as plastic bounded explosives, in the USA. RDX replaced TNT in importance during World War II due to its enhanced explosive power (Urbanski, 1977).

Most commercial grade RDX contains 9% of the homologue HMX, which is a by-product of the synthesis of RDX (McCormick *et al.*, 1981). Today, HMX has replaced RDX for new applications because of its greater energetic yield and greater resistance to unwanted detonation (Dobratz, 1981).

This thesis provides the information necessary to understand the basic procedure of adsorption onto activated carbon, and the regeneration of loaded activated carbon using alkaline hydrolysis (Chapter 2). The following experiments were conducted in order to verify Heilmann's (1996) findings and to prove the feasibility of the regeneration of RDX-laden activated carbon fixed-beds using alkaline hydrolysis:

- kinetic batch experiments in order to find the surface diffusion coefficient D_s (Chapter 3.3.1)
- RDX adsorption onto activated carbon fixed-beds (Chapter 3.3.2)
- regeneration of RDX-laden activated carbon fixed-beds using alkaline hydrolysis (Chapter 3.3.3)

The best process conditions were identified for both RDX adsorption onto activated carbon fixed-beds and regeneration of RDX-laden activated carbon fixed-beds using alkaline hydrolysis.

The study was conducted primarily at the University of California Los Angeles, CA, and submitted to the Technical University of Berlin, Germany.

2. Literature Review

This chapter provides the information necessary to understand the basic procedure of adsorption and regeneration of activated carbon. The qualities and production of activated carbon are described. The procedure of adsorption is presented and activated carbon adsorption contactors are introduced. Regeneration techniques are reviewed, particularly with respect to alkaline hydrolysis.

2.1. Adsorption

Adsorption is the adherence of molecules onto the surface of a solid. It has to be distinguished from absorption which is the solution of molecules in a fluid or solid.

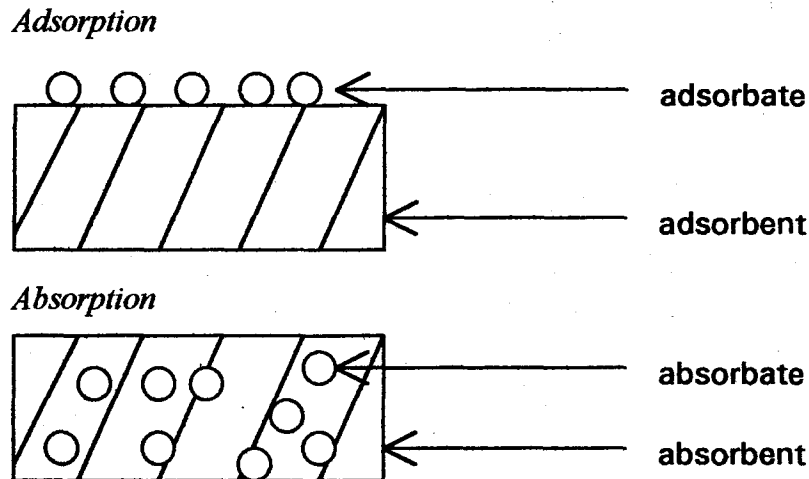


Figure 2.1 ad/absop: Principle of Adsorption and Absorption. With adsorption, the adsorbates adhere on the adsorbent surface only while absorption is the solution of the adsorbate in the adsorbent.

Due to intermolecular surface forces such as the Van der Waals force, molecules attach to the surface of the adsorbent, and energy is released. This is called physical adsorption. Additionally, there may be chemical forces such as ion exchange, causing a chemical bond between adsorbate and adsorbent. This is called chemical adsorption. Forces such as different electrical charges try to keep adsorbate and adsorbent apart. Therefore, the adsorbate must have enough energy to overcome these forces. Chemical adsorption appears more often when high temperatures are present.

Compared to physical adsorption, the bond between adsorbent and adsorbate is stronger when a molecule is chemically adsorbed, and more energy is released. Due to the strong bond, film diffusion is smaller when molecules are chemically adsorbed (see Chapter 2.5). Nevertheless, adsorption onto activated carbon is usually physical rather than chemical (Normann, 1987; Wiesmann, 1994a).

2.2. Activated Carbon

Adsorptive activated carbon (AC) treatment is a physico-chemical process which removes particularly organic contaminants from liquid or gas (Voice, 1989). The contaminants are concentrated on the activated carbon surface area. Exhausted activated carbon usually requires further treatment or is stored as hazardous waste (EPA, 1986).

Activated carbon usually adsorbs unspecifically. It is used in waterworks for dechlorination, removal of taste, odors, and organic pollutants. The concentration of many compounds in wastewater can be reduced using activated carbon.

The concentration of contaminants such as dissolved organic carbon (DOC) and humic acids can sometimes be reduced using more inexpensive procedures such as biological treatment. Pollutants which can not be degraded using conventional biological treatment can be separated in wastewater treatment plants using activated carbon. Therefore, activated carbon is more often used to reduce the concentration of compounds such as mineral oil hydrocarbons, heterogeneous compounds, or nitrogen or phosphorus based pesticides (Normann, 1987; Sontheimer *et al.*, 1988; Masschelein, 1992).

Activated carbon may further be used as a biological filter to degrade organic compounds and ammonia (Normann, 1987). The treatment is necessary because these compounds contaminate the surface-, ground-, and potable water and accumulate in plants and animals (Wiesmann, 1992).

Particles of powdered activated carbon (PAC) have a size ranging from 1 to 100 μm , the size of granular activated carbon (GAC) particles ranges from 0.5 to 4 mm. In general, the inner porosity reaches from $0.3 \cdot 10^{-6}$ to $1.5 \cdot 10^{-6}$ m^3/g , the inner surface area from 500 to 1500 m^2/g , respectively.

Different kinds of pores can be found inside the particles. These are micropores (diameter ≤ 20 nm), transitional pores (diameter 100 nm), and macropores (diameter ≥ 1000 nm). The micropores provide about 95% of the inner surface area and most of the adsorbate will adsorb there. The transitional- and macropores are responsible for the transport of the adsorbate to the micropores (Masschelein, 1992).

The internal surface of an activate carbon is usually expressed as the BET surface in m^2/g . This surface can be determined according to the adsorption theory of Brunauer, Emmett, and Teller by measuring the saturation characteristics of the carbon with a single compound. The efficiency of an adsorbent is not necessarily directly related to the internal surface (Masschelein, 1992).

The following properties of an adsorbate are very closely related to adsorption potential: molecular size, solubility, functional groups, polarity, and ionization. The solvent properties including the pH, temperature, solubility, and interactions with other compounds may also affect the adsorption capacity for a particular system (Chiang and Wu, 1989).

2.3. Production of Activated Carbon

The most common raw materials used in activated carbon production for water treatment are bituminous coal, peat, lignite, petroleum coke, wood, and coconut shells. Different raw materials will produce dramatic differences in the pore structure, which have an impact on the diffusive transport of molecules to the adsorption sites. For example, wood based carbons have uniform distribution. Most activated carbons have a more random distribution of macropores.

A consistent product quality is important for the initial design and long term maintenance of an efficient adsorption process. Changes in the raw material, as well as the activation process, can have major impact on activated carbon adsorption capacity and kinetics. The production of activated carbon consists of the pyrolytic carbonization of the raw material and subsequent or parallel activation. During the carbonization, volatile components are released to the carbon to form a pore structure that is developed during the activation process. The activation process selectively removes carbon resulting in an opening of closed pores and an increase in the average size of the micropores (Sontheimer *et al.*, 1988).

Carbon is activated either chemically or physically. If chemical activation is used, dehydrating chemicals, such as zinc chloride ($ZnCl_2$) and phosphoric acid (H_3PO_4), are added to the raw material at elevated temperatures. This product is heated pyrolytically (causing a degradation of the cellulose), cooled, and the activating agent is then extracted.

A disadvantage is the possible remaining activating agent. This can cause biological activity if the carbon is used for water treatment in fixed-bed adsorbers. Furthermore, the activating agent can be released into the process effluent with the treated water. This leakage cause algal blooms in lakes (Jekel, 1992; Wiesmann, 1994).

Physical or thermal activation of a carbonized char is more common (Masschelein, 1992). The endothermic process involves the contracting of gaseous activating agents such as steam (most often used), CO_2 , and air, with a char at elevated temperatures of 850°C to 1000°C.

The type of activating agent used, the length, and temperature of the activation have a major influence on adsorbent properties (Sontheimer, 1988).

2.4. Adsorption Isotherms

The solid phase equilibrium concentration of a compound on activated carbon is a function of the liquid phase equilibrium concentration in the solution:

$$q_e=f(C_i) \quad (2.1)$$

The equation is also related to the type of both, adsorbate and adsorbent, and physical conditions such as temperature. In order to find the best parameters for special conditions, isotherms conducted under different conditions are compared (Sontheimer, 1988; Jekel, 1992; Masschelein, 1992; Wiesmann, 1994a).

Many models are available to describe the adsorbate/adsorbent system. The Langmuir and the Freundlich model are the most often used. The latter is particularly good if the concentration of the compound in the liquid is very low. Therefore, it is usually preferred over the Langmuir isotherm. The Freundlich model is described by the following equation:

$$q_e=k*C^{1/n} \quad (2.2)$$

where the capacity constant k and the intensity constant $1/n$ are parameters related to the system of adsorbent and adsorbate (Sontheimer, 1988; Jekel, 1992; Masschelein, 1992; Wiesmann, 1994a).

In order to determine the parameters K and $1/n$, isotherm experiments need to be conducted. An aqueous solution containing a defined mass of the desired compound and a defined mass of activated carbon is mixed in a flask. Samples are taken after defined time periods. Adsorption equilibrium occurs when the concentrations of the compound in the solution and on the carbon are stable.

The amount of adsorbate can be calculated from the concentration difference in the solution at the beginning and the end of the experiment, multiplied by the volume of liquid. Each experiment defines one point in the isotherm. The next point can be determined by adding a defined mass of the same adsorbate to the system and repeating the same procedure. Another way to determine several points of the isotherm is using individual flasks for several compound concentrations or liquid volumes. The parameters K and $1/n$ can be calculated using the Freundlich model (Wiesmann, 1994a).

2.5. Adsorption Kinetics

Before an adsorbate can adsorb onto the adsorbent, it has to diffuse to its surface. Three kinds of diffusion exist and should be distinguished: bulk diffusion, film diffusion, and intraparticle diffusion. When the adsorbate has reached the adsorbent surface it can adsorb onto the surface (Normann, 1987).

Bulk diffusion is the transport of the adsorbate through the bulk liquid to the boundary layer. It is seldom limiting in engineered applications of activated carbon.

Film diffusion is also known as external mass transfer. Adsorbate molecules, which migrate from the bulk solution to the adsorbed state, are transferred to the outer surface of the adsorbent by liquid-phase diffusion. This mass transfer step occurs within the boundary layer around the adsorbent as shown in Figure 2.2 (Sonthaimer *et al.*, 1988).

If the boundary layer is thick and the compounds need to diffuse a large distance, film diffusion may be rate limiting. The boundary layer will become thinner if the liquid is agitated, and compounds will more rapidly diffuse through the boundary layer. Therefore, agitating the liquid reduces the influence of film diffusion (Hand *et al.*, 1983).

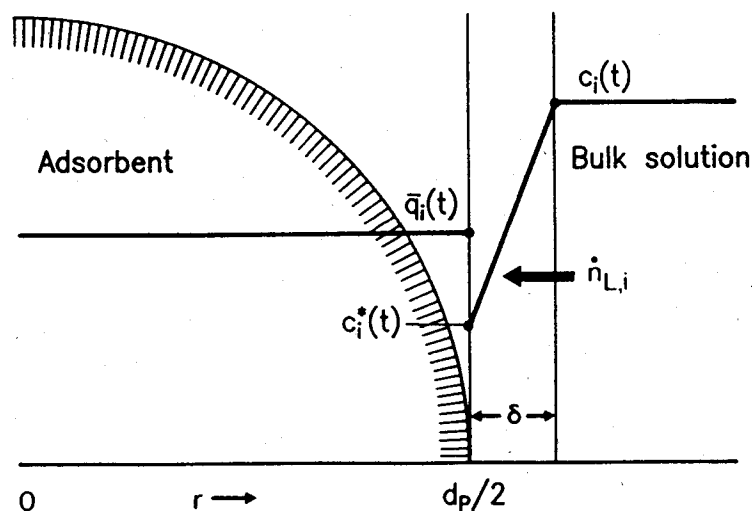


Figure 2.2: Concentration Profiles for a Single Particle Assuming no Internal Mass Transfer Resistance

Particle diffusion is also known as internal mass transfer. Once the adsorbate molecules have reached the outside surface of the adsorbent grain, they diffuse to the inside of the porous adsorbent, because of the high internal surface of the adsorbent, as shown in Figure 2.3 (Sonthaimer *et al.*, 1988).

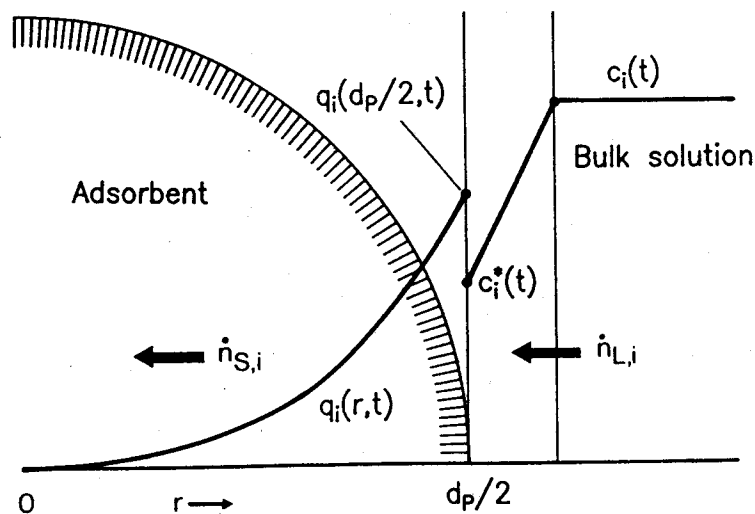


Figure 2.3: Concentration Profiles According to the Film-Surface Diffusion Model

Inside the particle, adsorbates can either diffuse in the adsorbed state along the pore surface, which is called surface diffusion, or within the fluid in the pores, which is called pore diffusion (see Figure 4.1).

For surface diffusion, molecules migrate along the surface when an adjacent adsorption site is available, and the molecule has enough energy to leave the site it is presently occupying (Hand *et al.*, 1983). It is described by the surface diffusion coefficient D_s . The driving force is the local adsorbent phase gradient (Jekel, 1992).

If the adsorbate is desorbed and repeatedly dissolved in the liquid, pore diffusion is prevalent. The adsorbate diffuses through the liquid within the pores. It is described by the pore diffusion coefficient. The driving force is the local concentration gradient in the liquid (Jekel, 1992).

The surface diffusion flux was found to be many times greater than the pore diffusion flux for strongly adsorbed species (Hand *et al.*, 1983) such as RDX and HMX. Hence, pore diffusion can often be neglected (Dobratz, 1981).

In order to design an activated carbon treatment procedure, the activated carbon adsorption capacity under defined conditions has to be known. The capacity is related to the kind of the adsorbate and adsorbent, the temperature, and the compound concentration in the solution (Normann, 1987).

The stable condition which is obtained between the adsorbate concentration in the liquid- and solid-phases after a sufficiently long contact time is called adsorption equilibrium. The adsorption equilibrium is not instantaneous because the adsorbate molecules must first diffuse from the solution to the external surface of the adsorbent and then diffuse into the internal surface of the adsorbent.

Adsorption kinetics are usually limited by mass transfer, and depend on the properties of the adsorbate and adsorbent. Additionally, the hydrodynamics of the system influence mass transfer and must be understood if dynamic processes such as fixed-bed adsorbers are to be designed (Sontheimer, 1988).

2.6. Contactors

Activated carbon must be contacted with the water being treated. A variety of methods can be used, such as fixed-beds, upflow adsorbers, continuous stirred tank reactor, filtration with powdered activated carbon, or fluidized bed adsorption.

Powdered activated carbon (PAC, particle size: 1-100 μm) is normally used in complete mixing reactors, and must be then removed by sedimentation and/or filtration. When used in complete mixing reactors, PAC is continuously added to the liquid which flows through a treatment plant. It has a very large outer surface area. Therefore, adsorption proceeds fast. Retention times of approximately 10 to 30 minutes are usually sufficient. The powdered activated carbon has to be separated from the liquid after the treatment. Most often flocculation, sedimentation, and following filtration is used.

When PAC is used for filtration, the amount of carbon needed for one run of a filter is stored in the filter-bed. When the contactor is exhausted, the activated carbon is flushed out of the filter and replaced with virgin activated carbon. The filter can be used for another charge of liquid (Jekel, 1992; Masschelein, 1992).

Granular activated carbon (GAC, particle size: 0.5-4 mm) is normally used in fixed beds or upflow adsorbers. When GAC is used in fixed-bed filters, also called granular activated carbon adsorbers, it may be utilized in the filters for the adsorption as well as for the regeneration. After regeneration, the fixed-bed can be used to treat another charge of liquid. Nevertheless, since regeneration techniques are often unavailable, unknown, or more expensive than the discharge of exhausted activated carbon, its disposal as hazardous waste is very common.

In order to characterize a granular activated carbon adsorber, the following design parameters are used (Sontheimer, 1988):

- The volumetric flow rate, \dot{V} , is the quantity of water fed per unit time;
- The carbon-bed volume, V_F , is the total volume of the granular activated carbon packed bed, which accounts for both the activated carbon grains and the void fraction;
- The void fraction, v_F , corresponds to the part of the fixed-bed volume which is not occupied by activated carbon particles;
- The filter velocity, ε , also termed superficial linear velocity or surface loading rate, is the velocity in an empty bed with the filter cross-sectional area, A_F ;

$$\varepsilon = \frac{\dot{V}}{A_F}$$

- The effective contact time, τ , is the residence time within the granular activated carbon bed. This time is available for the mass transfer of the substances from the bulk solution to the granular activated carbon particles;

$$\tau = \frac{V_F \cdot \varepsilon}{\dot{V}}$$

- The empty-bed contact time (EBCT), or t_A , is calculated from the carbon-bed volume and the volumetric flow rate or the length, l , and the filter velocity;

$$EBCT = t_A = \frac{V_F}{\dot{V}} = \frac{L}{v_F} = \frac{\tau}{\varepsilon}$$

- The filter operation time, t_F , is the operation time of a granular activated carbon bed;
- The throughput volume, V_L , is the water volume which passes through the filter during a time unit, t_F ;

$$V_L = t_F \cdot \dot{V}$$

- The specific throughput, V_{sp} , is the throughput volume divided by the mass of activated carbon in the bed;

$$V_{sp} = \frac{V_L}{V_F \cdot \rho_F}$$

The product of the filter density, ρ_F , and bed volume, V_F , correspond to the mass of dry granular activated carbon in the filter;

- Another parameter which allows a comparison of removal efficiencies regardless of bed size is the throughput in bed volumes, BV ;

$$BV = \frac{V_L}{V_F} = \frac{t_F}{EBCT}$$

Typical values for granular activated carbon adsorbers parameters are given in Table 2.1

Parameter	Symbol	Typical values in practice	Unit
Volumetric flow rate	\dot{V}	50-400	m^3/h
Bed volume	V_F	10-50	m^3
Cross-sectional area	A_F	5-30	m^2
Length	l	1.8-4	m
Void fraction	v_F	0.38-0.42	m^3/m^3
Filter density	ρ_F	350-550	kg/m^3
Filter velocity	ε	5-15	m/h
Effective contact time	τ	2-10	min
Empty bed contact time	EBCT or t_A	5-30	min
Operation time	t_F	100-600	days
Throughput volume	V_L	10^4 - 10^5	m^3
Specific throughput	V_{sp}	50-200	m^3/kg
Bed volumes	BV	2,000-20,000	m^3/m^3

Table 2.1: Typical Values for Granular Activated Carbon Adsorber Parameters (Sontheimer, 1988)

2.7. Mass Transfer Zone and Breakthrough Curve

When a liquid containing adsorbates is flushed through an activated carbon fixed-bed, the activated carbon particles will develop an adsorption equilibrium with the adsorbate. In the beginning only the particles at the entrance will adsorb. Their adsorption capacity will be exhausted first while activated carbon particles at the end of the fixed-bed might not have adsorbed any adsorbate because all adsorbent is adsorbed on the first activated carbon particles (see Figure 2.4).

Ideal fixed-bed adsorber show a piston flow profile and the adsorption equilibrium develops spontaneously. No adsorbent is in the effluent in the beginning of the experiment. The adsorbate concentration increases to the influent concentration immediately when the fixed-bed is exhausted (see Figure 2.5). The border between exhausted activated carbon particles and unloaded particles is called mass transfer zone.

The dependence between effluent concentration and elapsed time is called the breakthrough curve. When a defined concentration limit in the effluent is reached or exceeded (e.g. detection limit, discharge limit) the fixed-bed *breaks through*. The activated carbon has to be discharged or regenerated.

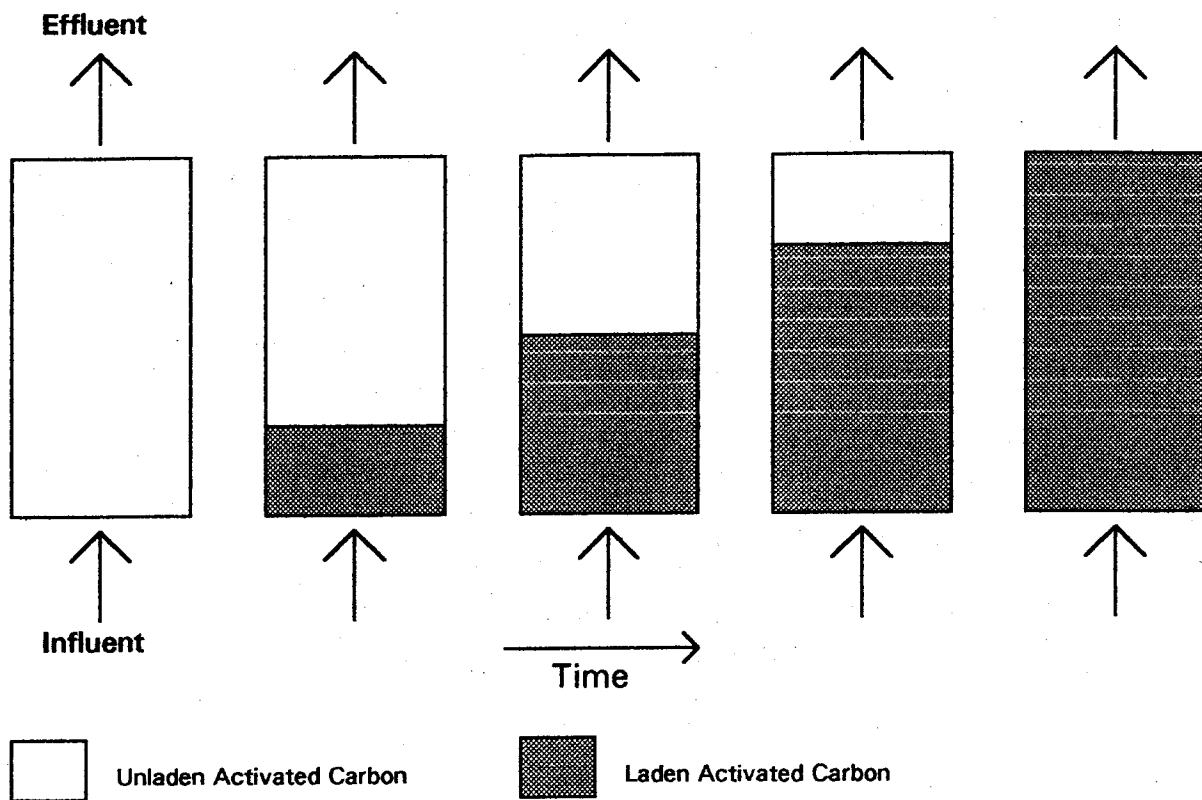


Figure 2.4: Move of the Laden Area or Mass Transfer Zone of a Activated Carbon Fixed-Bed

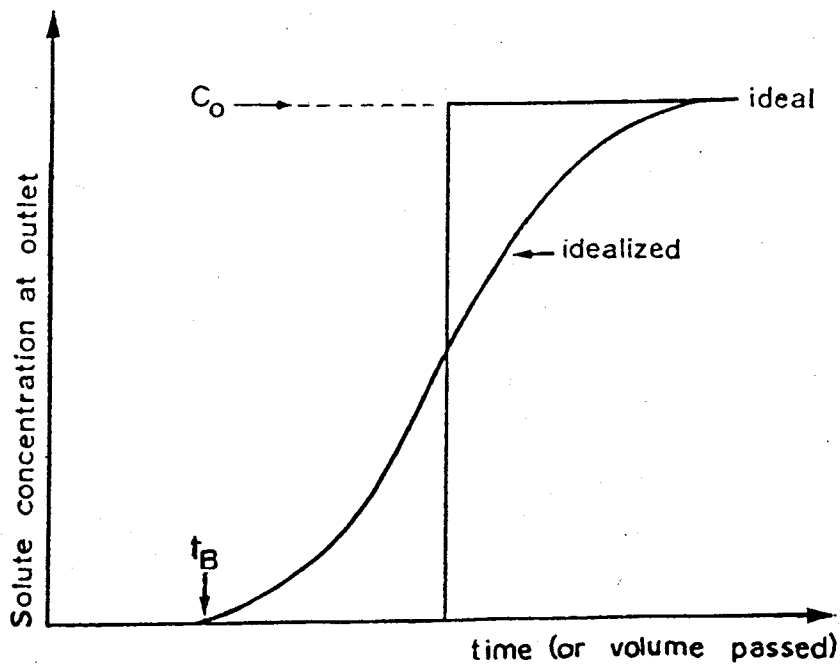


Figure 2.5: Breakthrough Profile (Schematic) of Activated Carbon Filters

In real fixed-beds, no piston flow exists and the adsorption equilibrium does not develop spontaneously. Therefore, the adsorbent concentration in the effluent will increase slowly over time until it reaches the influent concentration (see Figure 2.5).

2.8. Regeneration of Exhausted Activated Carbon

Although activated carbon is very effective for removing wastewater compounds, its operation and maintenance in wastewater plants is very cost intensive (Chiang and Wu, 1989). In order to use activated carbon economically and in an environmentally good fashion, it should be regenerated after it is exhausted. During regeneration, the adsorbed contaminants may be released (desorption) and recovered, or they may be destroyed through reactions, such as oxidation. After regeneration, the former exhausted carbon can be used for the treatment of another charge of liquid (EPA, 1991). When exhausted activated carbon is not regenerated, it has to be disposed, most likely as hazardous waste, which makes its use in a treatment system more expensive. Nevertheless, this procedure is still common (Johnson and Bacon, 1990).

Several techniques are available to regenerate exhausted activated carbon. The adsorbent can be desorbed from the activated carbon and transferred into a different medium such as air or liquid. The adsorbate can also be desorbed *and* transformed to other, less hazardous, compounds. The following regeneration techniques found in a literature review: thermal treatment or burning of activated carbon which is often used (Beccari *et al.*, 1977; EPA, 1991; Masschelein, 1992), chemical treatment (Beccari *et al.*, 1977; Martin and Ng., 1985; Masschelein, 1992; Newcombe and Drikas, 1993), electrochemical treatment (Narbaitz and Cen, 1994), biological treatment (Hutchinson and Robinson, 1990; Masschelein, 1992), and alkaline hydrolysis (Spitzer *et al.*, 1993; Heilmann, 1996).

2.9. Alkaline Hydrolysis of RDX

Alkaline hydrolysis is a new chemical process which can be used for regeneration of exhausted activated carbon. The exhausted activated carbon is flushed with water at high pH and temperature. Spitzer *et al.* (1993) investigated the alkaline hydrolysis of methylparathion. Heilmann (1996) found that high explosives such as RDX and HMX are desorbed and hydrolyzed from activated carbon using alkaline hydrolysis.

With alkaline hydrolysis, the hazardous compound adsorbed onto the activated carbon is not only transferred into a new medium but also destroyed or transformed to less dangerous compounds. The regeneration liquid may receive further treatment in regular sewage treatment plants with nitrification and denitrification stages. A potential advantage of this technique is that the end-products may be less dangerous or even harmless to human beings and the environment (Heilmann, 1996).

Alkaline hydrolysis of RDX proceeds faster at elevated pH and temperatures. Appropriate conditions are a pH of approximately 12 and a temperature in the range of 80°C to 90°C.

Hoffsommer *et al.* (1977) found the first step of the RDX hydrolysis to be an E2 elimination. Provoked by the attack of an hydroxide ion, RDX simultaneously loses a proton and a nitrite (NO_2^-) group, and is transformed to RDX-h5 (Figure 2.8). RDX-h5 reacts rapidly with hydroxide ion to generate a number of products which indicates opening of the ring. The hydrolyses of both RDX-h6 and RDX-h5 showed first-order dependence on hydroxide ion in Hoffsommer *et al.*'s study (1977).

The second-order rate constant for the RDX-h6 hydrolysis is many times greater than the appropriate RDX-h5 constant:

$$\frac{k_2(\text{RDX-h5})}{k_2(\text{RDX-h6})} = 10^5 \quad \text{at } 25^\circ\text{C} \quad (2.3)$$

Therefore, the RDX-h6 hydrolysis is rate determining.

According to Hoffsommer *et al.* (1977), HCOO^- is generated due to both the hydrolysis of RDX-h5 and the hydrogen ion attack on CH_2O under Cannizzaro conditions. Hoffsommer *et al.* (1977) found N_2 , NH_3 , N_2O , CH_2O , and the anions NO_2^- and HCOO^- as end-products.

Based on his kinetic studies, Heilmann (1996) proposes a new reaction pathway (Figure 2.8). In addition to conforming the end-products found by Hoffsommer *et al.* (1977), he also found CH_3COO^- . He confirmed that the hydrolysis of RDX-h5 is much faster than the hydrolysis of RDX-h6. RDX-h5 is not stable and could not be detected at any time. According to Heilmann (1996), the hydrolysis of RDX-h5 leads to complex intermediates. Their mineralization, generating the known end-products, is thought to be slower than the hydrolysis of RDX-h6.

Furthermore, Heilmann (1996) found the fourth-order Cannizzaro reaction to be the slowest reaction step of the proposed formation. Even when experiments were conducted at the most rapid conditions (pH 12, $T=80^\circ\text{C}$), it took at least 6 hours to obtain the HCOO^- equilibrium (Heilmann, 1996).

Therefore, the amount of NO_2^- indicates the rate of RDX-h5 production, and thereby the destruction of RDX-h6. The rate of HCOO^- production indicates the rate of production of the final end-products. When the concentration of HCOO^- is stable, hydrolysis is complete. Heilmann (1996) found ratios of 1.7 mol nitrite/mol RDX and 1.6 mol formate/mol RDX with a complete regeneration of laden carbon using alkaline hydrolysis in his study.

No other side or end-products than mentioned above were found in Heilmann's (1996) research. A carbon- and nitrogen- balance is presented in Table 2.2.

	Carbon (M)	Nitrogen (M)
RDX ($\text{C}_3\text{H}_6\text{N}_6\text{O}_6$)	3	6
Formate (HCOO^-)	1.5	
Acetate (CH_3COO^-)	0.2	
Formaldehyde (HCHO)*	1.1	
*data from Hoffsommer <i>et al.</i> (1977)		
Nitrite (NO_2^-)		1.6
Ammonia (NH_3)		0.9
Nitrous Oxide		2.2
Nitrogen (N_2)		0.7
Sum	2.8	5.4
Difference (RDX-Sum)	-0.2	-0.6
Recovery	94%	90%

Table 2.2: Carbon and Nitrogen Mass Balance for the Hydrolysis of RDX (Heilmann, 1996)

The recovery of carbon (94%) and nitrogen (90%) is better than the results presented by Hoffsommer *et al.* (1977) where only 60% and 77% could be recovered, respectively.

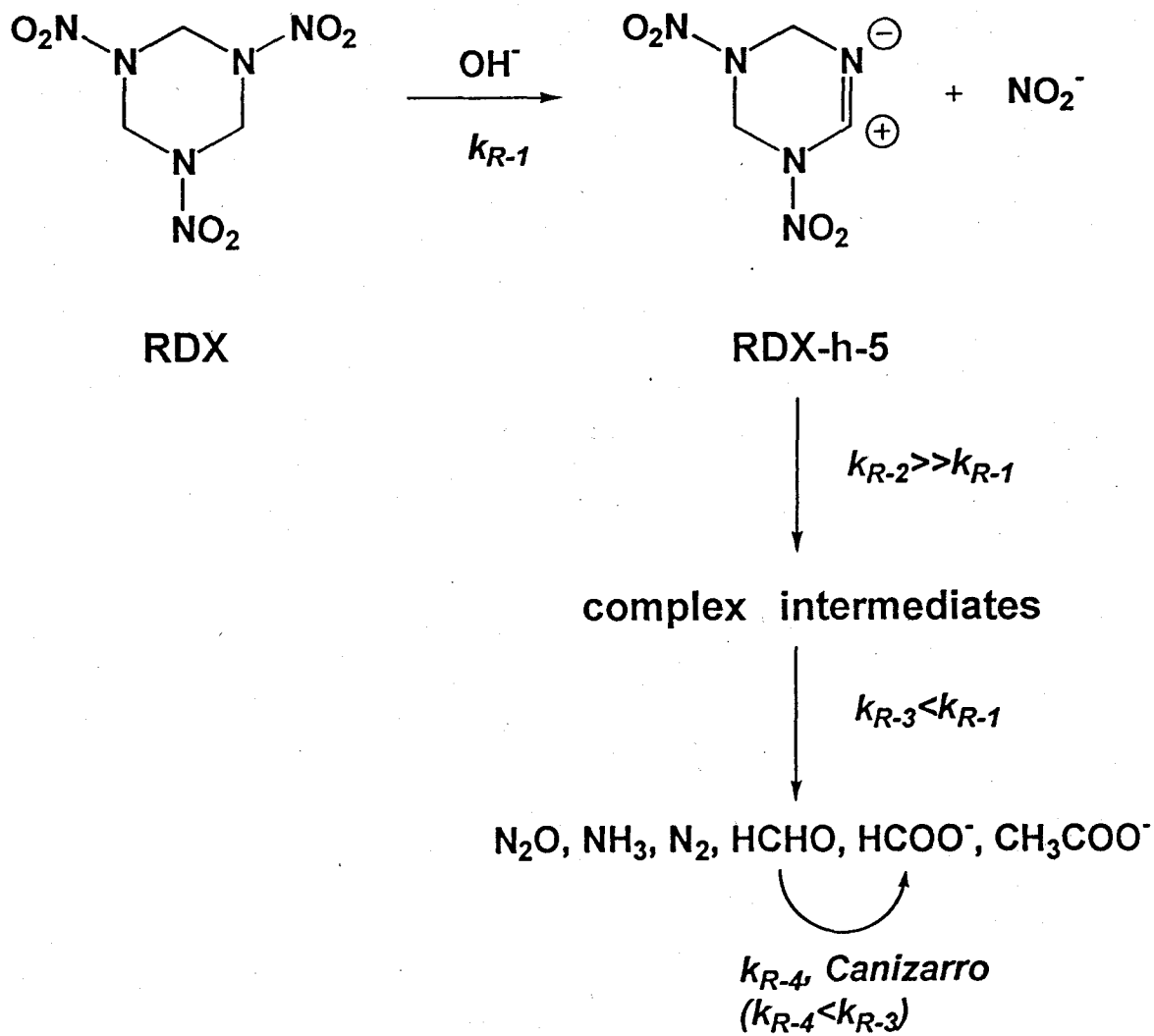


Figure 2.6: Lose of a Nitrite as Proposed by Hoffsommer *et al.* (1977) and Heilmann (1996), and the Following Hydrolysis of RDX-h5

3. Materials and Methods

This chapter describes the analytical procedures and experimental methods used in this study.

3.1. Analytical

3.1.1. High Performance Liquid Chromatography

The samples were filtered through sterile Acrodisc-13 0.2 μm syringe-microfilters (Gelman Sciences, product No. 4454, Ann Arbor, MI, USA) before analysis with High Performance Liquid Chromatography (HPLC). The HPLC was equipped with a variable wavelength UV-detector (HPLC/UV, Hewlett-Packard Series 1050) set to 236 nm. A mobile phase consisting of 40% water, 30% methanol and 30% acetonitrile (volume-%, all solvents HPLC-grade, Fisher scientific, Springfield, NJ, USA) was used with a flow rate of 1 mL/min. An Adsorbosphere-C-18-10 micron reversed-phase column (Alltech, Deerfield, IL, USA) with pre-filter element and guard column (C-18-5 micron, Alltech) was used. The injection volume was set to 20 μL using the autosampler.

Samples of approximately 0.5 mL were taken by sterile 1mL plastic syringes (Monoject, Sterile disposable tuberculin syringe) and transferred into HPLC vials. The samples were either analyzed directly after sampling or stored in a refrigerator until analysis.

Peaks were detected at retention times between 4.1 and 4.3 minutes. The peak area was a linear function of the concentration between 0.1 and 40 mg/L. The detection limit was 0.1 mg/L with this method. Standards prepared by Heilmann (1996) were used for this study. When necessary, the HPLC column was replaced, and new standards and calibrations were prepared. The standards containing 2, 4, 10, 20, 40, and 80 mg RDX/L were injected at least three times. Three data points were gathered for each standard concentration and the mean was then used for the calibration curve.

3.1.2. Ion Chromatography

The samples were analyzed for nitrite (NO_2^-) and formate (HCOO^-) directly without any storage using a Dionex Ion Chromatograph (IC) (basic chromatography module CMB-2, gradient pump GPM-1; Dionex, Sunnyvale, CA, USA). The IC was equipped with a suppressed conductivity detector (conductivity detector CDM-1). An Ion Pac AS9-SC column (4 mm I.D.) and a suppressor column were applied. The mobile phase consisted of 0.75 mM NaHCO_3 and 2 mM Na_2CO_3 dissolved per 1L of milli-q-water at a flow rate of 2 mL/min.

Samples containing less than 15 mg nitrite/L were measured undiluted. Approximately 2.5 mL liquid were taken using a sterile 3 mL syringe (Monoject, Sterile disposable tuberculin syringe). If the concentration of nitrite exceeded 15 mg/L, approximately 0.5 mL liquid was taken with a sterile 1 mL syringe (Monoject, Sterile disposable tuberculin syringe) and diluted in DI-water. All samples were filtered through sterile Ion Chrom Acrodisc 0.2 µm syringe-microfilters (Gelman Sciences, Ann Arbor, MI, USA) before injection.

The samples were manually injected into a 50 µL sample loop. Peaks were detected at retention times between 1.0 and 1.1 minutes (HCOO^-) and 1.7 and 1.8 minutes (NO_2^-), respectively. The peak area was a linear function of the concentration between 0.33 and 13.24 mg/L (HCOO^-) and 0.33 and 13.33 mg/L (NO_2^-), respectively.

For external calibration, at least three data points were gathered for each standard concentration. The mean was used for the calibration curve. Since there is an influence of the pH value in the determination of the HCOO^- and NO_2^- concentration with the described method, standard curves for pH 10, 11 and 12 were obtained.

3.1.3. Miscellaneous Analytical Methods

A Fisher Accumet (Fisher Scientific, Accumet pH/ion meter, Model 25) pH/Ion meter was used to measure the *pH*. It was equipped with a Fisher pH electrode. The pH/Ion meter was calibrated at least once per day using Fisher calibration solutions for pH 7 and pH 10.

For *temperature* measurements a precision scientific thermometer with an 0.1°C scaling was used. 1°C was equivalent to approximately 1 cm of the scale.

3.2. Materials

3.2.1. Activated Carbon

For all experiments the activated carbon brand Filtrasorb-400 (Calgon Corporation, Prittsburg, PA) was used. Filtrasorb-400 is used for commercial and technical applications. It is also widely used for scientific research. Therefore, results found in this study should be comparable to other studies on Filtrasorb-400.

The manufacturer specifications are given in Table 3.1:

Surface Area, N ₂ -BET	950-1050 m ² /g
Density	0.43 g/cm ³
U.S. Standard Sieve Size Fraction	12x40
Iodine Number (min)	1000
Abrasion Number	75
Effective Size	0.8-1.0 mm

Table 3.1: Filtrasorb-400 Qualitys (Product Information, Calgon Corporation)

3.2.2. Activated Carbon Pretreatment

The granulated activated carbon for both the kinetic and fixed-bed experiments was pretreated before it was used.

The carbon was heated and agitated in a water bath for at least 24 hours at temperatures of 80°C to 90°C. Furthermore, the carbon was sized. It was put onto a screen (mesh size 40) and rinsed thouroughly.

3.2.3. RDX

RDX is the British code name for Research Department, Royal Detonation, or Rapid Detonation Explosive (Rosenblatt, 1991).

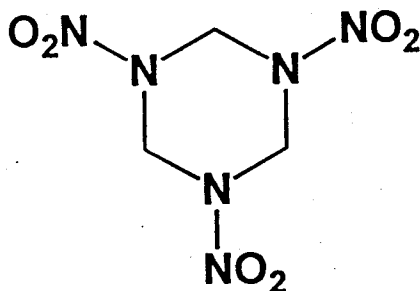


Figure 3.1: Hexahydro-1,3,5-Trinitro-1,3,5-Triazine (RDX), C₃H₆N₆O₆, CAS 121-82-4

The heterocyclic nitroorganic explosive RDX has a low solubility in water (approximately 50 mg/L at 25°C) (Gibbs and Popolato, 1980). It has a molecular weight of 222.1 g/mol, a density of 1.806 g/cm³, and a vapor pressure of 5.37*10⁻⁹ mbar (at 25°C). Therefore, volatilization can be neglected. The melting point of RDX is 204°C and the heat of explosion is 5757 kJ/kg.

Due to its low polarity and solubility, RDX adsorbs onto activated carbon very well (Dobratz, 1981). The molecule is destroyed by alkaline hydrolysis (see Chapter 2.9).

RDX is classified as a Group C Possible Human Carcinogen by the U.S. Environmental Protection Agency. This classification is based on limited animal data. Furthermore, it has adverse effects on the central nervous system. A lifetime health advisory of 2 µg RDX/L is defined for drinking water in the USA. No maximum containment standard has been defined, yet (McLellan *et al.*, 1988).

RDX used in this research was obtained from the Lawrence Livermore National Laboratory (LLNL). This RDX is also used in commercial applications. It had an impurity of approximately 9% HMX by weight.

3.2.4. Preparation of the synthetic RDX-solution

RDX in powdered form was dissolved in DI-water by heating and stirring at T=80°C. Approximately 80 mg RDX/L were added into the vessel and stirred for at least 24 hours. When all RDX was completely dissolved, another charge of DI-water of the same volume was heated to 80°C and added into the vessel. The accurate RDX concentration was analyzed using an HPLC. The volume of DI-water necessary to reach the desired RDX concentration was then added. The RDX concentration was verified using at least two independent samples and analyses.

3.2.5. Glass Columns

In order to conduct the fixed-bed adsorption and regeneration experiments, Omni-glass columns (10 mm I.D., 250 mm length) with water jackets and low-pressure Omnifit-fittings (Rainin, Emeryville, CA) were filled with 1g or 2.4g activated carbon (Filtrisorb-400), respectively. The activated carbon bed had a diameter of 10 mm and a length of 30 mm (1g AC) or 70 mm (2.4g AC). At the entrance and the exit of the 1g columns glass beads (3 mm, Fisher Scientific) were placed with a height of approximately 15 mm to fineadjust the bed height and homogenize the volumetric flow (see Figure A.1).

The activated carbon and the glass beads were separated using nylon filters (143 µm). In order to protect the tubes connecting the columns with the pump and the influent and effluent container from small activated carbon particles, another set of nylon filters (53 µm and 143 µm) were put at both ends of the columns.

3.2.6. Miscellaneous Materials

A peristaltic cartridge *pump* (Masterflex Microprocessor Pump Drive, Model No. 752400; pump head: 751920; cartridge: 751965; Cole Palmer, Chicago, Illinois 60648) was used to flush the RDX-solution through the columns or to flush the regeneration liquid through the columns and the Erlenmeyer-flask, respectively.

In order to heat and stir the regeneration liquid, a *heater/stirrer* (Fisher Scientific, Model 8005) was used.

A *circulation heater* was used for heating the activated carbon columns to 70°C or 80°C in the regeneration experiments. The heated water was flushed through the water-jackets of the columns with a constant temperature.

Nylon filters (Spectra/Mesh macroporous filters, 53µm, Cat.No. 08-670-201; Spectra/Mesh macroporous filters, 143µm, Cat.No. 08-670-181) were put between the glass beads and the activated carbon particles. The same glass beads were put at the entrance and the exit of the columns (see Figure A.1).

The columns were connected with the influent and effluent vessels or the Erlenmeyer-flask, respectively, using *plastic tubing* (Masterflex, 96410-14, Masterflex, 96410-13; Rainin Teflon Tubing, ID 1.5mm, Cat.No. 200-32).

3.3. Experiments

Three different experimental series were conducted: batch experiments to develop the surface diffusion coefficient D_s , fixed-bed adsorption experiments, and fixed-bed regeneration experiments using alkaline hydrolysis.

3.3.1. Kinetic Batch Experiments of RDX-Adsorption onto Activated Carbon

Experiments were performed to estimate the surface diffusion coefficient (D_s). In order to determine D_s , Hand *et al.*'s (1983) suggestions in their "User-Oriented Batch Solutions to the Homogeneous Surface Diffusion Model" (HSDM) were used. The HSDM model is described in Chapter 4.

Experimental Procedure

A 1 L Erlenmeyer-flask was filled with 1 L DI-water containing approximately 35 mg RDX/L. Three independent samples of the RDX solution were taken and analyzed before the experiment was started because it is very important to know the precise initial RDX concentration. Activated carbon was next added. The necessary dosage to reach an equilibrium concentration (0.067 g) of $C_e/C_0=0.5$ was calculated from the Freundlich isotherm, as follows:

$$C_{AC} = \frac{C_0 - C_e}{K \cdot C_e^{1/n}} = \frac{36.35 - 18.175}{96.97 \cdot 18.175^{0.35}} = 0.067 \text{ g} \quad (3.1)$$

The Freundlich parameters such as K and 1/n were estimated by Heilmann (1996).

The RDX solution in the Erlenmeyer-flask was contacted with 0.067 g granular activated carbon (Filtrisorb-400) and agitated with an overhead driven propeller at an RPM of 1350 1/s.

Samples were taken at least every 30 minutes during the first 12 hours and analyzed for RDX using an HPLC. The most sensitive time period in this study was between 180 and 723 minutes. Data from samples taken before and after this time period do not belong to the sensitive period. $D_{s,i}$ values were calculated as described in Chapter 4 and an optimal D_s was determined.

In order to determine the mixing required to make film diffusion neglectible, experiments utilizing different RPM's (500, 750, 1250, 1350, and 2000 1/s) were conducted. The RDX concentration in the liquid was measured at four times (0, 150, 270, 240 minutes), and compared.

To properly measure the surface diffusion coefficient, a range of propeller RPM's was found where no significant concentration differences existed at the same elapsed times over a range of RPM's. Data developed from these experiments were compared in a graph showing the RDX-concentration in the liquid versus the elapsed time.

3.3.2. Fixed-Bed Experiments

Fixed-bed experiments were conducted to verify the feasibility of adsorption of RDX on activated carbon fixed-beds. It was necessary to create RDX-laden activated carbon in order to investigate column regeneration kinetics and stoichiometry. Experimental conditions were selected to approximate conditions in typically full scale adsorbers. The collected data are suitable for modeling of breakthrough curves. The regenerated carbon was compared to virgin carbon in other fixed adsorption experiments.

Experimental Procedure

Glass columns were filled with granular activated carbon (Filtrisorb-400). The activated carbon fixed-bed itself had a diameter of 10 mm and a length of 30 mm or 70 mm, respectively. This ratio of length/diameter is used in other investigations such as Wiesmann (1994) (ratio 1/3) and the DOE Pantex pilot plant near Amarillo, Texas (ratio 1/7). The mass of dry activated carbon was 1.0 g or 2.4 g, respectively. The activated carbon was rinsed and washed thoroughly before it was added to the column in order to prevent clogging of filters or tubes due to small activated carbon particles.

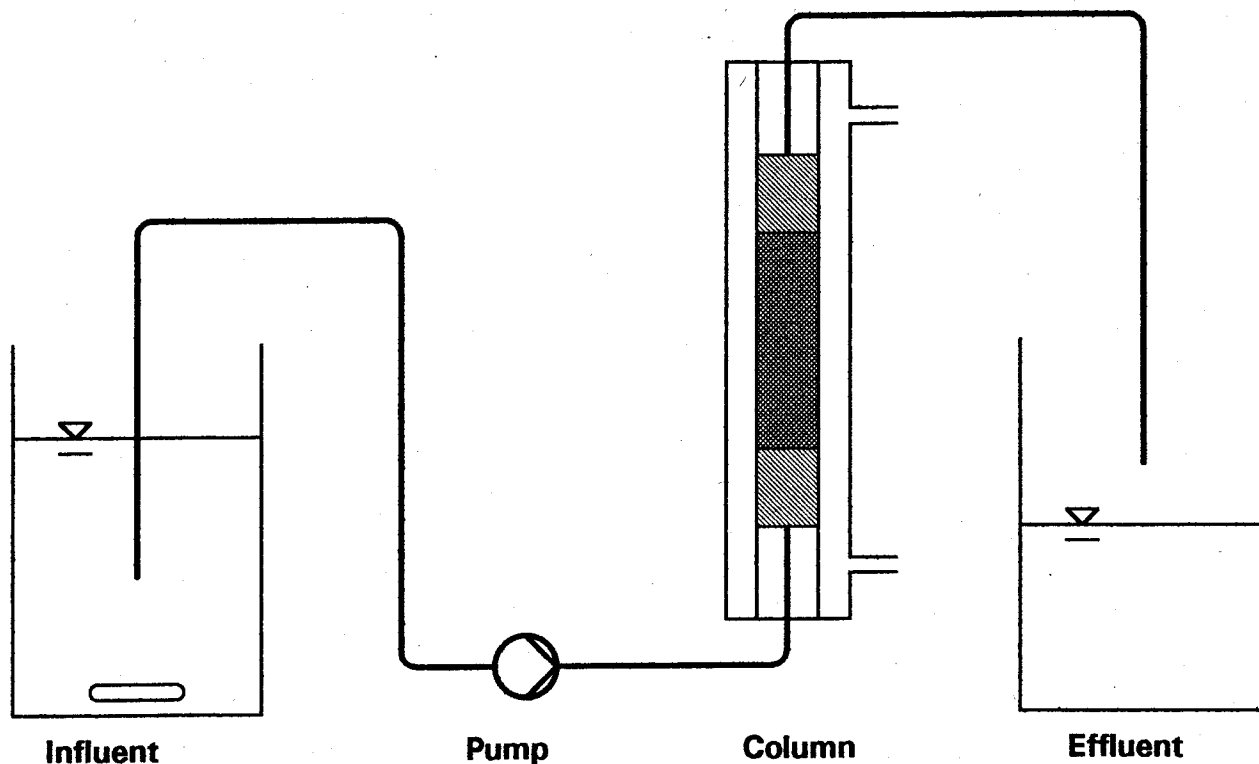


Figure 3.2 setup 2: Activated Carbon Fixed-Bed Adsorption Experiment, Experimental Setup
Glass beads (diameter 4 mm) were used at both ends of the activated carbon layer. Nylon filters were placed between the glass beads and the activated carbon. Furthermore, the same types of filters were placed at the entrance and the exit of the columns to keep solid particles out of the fixed-bed and prevent small activated carbon particles from plugging the tubes (see Figure A.1).

Synthetic RDX solution with a concentration of approximately 17.5 mg RDX/L was stirred in a storage tank. A pump flushed the solution into the columns. The effluent was collected in a separate container. The containers, pump, and column were connected using plastic tubes. The flow rate was adjusted to different flow rates between 0.5 mL/min and 3.9 mL/min.

Several influent samples were drawn during an experiment. At least two effluent samples were taken in each 24 hours period. 1 mL syringes were used to transfer samples into HPLC vials. The samples were analyzed using HPLC (see Chapter 3.1.1).

The flow rate was measured at least two times during 24 hours. If the flow rate dropped significantly, plugged tubes or filters were exchanged to restore the flow rate to the original value.

At the end of an adsorption experiment, the volume and the RDX concentration of the collected effluent were measured. The formula

$$m_{RDXonAC} = (C_i - C_e) \cdot V_{eff} \quad (3.2)$$

where C_i equals the influent RDX concentration, C_e equals the average effluent RDX concentration, and V_{eff} equals the volume of treated solution, was used to determine the mass of RDX adsorbed onto the activated carbon ($m_{RDXonAC}$).

3.3.3. Regeneration Experiments of Exhausted Activated Carbon Columns

Regeneration experiments were conducted in order to determine if RDX-laden activated carbon fixed-beds can be regenerated using alkaline hydrolysis. It was hoped to determine experimental conditions that would make alkaline hydrolysis of activated carbon commercially feasible.

Experimental Procedure

The same columns previously loaded during the adsorption experiments were used for the regeneration experiments (see Chapter 3.3.2).

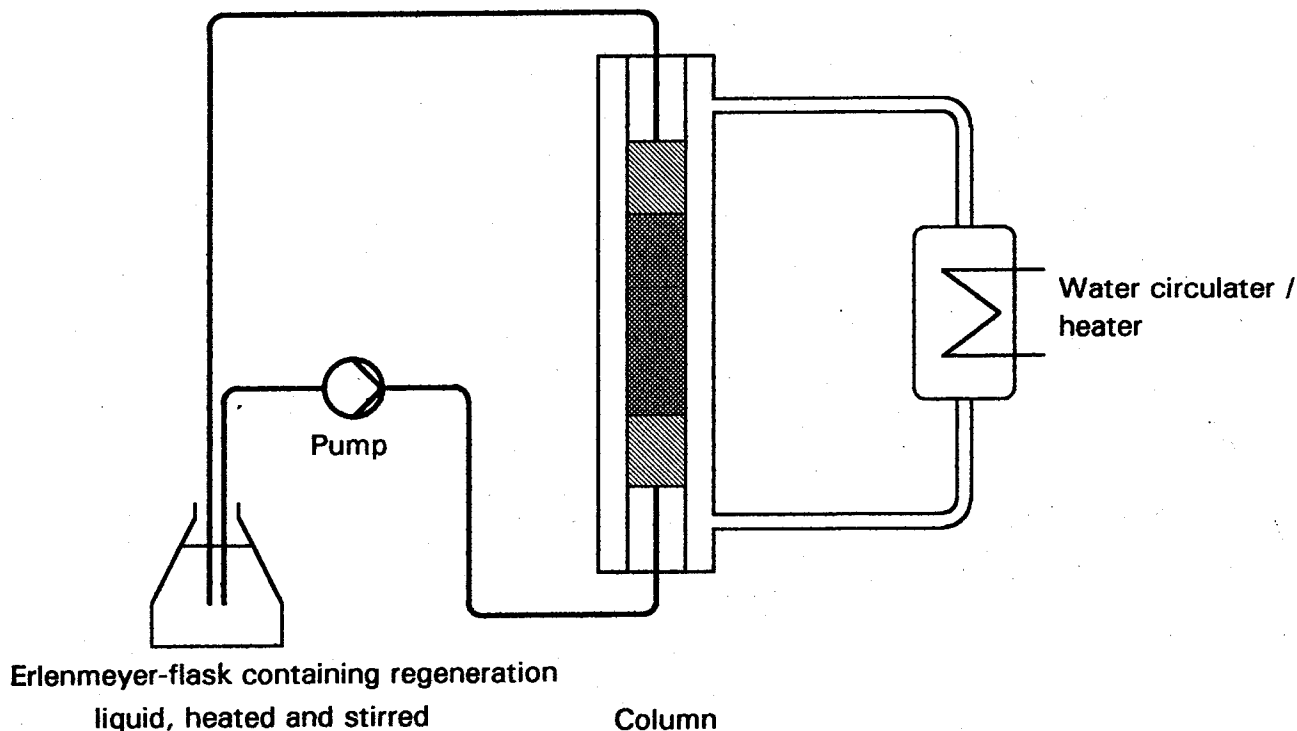


Figure 3.3: setup 3: Activated Carbon Fixed-Bed Regeneration Experiment, Experimental Setup

A 1 L Erlenmeyer-flask containing 1 L regeneration liquid (DI-water, adjusted to pH 11 or 12, respectively, using NaOH) was connected to a pump and the column using plastic tubes as shown in Figure 3.3. The regeneration solution was circulated through the Erlenmeyer-flask, the pump, and the column. In order to stir and heat the regeneration liquid to a temperature of 70°C or 80°C, respectively, the Erlenmeyer-flask was placed on a stirrer/heater. The activated carbon fixed-bed was heated by circulating water through a jacket, using a water circulation heater. The temperature of the water in the circulator was maintained constant.

Samples were taken from the Erlenmeyer-flask every 15 minutes during the first hour. Between 1 and 4 hours, samples were taken every 30 minutes, and then every hour until an elapsed time of 10 hours. Some samples were taken several hours later.

In order to take the samples, approximately 2.5 mL regeneration liquid was transferred from the Erlenmeyer-flask using a 3 mL syringe. If the concentration of nitrite exceeded 15 mg/L, samples of approximately 0.4 mL were taken using 1 mL syringes, and diluted using DI-water. All samples were analyzed for nitrite (NO_2^-) and formate (HCOO^-) using an IC (see Chapter 3.1.2.).

Several samples were taken to measure the pH. The effluent tube was transferred into a 25 mL beaker. This beaker was filled with approximately 10 mL regeneration liquid to measure the pH using an electrode of a pH meter which compensates for temperature. After this measurement, the solution was returned to the Erlenmeyer-flask.

3.3.4. Multipoint BET-Surface Area Measurements

The multipoint BET-surface area is the overall surface area of activated carbon available for adsorption. When virgin carbon is analyzed, the total surface area is determined. The difference between the surface area of exhausted and virgin activated carbon gives the surface area occupied from the adsorbed species.

Heilmann (1996) measured several sets of activated carbon for the multipoint BET-surface area using a Gemini 2360 surface area analyzer. His results are presented in Table 3.2.

Sample	Treatment applied on sample	BET-surface area (m ² /g)	BET-surface area of blank (m ² /g)*
Virgin F-400	no treatment	910	
Virgin F-400, pretreated	stirred in D.I.-water at 80°C for 16 hours	917	
F-400, loaded	loaded to q=180 mg RDX/g	488	
F-400, regenerated	loaded to q=195 mg RDX/g, regenerated at pH 13 and 80°C for 6 hours	884	911
F-400, regenerated and acid-post treated	loaded to q=195 mg RDX/g, regenerated at pH 13 and 80°C for 6 hours, then 16 hours on a shaker in 0.01-M HCL	905	941

*In order to evaluate the effect of alkaline treatment and acid-post treatment on the surface area of activated carbon alone, a blank experiment was defined for control purposes: Virgin activated carbon was contacted with a regeneration solution under the same conditions as the exhausted activated carbon. The BET-surface area was measured after the contact with the regeneration solution

Table 3.2: Results of the BET-Surface Area Measurements of Activated Carbon (from Heilmann, 1996)

The findings of Heilmann's (1996) BET-surface area investigations are:

- The BET-surface area of exhausted granular activated carbon (Filtrisorb-400) is approximately one half the surface area of virgin carbon. Even if the carbon is exhausted, significant unused surface spaces still exist.
- The activated carbon surface area regains very well to its previous amount after exhaustion and regeneration using alkaline hydrolysis. Therefore, almost the full carbon capacity is available after regeneration. Nevertheless, the surface area even increases when the regenerated carbon is treated with subsequent acid treatment.
- Alkaline hydrolysis has no significant effect on virgin carbon. Therefore, the increase of the surface area of exhausted activated carbon must be due to desorption of previously adsorbed species.

4. Homogeneous Surface Diffusion Model

In order to determine the surface diffusion coefficient D_s , the Homogeneous Surface Diffusion Model (HSDM) described by Hand *et al.* (1983) was used. The HSDM is described in this chapter. Its derivation is given in Appendix VII.

4.1. Assumptions

Although most of the adsorbents used to remove organic chemicals in water treatment have very heterogeneous and porous structures, the homogeneous surface diffusion model assumes that the adsorbent particle is spherical and homogeneous. This assumption is correct for activated carbon, if the heterogeneity of the porous structure is limited to microscopic ranges which are small compared to the geometric size of the total adsorbent grain. Stated another way, homogeneity implies that the solid-phase concentration, adsorbent density, and surface area are only a function of the radial location in the particle.

In order to develop kinetic models the following assumptions are made (see Figure 4.1) (Hand *et al.*, 1983):

- The surface diffusion can be described by Fick's first law of diffusion.
- Adsorption occurs under isothermal conditions and is a completely reversible process.
- The attachment rate of the adsorbate onto the adsorbent surface is much faster than the diffusion rate, i.e., near the adsorbent surface, local adsorption equilibrium exists between the adsorbed phase and the liquid phase.
- The bulk solution near a given adsorbent particle is completely mixed.
- The surface diffusion flux is many times greater than the pore diffusion flux. Therefore, pore diffusion can be neglected.
- External mass transfer can be neglected due to appropriate agitation. This has to be proved using either the Biot number or extra experiments.

Surface diffusion is rate limiting only if film diffusion is large enough to be neglected. It is necessary to achieve this condition in order to perform experiments to estimate the surface diffusion coefficient. Sufficient agitation must be provided to increase the film diffusion coefficient so that it will not be rate limiting and can be neglected (Sontheimer, 1988).

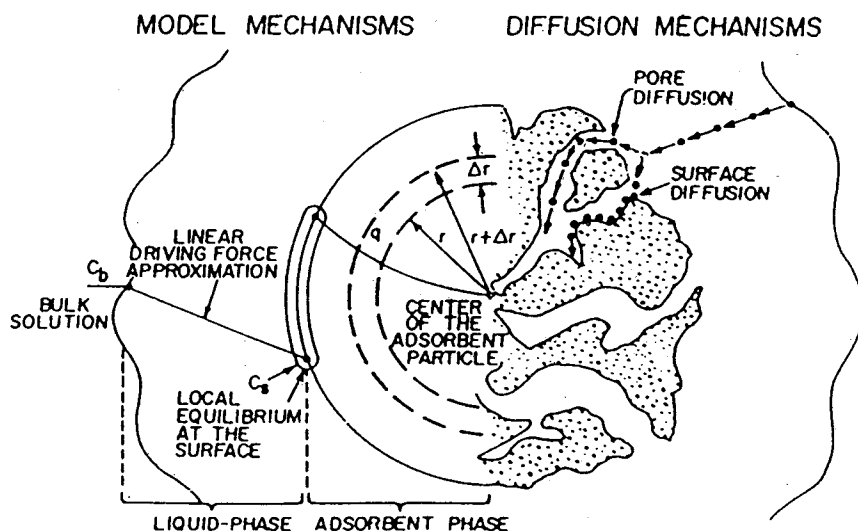


Figure 4.1: Mechanisms and Assumptions that are Incorporated in the Homogeneous Surface Diffusion Model (after Hand *et al.*, 1983)

4.2. Experimental procedure

An 1L Erlenmeyer-flask was filled with DI-water, containing the desired concentration of adsorbate. The amount of adsorbent, according to Hand *et al.*'s (1983) protocol, was added and the solution was stirred with an appropriate stirrer RPM.

Samples were taken from the solution in defined time periods. During the time where the model is most sensitive to the surface diffusivity, the time periods were very small. Before and after that time period fewer samples were taken. The last sample were taken after adsorption equilibrium was achieved. Three samples were taken from the initial solution because the accuracy of the initial concentration has a major influence on the entire calculation.

In order to find a sufficient stirrer speed, either the Biot number needs to be calculated or, as done in this research, extra experiments need to be conducted using different stirrer speeds. If the results meet within a predicted experimental error the agitation is sufficient. A decreasing concentration with increasing RPM's suggests that the film coefficient is not neglectible, because the coefficient increases with increasing RPM's. A problem with high propeller RPM's is carbon pulverisation. With higher RPM's the propeller may strike the carbon and reduce its size. To obtain valid results, carbon size must be constant during the course of the experiment.

The adsorbate concentration versus the elapsed time was drawn in a graph. The curve was modeled using the following calculations.

4.3. Calculations

The amount of activated carbon needed is determined by the equation

$$C_{AC} = \frac{(C_0 - C_e)}{K \cdot C_e^{1/n}} \quad \text{with} \quad \frac{C_e}{C_0} = 0.5. \quad (4.1)$$

K and 1/n have to be found in literature or isotherm tests have to be conducted. For the system Filtrasorb-400 and RDX, Heilmann (1996) developed isotherms and found K=96.97 and 1/n=0.3544.

For each sample taken $D_{s,i}$ is calculated using the equation

$$D_{s,i} = \frac{\bar{t} \cdot R^2}{t} \quad (4.2)$$

with

$$\bar{t} = \text{Exp} \left[A_0 + A_1 \cdot \bar{C}[\bar{t}] + A_2 \cdot \bar{C}[\bar{t}]^2 + A_3 \cdot \bar{C}[\bar{t}]^3 \right] \quad (4.3)$$

and

$$\bar{C}[\bar{t}] = \frac{C(\bar{t}) - C_e}{C_0 - C_e} \quad (4.4)$$

Values for A_0 , A_1 , A_2 , and A_3 are varying with the value of 1/n. For 1/n=0.3544 Hand *et al.* (1983) give the values following:

A_0	A_1	A_2	A_3
-1.085260	-9.17436	13.7597	-12.4017

The average of the calculated $D_{s,i}$ can be used for modelling. The following equation has to be used:

$$\bar{C}_{\text{mod}} = A_0 + A_1 \cdot \ln \bar{t} + A_2 \cdot (\ln \bar{t})^2 + A_3 \cdot (\ln \bar{t})^3 \quad (4.5)$$

with values for A_0 , A_1 , A_2 , and A_3 for 1/n=0.3544 as follows:

A_0	A_1	A_2	A_3
$-1.54082 \cdot 10^{-1}$	$-9.0934 \cdot 10^{-2}$	$3.51063 \cdot 10^{-2}$	$3.89262 \cdot 10^{-3}$

In order to estimate the best D_s for optimal model fit, s^2 has to be calculated:

$$s^2 = \frac{\sum_{i=1}^n \left[\bar{C}_{\text{data},i} - \bar{C}_{\text{mod el,calculated},i} \right]^2}{n-1} \quad (4.6)$$

s^2 should be as small as possible. The average of $D_{s,i}$ does not need to be the D_s that fits best. The best fit D_s is found if D_s is varied, or modeled. \bar{C}_{mod} is calculated using equation (4.5), s^2 has to be calculated using equation (4.6). This has to be done until the smallest s^2 is found. The $D_{s,\text{mod}}$ that gives the smallest s^2 is the best fit $D_{s,\text{mod}}$.

5. Results and Discussion

The Results of the kinetic, fixed-bed adsorption, and regeneration experiments, and BET-surface area and TOC measurements are presented and discussed in this chapter.

5.1. Homogeneous Surface Diffusion Model

In order to estimate the surface diffusion coefficient D_s , Hand *et al.* (1983) provides the User-Oriented Batch Reactor Solution to the Homogeneous Surface Diffusion Model (HSDM) (see Chapter 4). Several experiments were conducted using this program and are presented in this chapter. The Objectives of these experiments were to determine an appropriate stirrer speed which is required by Hand *et al.* (1983), and to collect data in order to develop D_s .

Furthermore, the experiments provide data for the modeling of breakthrough curves. Research on this subject is done at the UCLA, Department of Civil and Environmental Engineering, by Mr. Gross in order to write the Studienarbeit.

5.1.1. Stirrer Speed Experiment

Figure 5.1 and Table 5.1 show the results of the experiments conducted to find a valid stirrer RPM. The concentrations differ about 0.81 mg/L, maximum, only. This difference might be due to slightly different initial concentrations of 0.23 mg/L. Nevertheless, the results indicate that stirrer speeds of 500 to 1350 1/s produce stable consistent concentrations. This insures that film diffusion is not limiting, and carbon pulverisation is not occurring. Therefore, these stirrer speeds are suitable to develop D_s .

When a stirrer RPM of 2000 1/s was used, a pulverization was observed during the experiment. This led to a dramatically lower concentration after 139 minutes, which was even smaller than the concentration after 450 minutes elapsed time in all other experiments. Therefore, stirrer RPM's of 2000 1/s should not be used to develop D_s .

	RPM 400	RPM 500		RPM 1250		RPM 1350		RPM 2000
<i>time</i> <i>(min)</i>	C (mg/L)	C (mg/L)	<i>time</i> <i>(min)</i>	C (mg/L)	<i>time</i> <i>(min)</i>	C (mg/L)	<i>time</i> <i>(min)</i>	C (mg/L)
0	36.6	36.8	0	36.5	0	36.3	0	36.5
150	30.4	31.1	170	30.7	150	30.6	139	20.1
270	28.9	29.2	280	28.8	270	28.4		
450	27.0	27.3	450	27.2	450	26.5		

Figure 5.1: RDX Concentration in the Solution During the Kinetic Batch Experiment at Defined Elapsed Times

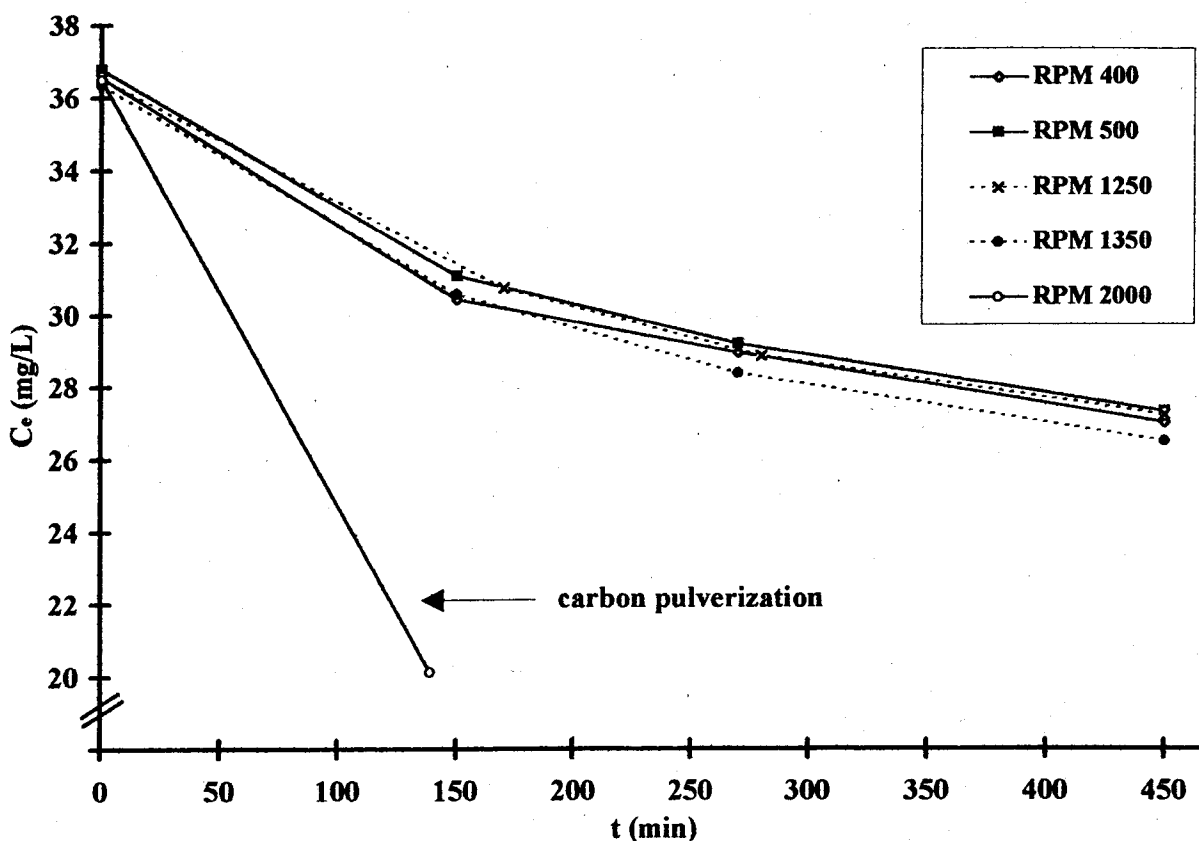


Figure 5.1: Comparison of Kinetic Experiments with Different Stirrer Speeds

5.1.2. Kinetic Experiment

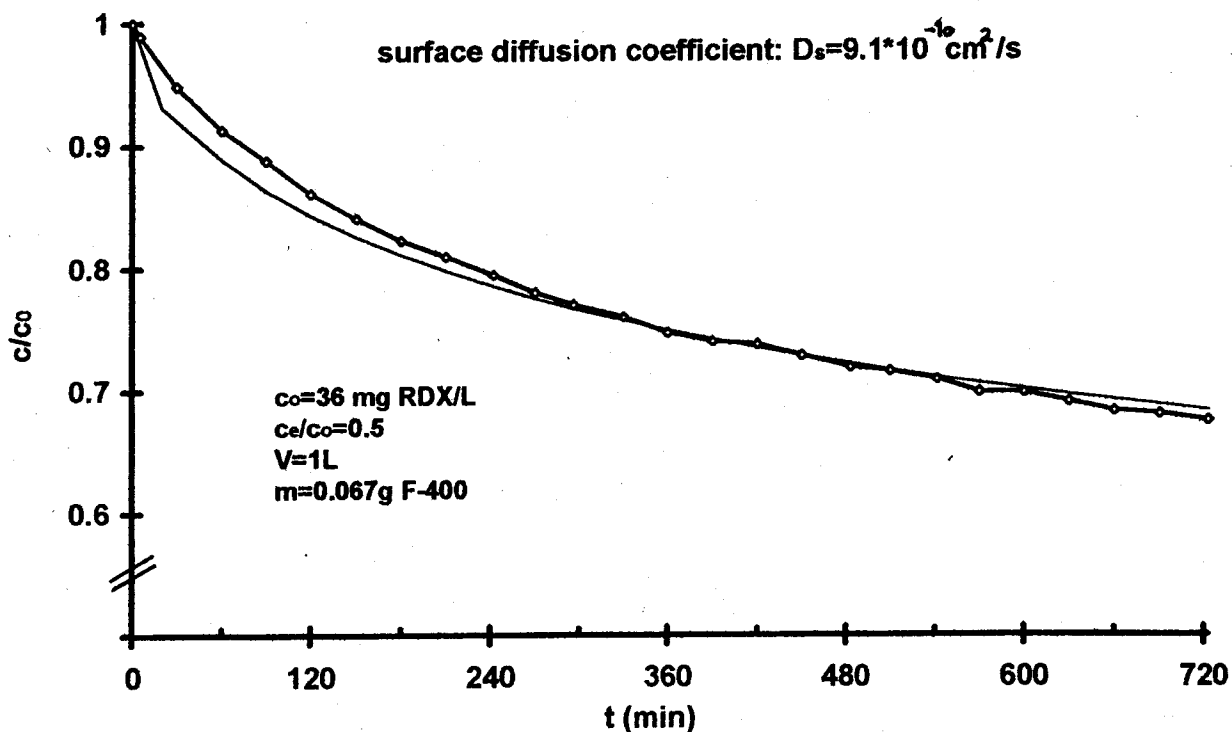
It is very important to know the initial RDX concentration because this concentration has a major effect on the calculation of D_s . Therefore, three independent samples of the RDX solution were taken and analyzed before the experiment was started. In order to calculate the necessary dosage of GAC (Filtrisorb-400) to reach an equilibrium concentration of $C_e/C_0=0.5$, the equation

$$D_0 = \frac{C_0 - C_e}{K \cdot C_e^{1/n}} = \frac{36.35 - 18.175}{96.97 \cdot 18.175^{0.35}} = 0.067g \quad (5.1)$$

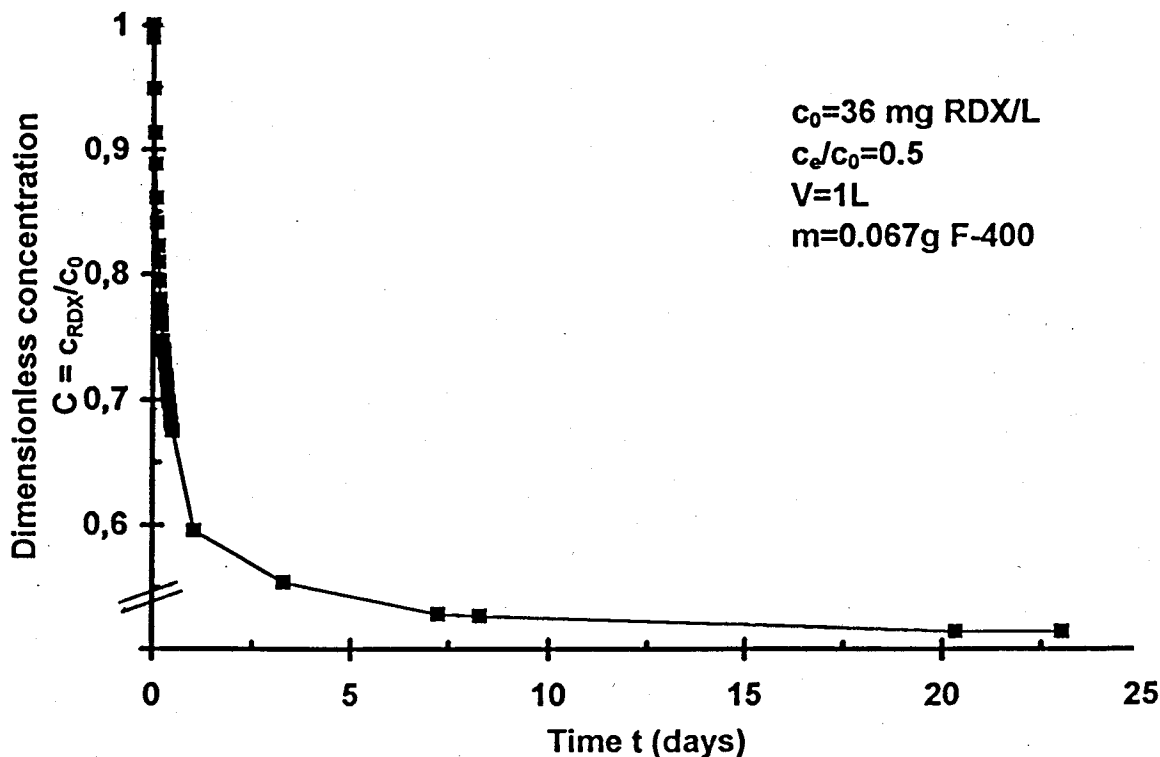
was used. The solution was agitated with an overhead driven propeller at an RPM of 1350 1/s.

Samples were taken at least every 30 minutes during the first 12 hours and analyzed for RDX. In this study, the model is most sensitive in the time between 180 and 723 minutes elapsed time. Data from samples taken before and after this time period do not belong to the most sensitive time and were therefore not used for the calculation of D_s . $D_{s,i}$ values were calculated as described in Chapter 4.3.

The average of the $D_{s,i}$ is $D_{s,orig} = 9.8 \cdot 10^{-10} \text{cm}^2/\text{s}$, s equals 0.04203. In order to evaluate the best fit D_s several estimations were calculated. The smallest s was found for $D_s = 93\% \cdot D_{s,orig}$ with $s = 0.04002$ and $D_s = 9.11 \cdot 10^{-10} \text{cm}^2/\text{s}$.



a) duration as relevant for HSDM-model estimations



b) complete duration of the experiment

Figure 5.2: Batch Rate Data and Model Calculations for the Adsorption of RDX Diluted in DI-Water onto Activated Carbon

Hand *et al.* (1983) distinguish between excellent fits ($s=0-0.04$), good fits ($s=0.04-0.08$), and satisfactory fits ($s=0.08-0.1$). Values larger than 0.1 should not be used for column model predictions. The results found in this study are good to excellent. The actual equilibrium concentration after 23 days was 17.95 mg/L. C_e/C_0 equals 0.49 which is well in the acceptable range for the model according to Hand *et al.* (1983).

Results from the kinetic experiment are presented in Figure 5.2 and in Table 5.2.

5.1.3. Findings

The external mass transfer can be neglected with stirrer speeds greater between 400 and 1350 RPM is used. Therefore, the only model parameters were the Freundlich-isotherm constant $1/n$ and c_e/c_0 . The surface diffusion coefficient D_s was found to be $9.1 \cdot 10^{-10} \text{cm}^2/\text{s}$ for the system Filtrasorb-400/RDX.

According to statistical analysis of the data and following the procedure suggested by Hand *et al.* (1983) the model fit was good to excellent.

percent of original estimate, $D_{s, \text{orig}}$	surface diffusion coefficient, D_s	sum of the squares of the residuals, s_2	standard deviation, s
%	(cm^2/s)		
85	8.33E-10	0.00188	0.04333
90	8.82E-10	0.00164	0.04051
93 (best fit)	9.11E-10	0.00160	0.0400
95		0.00161	0.0402
100	9.8E-10	0.00177	0.0420
110	1.08E-9	0.00252	0.0502

Table 5.2: Data Analysis for the Kinetic of RDX Adsorption onto Activated Carbon (F-400), Conducted in order to Develop the Best Fit D_s .

5.2. Adsorption of RDX onto Activated Carbon in Fixed-Bed Columns

The results of the adsorption experiments are presented and discussed in this chapter. Breakthrough curves are presented for various experiments. Table 5.3 lists all adsorption experiments and gives an overview over the experimental conditions.

Exp. Number	Column Number	Column height (mm)	Mass of AC (g)	Flow rate (mL/min)	EBCT (min)	RDX adsorbed (mg)	Water treated (L)	Temperature (°C)	Regenerations
FB1a	a	70	2.4	3.9	1.4	276	16.6	25-27	0
FB2a	a	30	1.0	1.2	2.0		6.1	25.5-27.5	0
FB2b	b	70	2.4	2.8	2.0	251	14.8	25.5-27.5	1
FB3a	a	30	1.0	1.1	2.2	123	6.9	26-27	1
FB3b	b	30	1.0	1.2	2.0	110	7.6	26-27	0
FB4a	a	30	1.0	0.62	3.8	132	8.1	25.5-27	2
FB4b	b	30	1.0	0.59	4.0	128	7.7	25.5-27	1
FB5a	a	30	1.0	0.60	3.9	198	19.4	23-25	3
FB5b	b	30	1.0	0.55	4.3	188	17.7	23-25	2
FB5c	c	30	1.0	0.59	4.0	256	19.0	23-25	0
FB6a	a	30	1.0	1.0	2.3	139	11.7	22-25	4
FB6b	b	30	1.0	1.1	2.1	136	12.6	22-25	3
FB6c	c	30	1.0	1.1	2.1	170	12.7	22-25	1

Table 5.3: Master Table for all Fixed-Bed Adsorption Experiments conducted. All experiments were conducted at room temperature (22°C to 27.5°C) and a RDX concentration of approximately 17.5 mg/L. The column diameter was 10 mm in each experiment.

Flow rates between 0.55 and 3.9 mL/min were used. The height of the activated carbon in the columns was 30mm and 70mm, respectively, the diameter was 10mm. The superficial velocity ranged from 0.55 to 3.9 mm/min and the empty bed contact time (EBCT) ranged from 1.4 min to 4.3 min. Virgin and one to four times regenerated columns were used. All experiments were conducted at room temperature and a RDX concentration of approximately 17.5 mg/L.

5.2.1. Results

5.2.1.1. Flow Rate

Figure 5.3 shows the results of experiment FB1b which was conducted using a 70 mm column, virgin activated carbon, and a flow rate of 3.6 mL/min. No RDX was detected in the effluent during the first 1200 minutes (857 bed volumes, BV, method detection limit = 0.1 mg/L).

In order to use the carbon which was exhausted in experiment FB1b for another adsorption, it was regenerated in place, using alkaline hydrolysis. After the regeneration, the second adsorption experiment was performed (FB2b) at identical conditions as the first experiment, except for a reduced flow rate of 2.8 mL/min.

In spite of the reduced flow rate, a RDX concentration of 0.07 mg/L was detected as early as 810 minutes elapsed time. However, the RDX concentration did not increase as fast as it did in experiment RG1b, where virgin activated carbon was used. The RDX concentration was lower even after 44 hours elapsed time (1873 BV, FB1b; 1354 BV, FB2b).

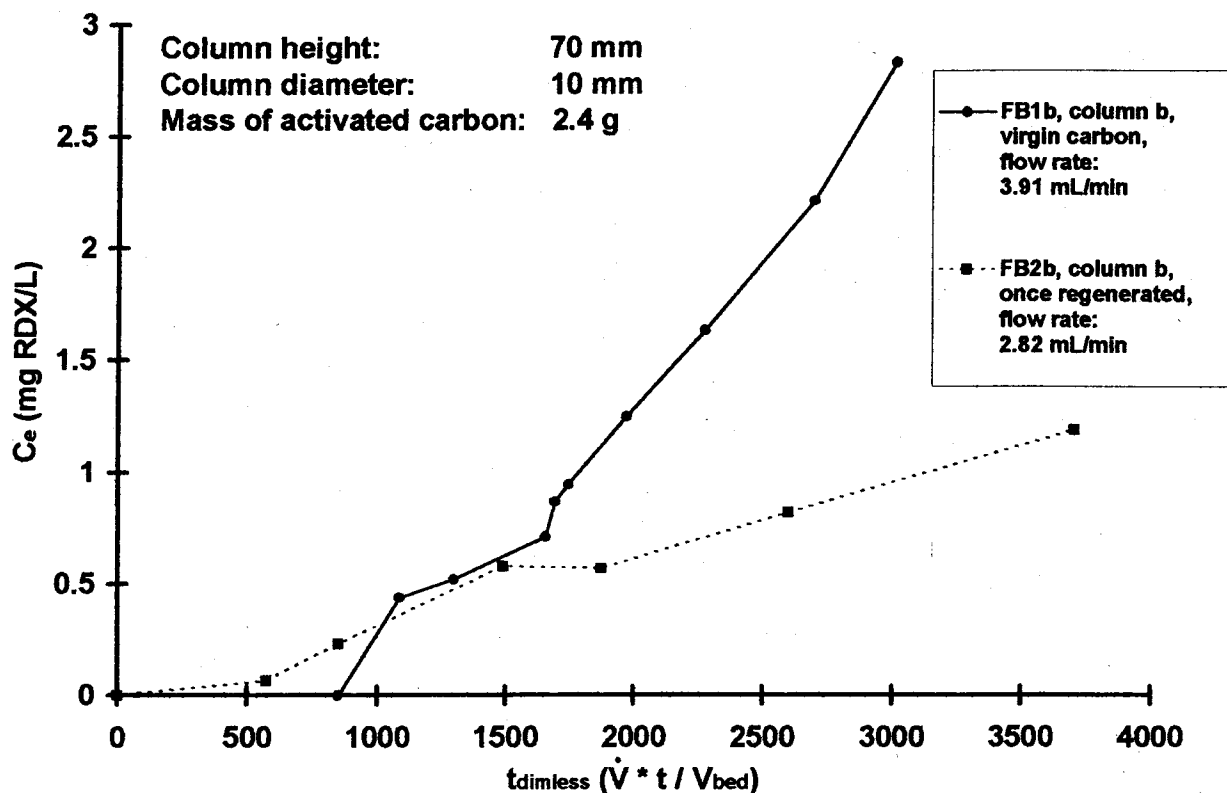


Figure 5.3: Breakthrough Curves for Adsorption of RDX in Continuous Flow Activated Carbon Fixed-Beds, Experiments FB1b and FB2b

Figure 5.4 shows the breakthrough curves for the experiments FB2a, FB3b, and FB5c. All columns used virgin carbon. The flow rates were 1.21 mL/min (FB3b), 1.16 mL/min (FB2a), and 0.59 mL/min (FB5c).

The curve of FB2a is not straight but jumps up and down during the entire breakthrough curve. The RDX concentration was found to be higher than the concentration in FB3a at some elapsed times and lower at other elapsed times. All effluent concentrations of FB5c were lower than the concentrations of both other experiments with a higher flow rate. Only samples taken in very early parts of the experiment had no detectable RDX concentration. The first RDX was detected after 1324 minutes (334 BV). For experiment FB3b, which was conducted with the highest flow rate, a concentration of 0.23 mg RDX/L was detected after 85 minutes (47 BV).

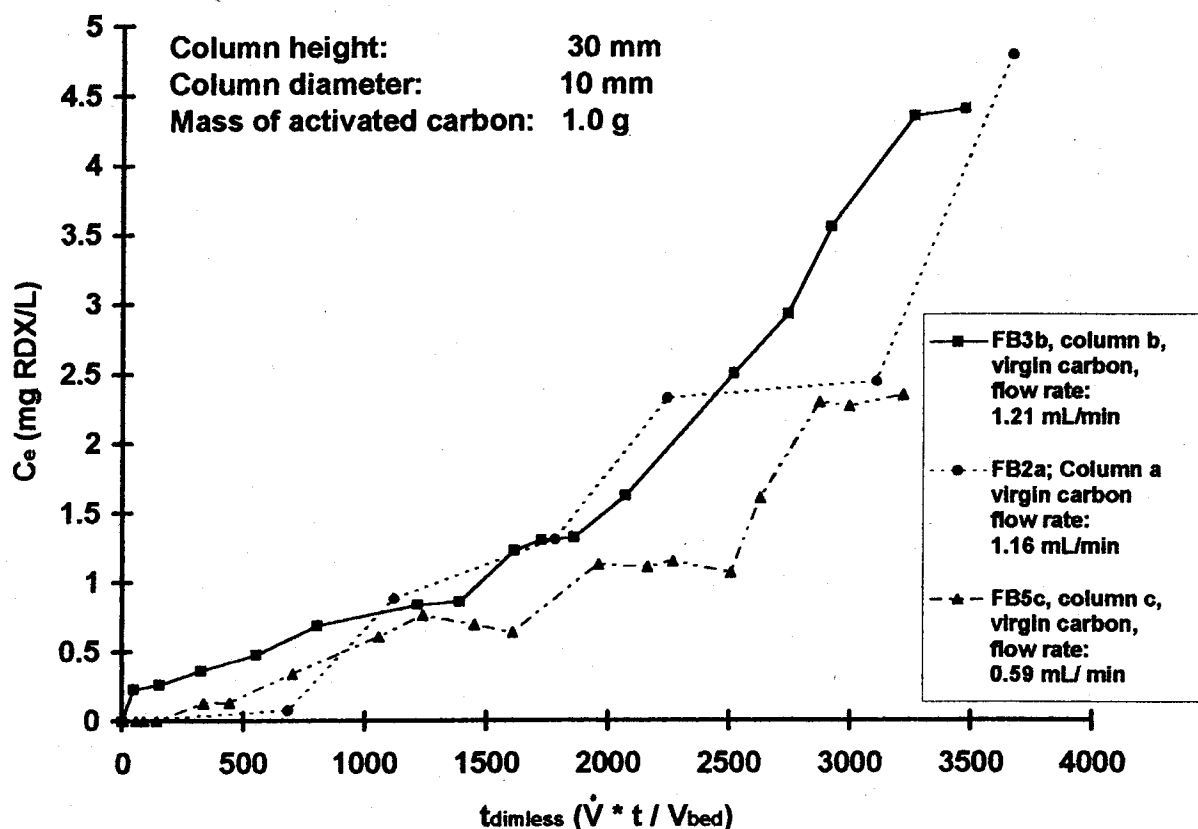


Figure 5.4: Breakthrough Curves for Adsorption of RDX in Continuous Flow Activated Carbon Fixed-Beds, Experiments BF2a, FB3b, and FB5c

5.2.1.2. Effect of Different Numbers of Regenerations

Figure 5.5 shows the breakthrough curves for adsorption experiments FB4a, FB4b, FB5a, FB5b, and FB5c. The flow rate ranged from 0.55 and 0.62 mL/min.

All breakthrough curves are approximately parallel and identical within experimental error in the beginning of the experiment. There was no RDX detectable in the effluent of these experiments until an elapsed time of approximately 560 minutes (130-160 BV). In experiment FB4a, no RDX was detected until 1320 minutes (364 BV). During all experiments the RDX concentration increased very slowly in the beginning and increased faster on the experiment progresses.

A trend can be detected in the experiment results. The effluent concentration is higher with increasing regeneration during the second half of the experiment. For example, at 3200 BV the RDX concentration for the virgin carbon is approximately 2.2 mg/L, for columns regenerated two and three times the concentrations ranged between 4.1 and 5.3 mg/L. The highest effluent RDX concentration was at FB5a which was run with activated carbon regenerated four times. The concentration was 5.92 mg RDX/L at an elapsed time of 13250 minutes (3402 BV). The lowest effluent RDX concentration at the same elapsed time (3340 BV) was 2.82 mg/L at FB5c where virgin activated carbon was utilized.

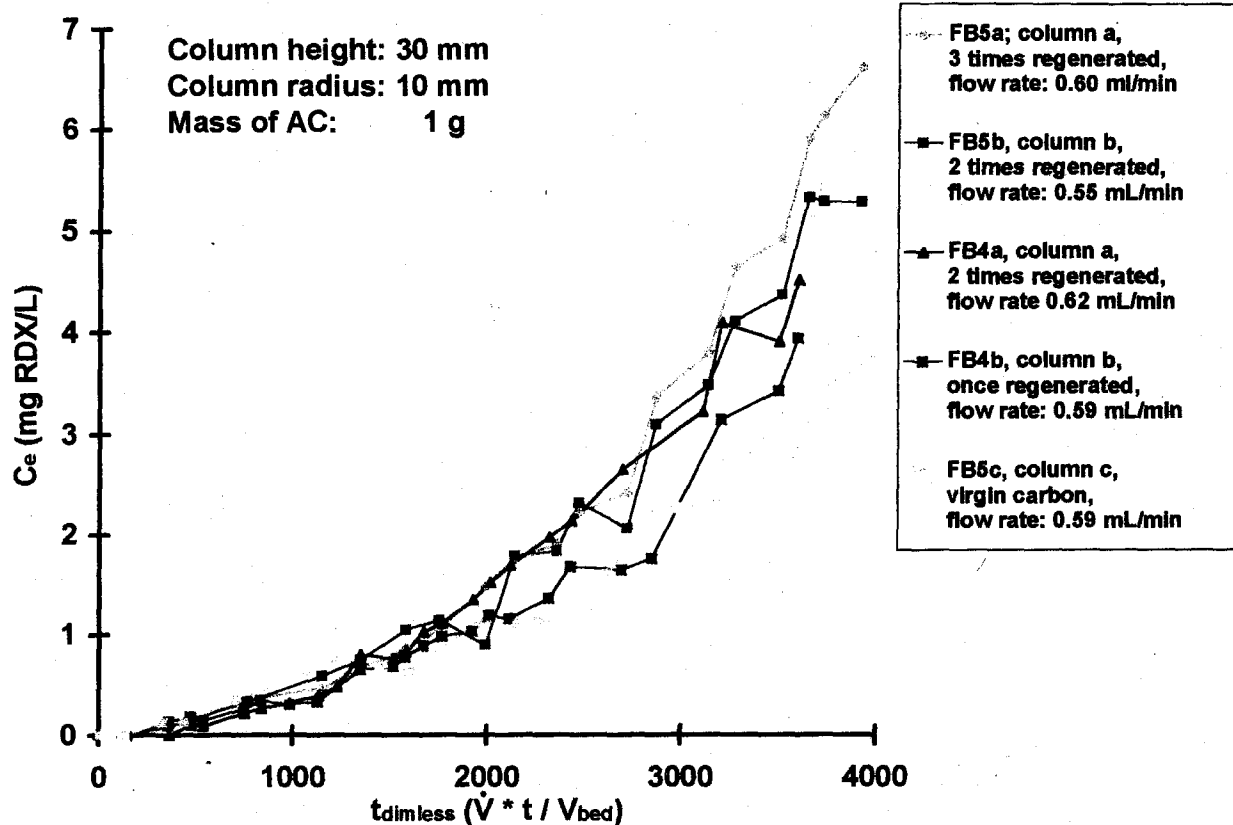


Figure 5.5: Breakthrough Curves for Adsorption of RDX in Continuous Flow Activated Carbon Fixed-Beds, Experiments FB4a, FB4b, FB5a, FB5b, and FB5c

Figure 5.6 shows the breakthrough curves for the adsorption experiments FB3a, FB3b, FB6a, FB6b, and FB6c. The flow rate ranged between 1.03 and 1.21 mL/min. The activated carbon of FB3b was virgin, the activated carbon for FB3a and FB6c was once regenerated, the activated carbon of FB6b was three times regenerated, and the activated carbon of FB6a was regenerated four times.

The breakthrough curves of FB6a, FB6b, FB6c, and FB3b are very nearly parallel. The slope of these curves do not change very much during the entire experiment. Compared to all other experiments shown in this graph, the RDX concentration in FB3a increased more slowly until 5340 minutes (2725 BV) and increased more rapidly compared to the other experiments after this time.

RDX was detected at all adsorption experiments shown in this graph even at the first sample taken.

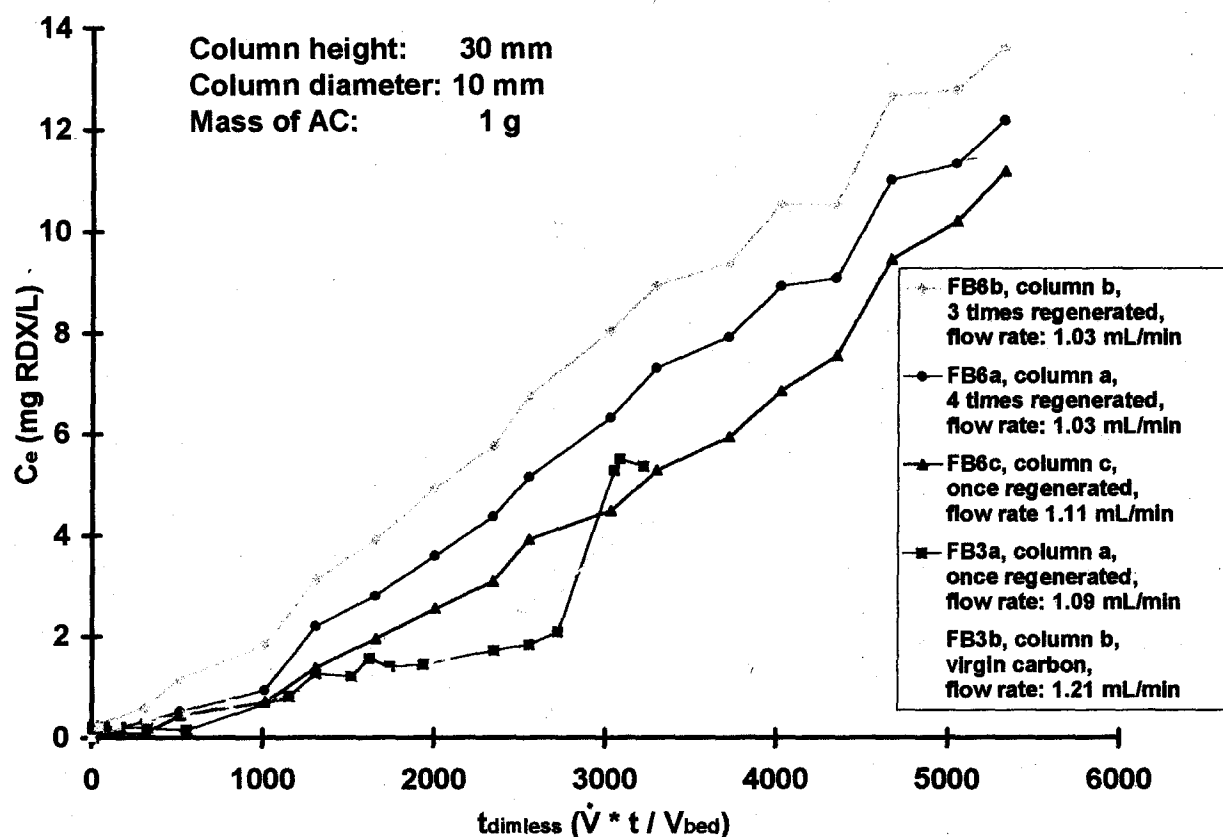


Figure 5.6: Breakthrough Curves for Adsorption of RDX in Continuous Flow Activated Carbon Fixed-Beds, Experiments FB3a FB3b, FB6a, FB6b, and, FB6c

5.2.1.3. Complete Breakthrough Curves

Figure 5.7 shows the breakthrough curves for the adsorption experiments BF5a, FB5b, and FB5c. This experiment was conducted for 32050 minutes (7508-8229 BV) with flow rates ranging between 0.55 and 0.62 mL/min.

The curves are very nearly parallel, even small changes and peaks appear at the same time. The first samples up to approximately 560 minutes (131-143 BV) did not have any detectable RDX. Between 2000 and 3000 BV (8000-12000 minutes), the increase of the RDX concentration in the effluent rose and became stable after 3500 BV (~13500-15000 minutes).

In experiments FB5a and FB5b columns which had been regenerated two and three times were used. Therefore, experiment FB5c, using virgin carbon, had lower effluent RDX concentrations than either of the other experiments through the entire time except of the very beginning.

The experiment was stopped when the effluent RDX concentration of FB5a equalled the concentration of the influent (17.3 mgRDX/L). The effluent concentrations of FB5b was about 1 mg RDX/L and the concentration at FB5c was about 3.5 mgRDX/L less than the influent concentration.

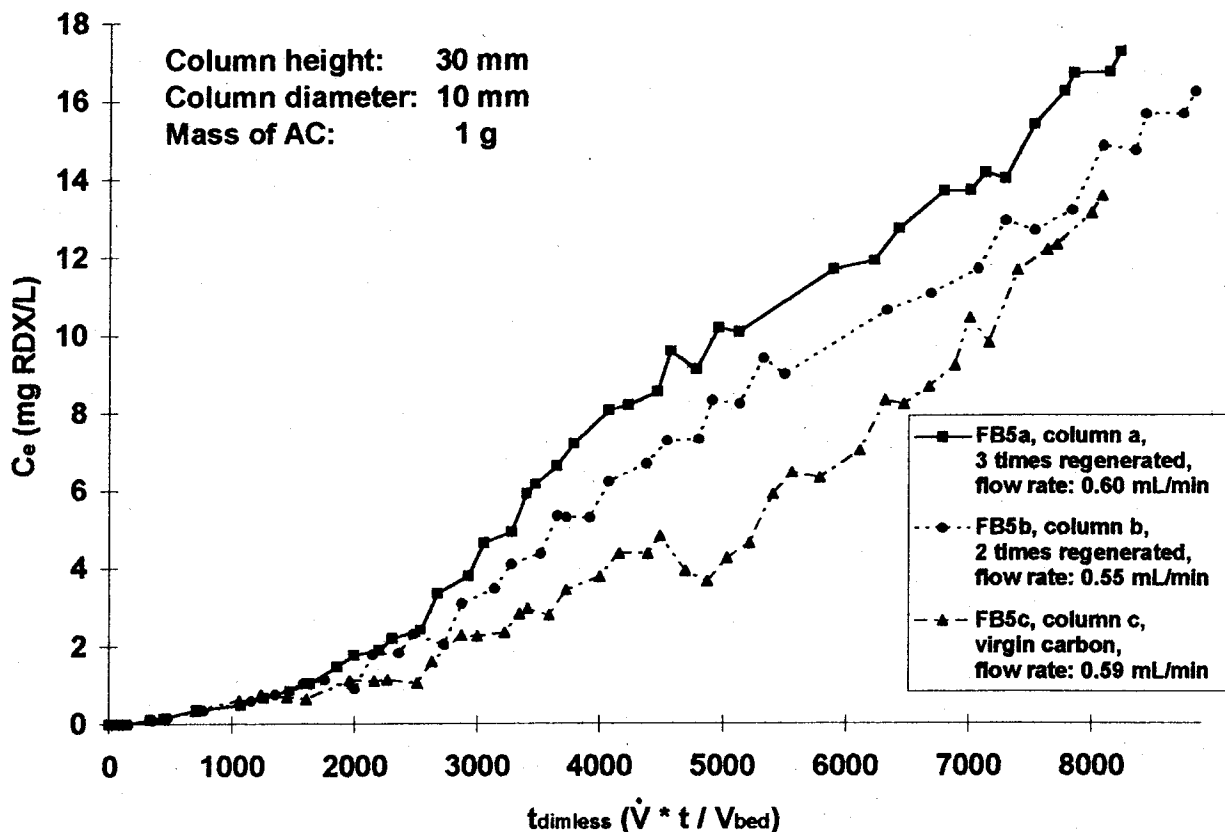


Figure 5.7: Breakthrough Curves for Adsorption of RDX in Continuous Flow Activated Carbon Fixed-Beds, Experiments FB5a, FB5b, and FB5c

5.2.2. Discussion

5.2.2.1. Errors

There are several sources of experimental errors in the column adsorption experiments.

In the beginning of the experiment series major flow rate changes appeared due to plugged screens in the system. Very small carbon particles were released from the fixed-bed and plugged the small pores of the nylon screens ($27 \mu\text{m}$) used. This led to a higher resistance in the screen and a decrease in flow rate. In the beginning of the experiment series, experiments had to be stopped because it was impossible to keep the flow rate stable. When the $27 \mu\text{m}$ screens were replaced by $53 \mu\text{m}$ screens, the flow rate became much more constant, even though it changed by as much as 0.1 mL/min , or 18% of the maximum flow rate.

The flow rate used for the calculation was derived from the volume of water treated and the elapsed time at the end of an experiment. Therefore, it is an average over the entire experiment. The flow rate changes can be neglected for all experiments conducted after the screens were changed in the beginning of the experiment series number 3.

Air bubbles plugged inside the fixed-beds during the adsorption. Higher flow rates, adjusted in order to flush the air bubbles out of the column, did not remove them. Most of them did not move during the entire adsorption experiment. Therefore, parts of the activated carbon did not have any contact to the liquid flushed through the column. This carbon did not adsorb any RDX, and less RDX was removed from the liquid which caused higher effluent concentrations. The error is suspected to be less than 10 percent.

The influent container had a volume of 20 L. Some experiments used more than 20 L liquid. The influent container had to be refilled during these experiments. The liquid added may have had slightly different RDX concentrations than the liquid in the influent container. This error would be less than 5 percent.

Midway experiments FB6a, FB6b, and FB6c, the HPLC column had to be replaced. New standards were to be developed. Minor errors may be caused due to the new column.

The main power supply does not provide 100% equal electric power. When changes appear in the electric power supply, the RPM of the pump will change causing a change in the flow rate.

5.2.2.2. Findings

Three parameters were changed in the fixed-bed adsorption experiments: the flow rate, the height of the activated carbon in the column, and the number of regenerations that had been conducted before running an adsorption.

As expected a higher flow rate lead to higher effluent RDX concentration if all other parameters mentioned above were equal (see Figures 5.3 and 5.4).

When 30 mm columns were used, RDX was detected after a few hours even if a small flow rate was used. When 70 mm columns were used, it took much longer before RDX was detected in the effluent.

The 30 mm columns were used because only a limited amount of RDX was available. The ratio 1/3 for diameter/height had to be used because only the height of the activated carbon in the columns could be changed, but not the diameter. Even if this ratio is used in other investigations, a ratio of 1/7 should be used for practical applications.

If columns were operated at the same flow rate and activated carbon mass, higher numbers of regenerations are associated with higher effluent RDX concentrations. This indicates that the capacity of the columns will decrease during each cycle of adsorption and regeneration. There are several possible reasons, and the following explanations are offered. They should be considered as speculations:

1. Small pores in the activated carbon particles can be plugged. Therefore, the surface area of these pores are not available for the RDX anymore.
2. The adsorption of TOC onto the carbon during the adsorption experiments. The TOC concentration in the DI-water used was relatively high compared to the low RDX concentration in the treated water. Furthermore, a large volume of water was flushed through the columns. Therefore, the amount of TOC flushed through the column was relatively high. During the regeneration, the adsorbed TOC might not be removed entirely from the carbon, thereby limiting its RDX adsorption capacity.
3. Even though the concentration of nitrite and formate indicates that all RDX was hydrolyzed and desorbed after every regeneration (except of RG5a, RG5b, and RG5c), there might still be some RDX adsorbed onto the activated carbon.
4. There may still have been some by-products such as formate and acetate generated by the hydrolysis adsorbed on the activated carbon

Further research is required to determine which reasons are most valid.

5.3. Regeneration Experiments of exhausted Activated Carbon Columns

Heilmann (1996) found that alkaline hydrolysis is feasible in batch experiments at pH=12 and T=80°C. When all RDX was hydrolyzed and desorbed, a ratio of 1.6 mol nitrite and 1.7 mol formate, respectively, per mol hydrolyzed RDX was found in the regeneration liquid. Heilmann (1996) proved that no RDX was adsorbed onto the activated carbon after regeneration. Therefore, nitrite and formate are suitable parameters to observe the regeneration process.

The following figures show the regeneration of laden columns using alkaline hydrolysis. The regeneration is measured by the evolution of end-products, such as nitrate and formate. The graphs are shown in mole ratios of the end-product to the original RDX that was present.

Most columns were regenerated by alkaline hydrolysis using pH 12, T=80°C, and one liter regeneration liquid. In experiments RG5a, RG5b, and RG5c, the pH and/or the temperature was reduced to pH 11 or T=70°C, respectively. The regenerations RG6a, RG6b, and RG6c were conducted using one liter regeneration liquid for all columns.

Flow rates between 3.2 mL/min and 8.8 mL/min were used. The activated carbon height in the columns was 30 mm or 70 mm, respectively, with a diameter of 10 mm in all experiments. The EBCT ranged between 0.27 min and 1.4 min. Table 5.4 lists all regeneration experiments in order to give an overview over the experimental conditions.

<i>Exp.</i> Number	<i>Column</i> Number	<i>Column</i> <i>height</i>	<i>Mass of</i> <i>AC</i>	<i>Flow rate</i>	<i>EBCT</i>	<i>Tem-</i> <i>perature</i>	<i>pH</i>	<i>RDX</i> <i>adsorbe</i> <i>d</i>	<i>Regen-</i> <i>erations</i>
		(mm)	(g)	(mL/min)	(min)	(°C)		(mg)	
RG1a	a	70	2.4	3.9	1.4	80	12	276	0
RG2a	a	70	2.4	8.0	0.69	80	12	251	1
RG3a	a	30	1.0	8.8	0.27	80	12	123	1
RG3b	b	30	1.0	8.5	0.28	80	12	110	0
RG4a	a	30	1.0	5.2	0.45	80	12	132	2
RG4b	b	30	1.0	5.7	0.41	80	12	128	1
RG5a	a	30	1.0	3.8	0.62	80	11	198	3
RG5b	b	30	1.0	3.9	0.61	70	12	188	2
RG5c	c	30	1.0	3.7	0.63	70	11	256	0
RG6a	a	30	1.0	3.3	0.67	80	12	139	4
RG6b	b	30	1.0	3.4	0.69	80	12	136	3
RG6c	c	30	1.0	3.2	0.73	80	12	170	1

Table 5.4: Master Table for all Fixed-Bed Regeneration Experiments Conducted. The column diameter was 10 mm in each experiment.

5.3.1. Results

5.3.1.1. Flow Rate

The experiments shown in Figure 5.8 were conducted using 70 mm columns, pH 12, and $T=80^{\circ}\text{C}$. The flow rate was 3.9 and 8.0 mL/min, respectively.

Nitrite and formate are very quickly produced in batch regeneration experiments, as indicated by the slope of the curve. The evolution is very rapid until approximately 240 minutes (170 or 349 BV, respectively).

Nitrite and formate were rapidly generated in experiments RG1b and RG2b until elapsed times of 362 minutes (251 BV) and 240 minutes (349 BV). The ratio for nitrite was greater than 1.5 in experiment RG1b after 362 minutes (251 BV) and for formate after 631 minutes (448 BV). In RG2b the ratios are greater than 1.5 after 3259 minutes (2311 BV) and 724 minutes (514 BV), respectively.

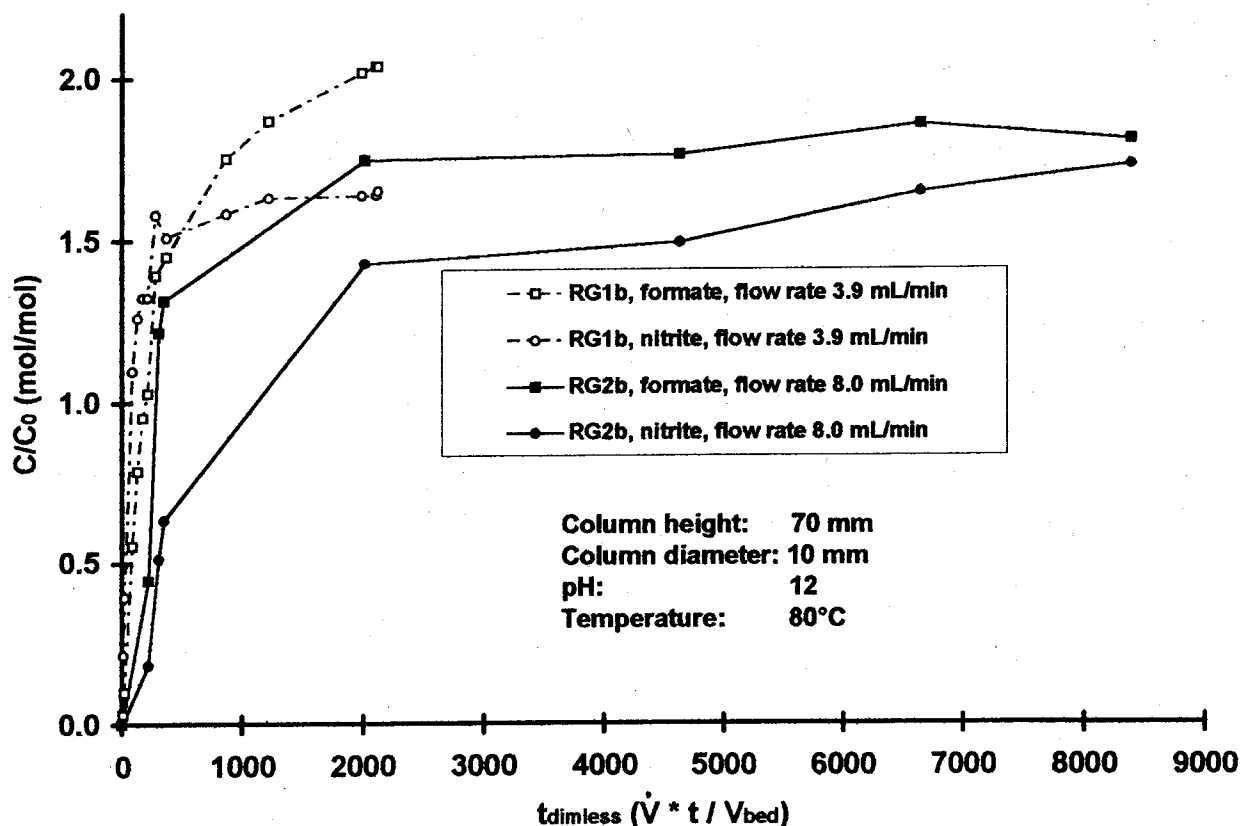


Figure 5.8: Mol End-product/Mol RDX Generated by Alkaline Hydrolysis of Laden Activated Carbon Fixed-Beds. Experiments RG1b and RG2b.

For RG1b a stable mol/mol ratio of 1.65 (nitrite) was found after 390 minutes (277 BV). The production of formate was also nearly complete after 2800 minutes (1986 BV) with 2.04 mol/mol. At RG2b this ratio was stable and detected to be 1.73 and 1.81, respectively, after 1380 minutes (2009 BV).

Experiments RG3a and RG3b were conducted using 30 mm columns, a pH of 12, a temperature of 80C, and flow rates of 8.8 and 8.5 mL/min, respectively (see Figure 5.9).

No difference in evolution rates can be detected in the beginning of the regeneration. After 400 minutes (1493 and 1444 BV, respectively) ratios greater than 1.5 for both nitrite and formate were obtained in both experiments. Stable concentrations were developed after approximately 600 minutes (2239 and 2166 BV, respectively). The ratio at the end of experiment RG3a after 3060 minutes (11,418 BV) was 1.66 mol/mol (nitrite) and 1.83 mol/mol (formate). In experiment RG3b a ratio of 1.95 and 2.17, respectively, had developed at the end of the experiment after 2500 minutes (9019 BV).

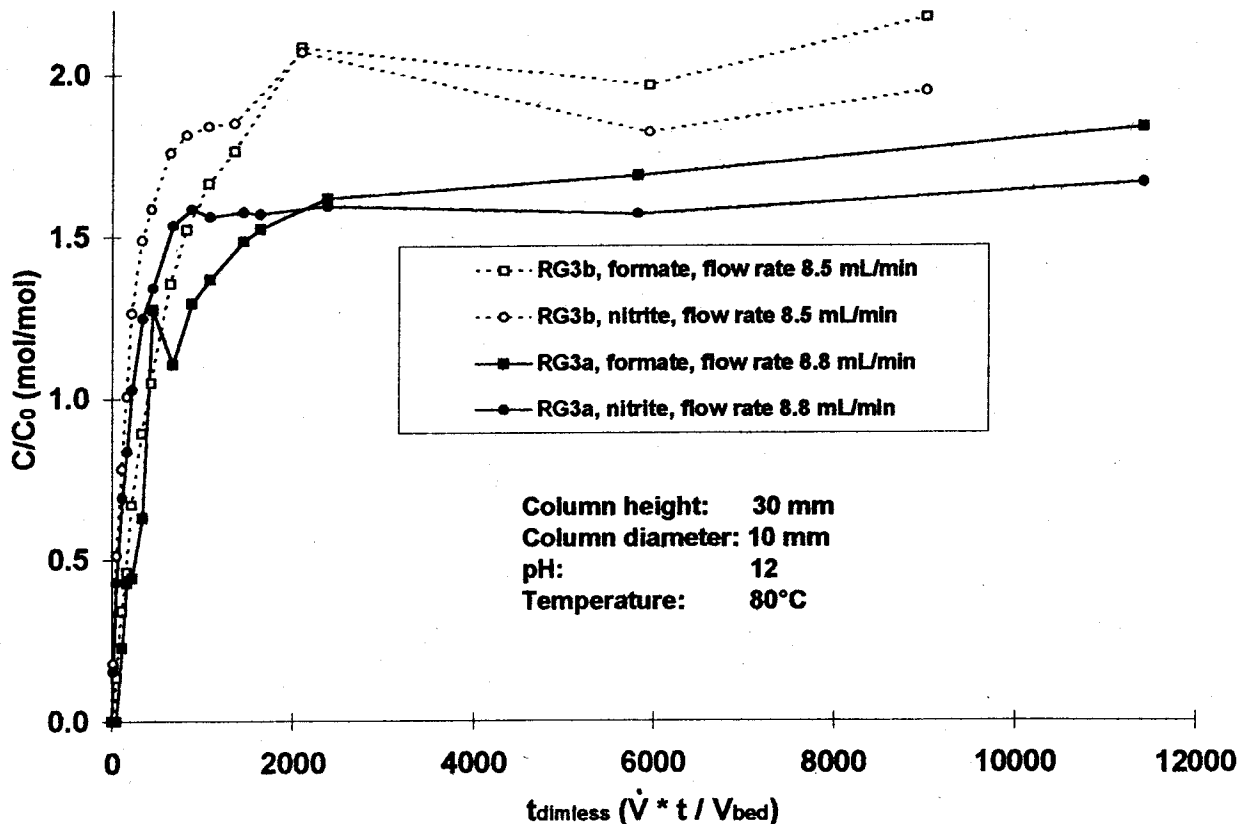


Figure 5.9: Mol End-product/Mol RDX Generated by Alkaline Hydrolysis of Laden Activated Carbon Fixed-Beds. Experiments RG3a and RG3b.

5.3.1.2. Comparison of Regeneration's With Equal Parameters

Experiments RG4a and RG4b were conducted using pH 12, $T=80^{\circ}\text{C}$, a column height of 30mm, and flow rates of 5.2 and 5.7 mL/min, respectively (see Figure 5.10).

The rates of production of nitrite and formate are approximately equal as indicated by the slopes of the curves. A ratio of 1.5 for nitrite and formate was reached at RG4a after 451 minutes (995 BV) and at RG4b after approximately 500 minutes (1224 BV). A stable concentration for nitrite was found after 451 minutes (995 BV) at RG4a and after 479 minutes (1173 BV) at RG4b. For formate a stable concentration was generated after 1398 minutes (3085 BV) and 1342 minutes (3286 BV), respectively. The ratio at the end of the regeneration of RG4a was for nitrite 1.78 and for formate 1.99. At RG4b the ratios were 1.82 and 2.00, respectively.

All data for these two experiments meet within the experimental error very well.

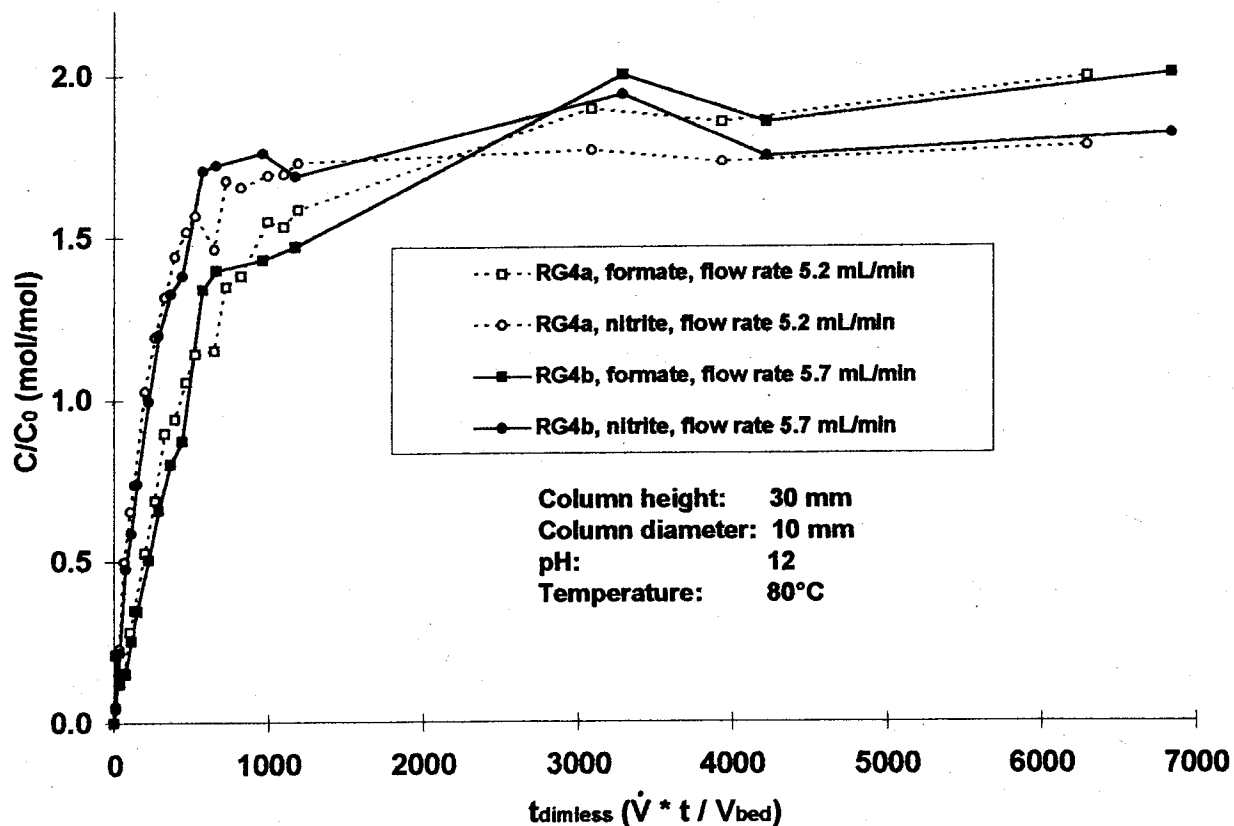


Figure 5.10: Mol End-product/Mol RDX Generated by Alkaline Hydrolysis of Laden Activated Carbon Fixed-Beds. Experiments RG4a and RG4b.

5.3.1.3. pH and Temperature Effects

In experiments RG5a, RG5b, and RG5c, pH or/and temperature were reduced to 11 and 70°, respectively, using 30 mm columns (see Figures 5.11 to 5.13).

Experiment RG5a was conducted at a pH of 11 and a temperature of 80°C. The flow rate was 3.8 mL/min. After an elapsed time of 2238 minutes (3609 BV) the mol/mol ratios for nitrite and formate in RG5a was 1.06 and 0.22, respectively. The experiment was stopped after 2238 minutes (3609 BV) before the concentration of nitrite or formate was stable. However, the generation of both nitrite and formate in this experiment was less than in all experiments at a temperature of 80°C and a pH of 12. After an elapsed time of 2238 minutes it was less than expected at an higher pH when RDX is fully hydrolyzed.

To regenerate the column sufficiently, 2mL NaOH, 10 Mol, was added to the Erlenmeyer-flask after 2773 minutes (4480 BV). Both the concentration of nitrite and formate increased to a ratio of 1.2. This indicates that not all RDX was hydrolyzed and desorbed from the activated carbon even after the pH was elevated.

Experiment RG5b was conducted at the temperature of 70°C and a pH of 12. During the first 715 minutes (1174 BV) the generation of nitrite and formate was fast. A stable nitrite and formate concentration was reached after approximately 2500 minutes (4105 BV). The ratio after 5915 minutes (9716 BV) was 1.1 mol/mol for nitrite and 1.64 mol/mol for formate. The ratios for both nitrite and formate at this time were smaller than it can be expected at a complete hydrolysis.

The smallest mol/mol ratio of both nitrite and formate was measured in experiment RG5c where the pH and the temperature were reduced to pH 11 and 70°C. The ratio for formate never exceeded 0.1 mol/mol and the ratio of nitrite was smaller than 0.8 mol/mol during the entire experiment, up to an elapsed time of 5910 minutes (9356 BV). The production of nitrite and formate is less than in experiments RG5a and RG5b, were only one parameter, pH or temperature were reduced. The production of nitrite and formate stabilized after 1385 minutes (2193 BV).

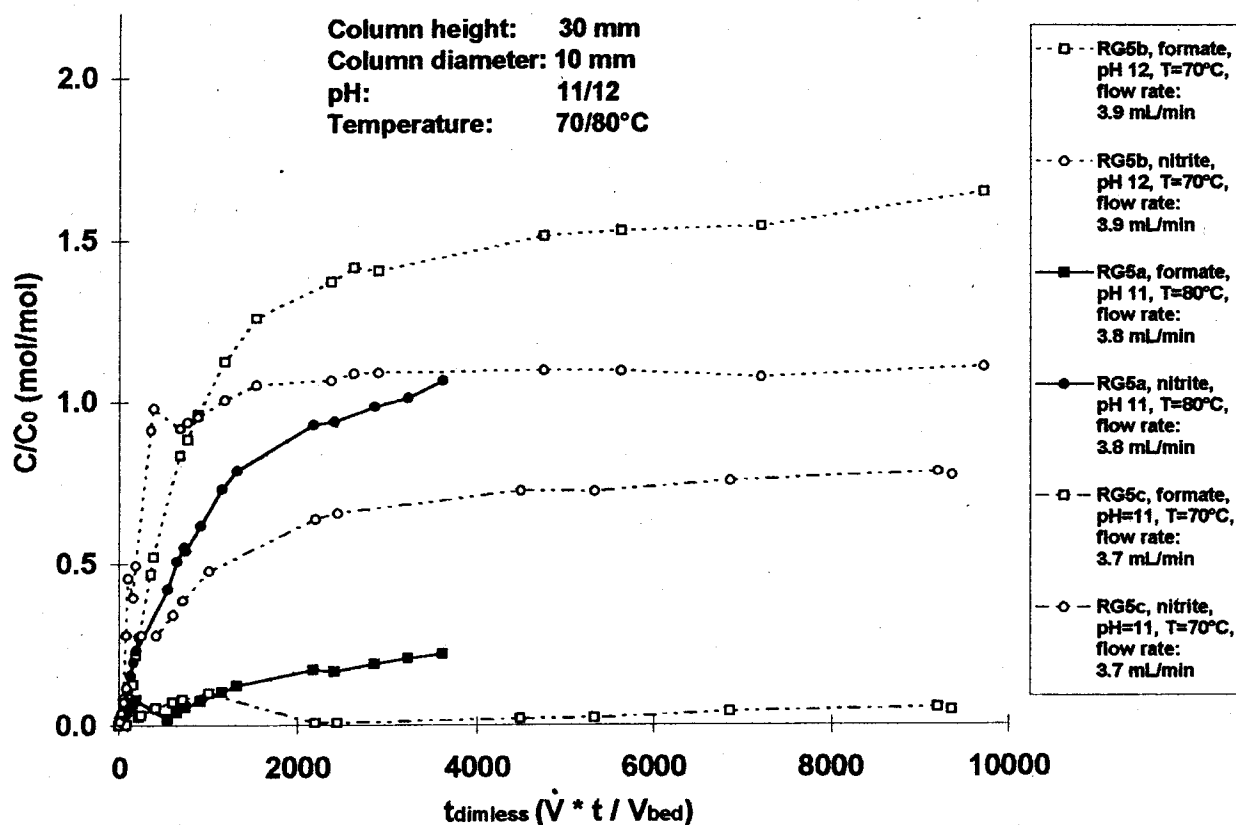


Figure 5.11: Mol End-product/Mol RDX Generated by Alkaline Hydrolysis of Laden Activated Carbon Fixed-Beds. Experiments RG5a, RG5b and RG5c.

As done in RG5a, 2mL NaOH, 10 Mol, was added to the Erlenmeyer-flask after 6025 minutes (9538 BV) in order to regenerate the column sufficiently. The ratio increased to 1.4 (nitrite) and 1.2 (formate). This indicates that not all RDX was hydrolyzed and desorbed from the activated carbon even after the pH was elevated.

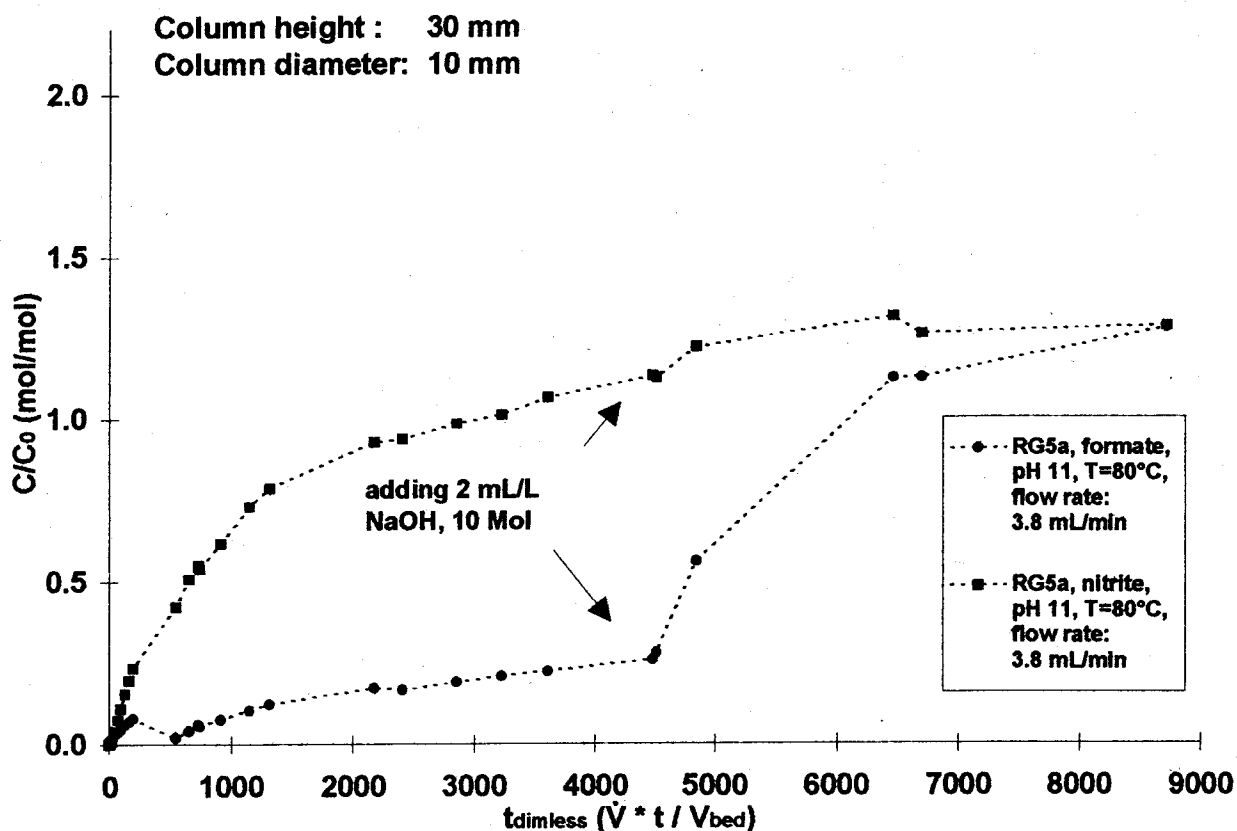


Figure 5.12: Mol End-product/Mol RDX Generated by Alkaline Hydrolysis of Laden Activated Carbon Fixed-Beds. Experiments RG5a. In order to rise the pH, 2 mL/L NaOH, 10 Mol, was added to the regeneration liquid after the dimensionless time of 4480 BV.

5.3.1.4. Regeneration of Three Exhausted Columns Using One Liter Regeneration Liquid

In experiments RG6a, RG6b, and RG6c, three exhausted 30 mm columns were regenerated using one liter regeneration liquid, pH 12, and $T=80^\circ\text{C}$. The total mass of RDX adsorbed on the columns was 446 mg.

The production of nitrite and formate for this multiple column experiment followed the expected trends from a single experiment at the same pH and temperature. The generation of nitrite and formate during experiment RG6a and RG6b and the generation of nitrite during RG6c was very fast in the beginning and the concentration became stable after approximately 500 minutes (~ 720 BV). The generation of formate in RG6c was fast in the beginning also but became stable after 1645 minutes (2234 BV) only.

When the regenerations were completed, the ratio of nitrite varied between 1.86 and 2.06, the ratio of formate varied between 1.63 and 2.61. In RG6c a relatively high ratio for both nitrite and formate has been found, 2.06 for nitrite and 2.61 for formate. The final ratios of the experiments RG6a and RG6b are comparable to results from other regeneration experiments.

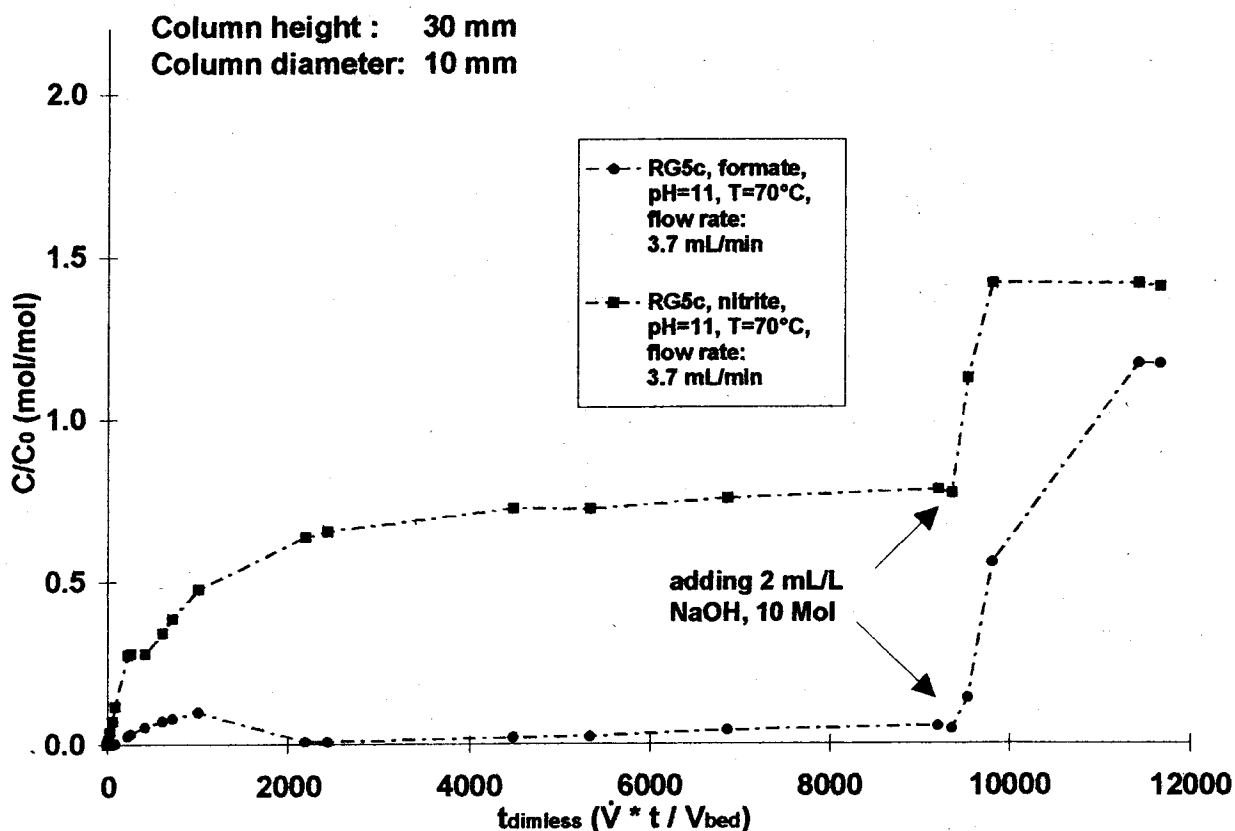


Figure 5.13: Mol End-product/Mol RDX Generated by Alkaline Hydrolysis of Laden Activated Carbon Fixed-Beds. Experiments RG5c. In order to rise the pH, 2 mL/L NaOH, 10 Mol, was added into the regeneration liquid after the dimensionless time of 9538 BV.

5.3.1.5. OH⁻ consumption

In order to compare the expected and measured OH⁻ consumption during carbon regeneration, a series of three experiments (RG6a, RG6b, RG6c) were performed using a single charge of regeneration liquid. One liter sodium hydroxide solution (pH ≈ 11.9) was used to regenerate three carbon beds. The regeneration liquid was not replenished with OH⁻ on the course of the experiments. Compared to the other regenerations, more RDX was hydrolyzed using one liter regeneration liquid.

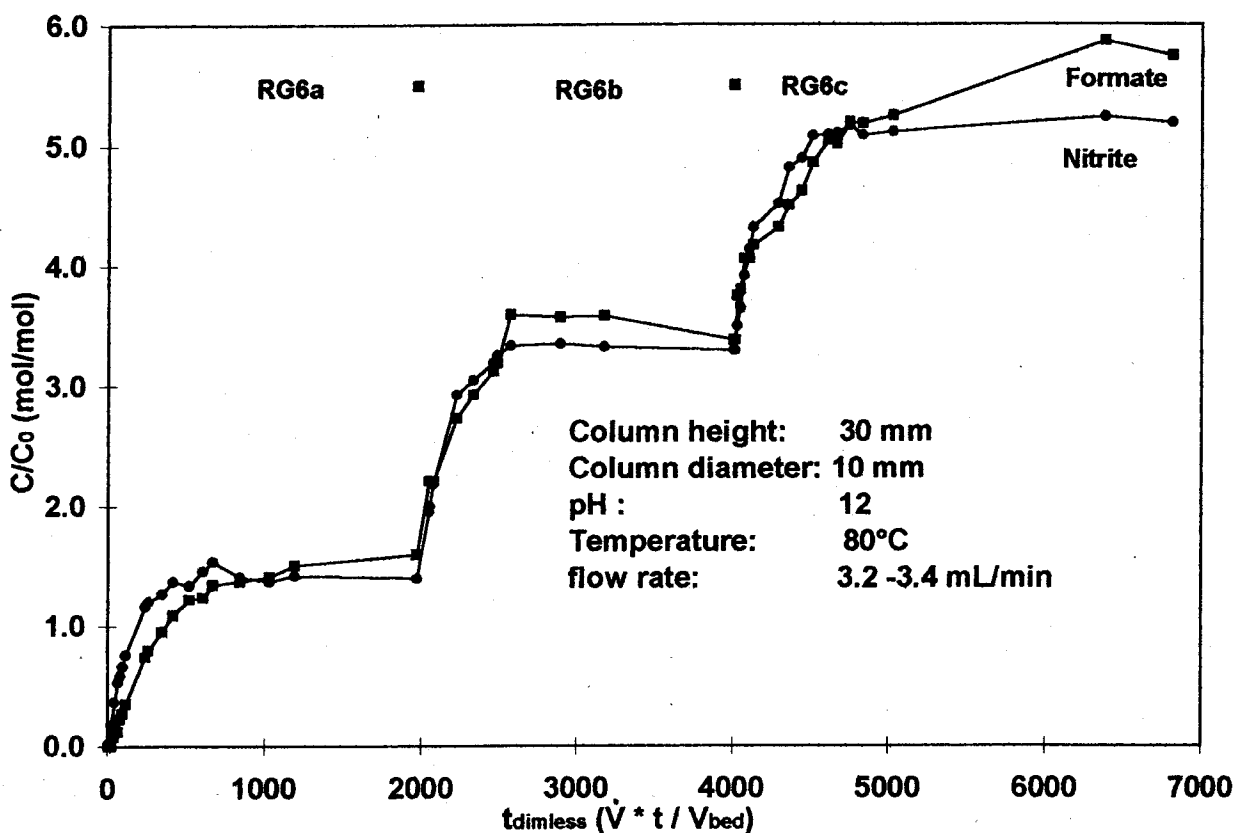


Figure 5.14: Mol End-product/Mol RDX Generated by Alkaline Hydrolysis of Laden Activated Carbon Fixed-Beds. Experiments RG6a, RG6b and RG6c. All regenerations were conducted immediately after the other using one liter regeneration liquid only. The total amount of nitrite and formate in the regeneration liquid is shown in this figure.

Measurement of the OH^- consumption:

The pH was measured before the start of RG6a, throughout the entire experiment, and at the end of experiment RG6c. In order to determine the actual OH^- consumption, the number of OH^- was calculated. The difference between the amount in the end and the beginning is the OH^- consumption:

	pH	mmol OH^-
beginning	11.913	8.18
after RG6c	11.334	2.16
delta		6.0223

Table 5.5pH drop measured: Calculation of the OH^- Consumption in RG6a, RG6b, and RG6c

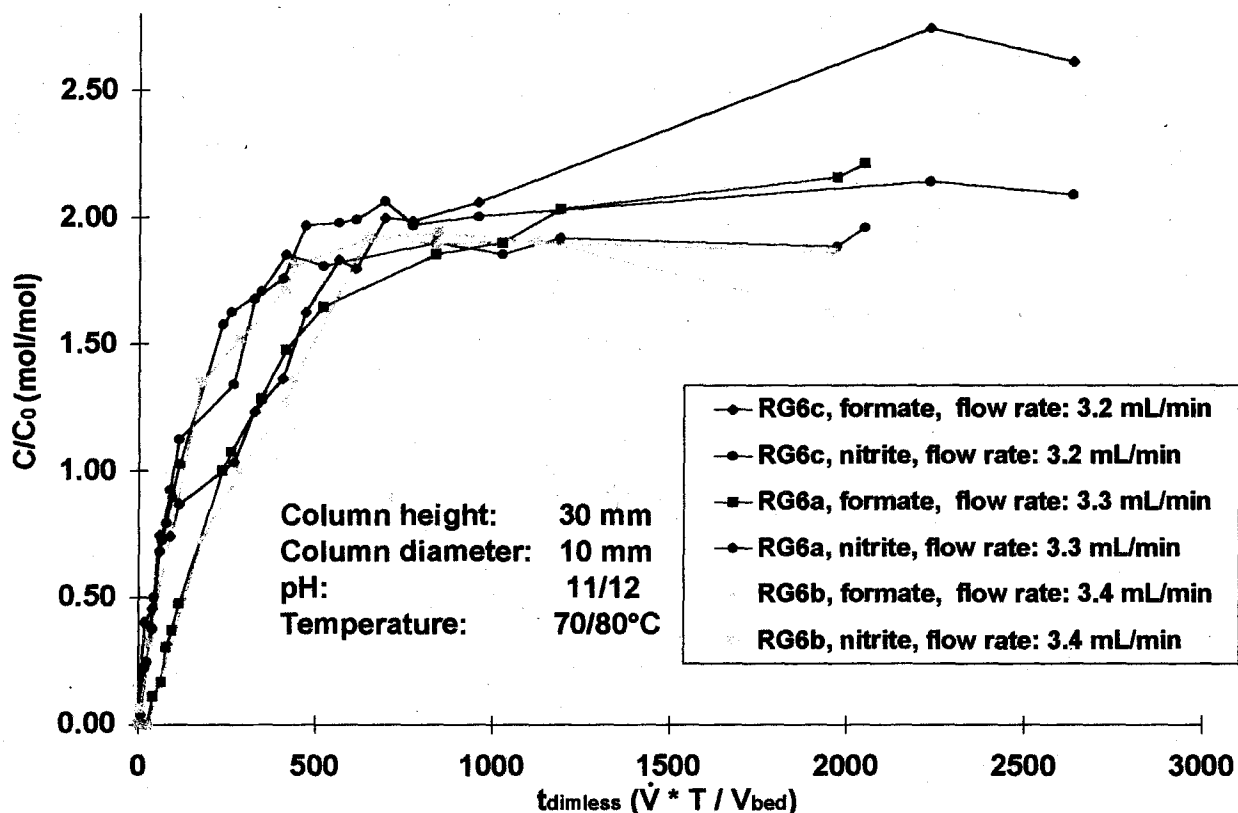


Figure 5.15: Mol End-product/Mol RDX Generated by Alkaline Hydrolysis of Laden Activated Carbon Fixed-Beds. Experiments RG6a, RG6b and RG6c. The nitrite and formate ratios of each regeneration is shown in this figure. The amount of nitrite and formate in the regeneration liquid resulting from earlier regenerations are subtracted in order to present the ratios for experiments RG6b and RG6c.

The measured OH^- consumption during the entire experiment was 6.0223 mmol.

Calculation of the OH^- consumption:

The total amount of RDX adsorbed onto the three activated carbon fixed-beds and hydrolyzed using one liter regeneration liquid was 446 mg, which equals 2.018 mmol.

According to Heilmann (1996), 1.7 mol nitrite (NO_2^-), 1.6 mol formate (HCOO^-), and 0.2 mol acetate (CH_3COO^-) are generated during the hydrolysis of one mol RDX (see Chapter 2.9). To maintain electrostatically, the charge of both sides of any equation must balance. Initially, all the electrons in the system are due to OH^- . Therefore, it is obvious that for each generated anion (NO_2^- , HCOO^- , and CH_3COO^-) one OH^- is used. The amount of anions generated must equal the difference between the OH^- amount at the beginning and the end of the alkaline hydrolysis.

In experiments RG6a, RG6b, and RG6c, more nitrite and formate were generated than expected. Therefore more OH^- was transferred.

Two calculations were made in order to compare the measured and calculated OH⁻ consumption. In calculation a) the ratios 1.7 mol/mol for nitrite and 1.6 mol/mol for formate were used. In calculation b) the measured amount of nitrite and formate generated in these experiments were used. For acetate, the ratio of 0.2 mol/mol were used in both calculations.

	a		b	
molecule generated	amount of molecules generated per mol RDX (mol/mol)*	amount of OH ⁻ needed (mmol)	measured molecules amount (mmol)	amount of OH ⁻ needed (mmol)
nitrite	1.7	3.431	3.976	3.976
formate	1.6	3.229	4.136	4.136
acetate	0.2	0.404	0.2*	0.404
sum		7.064		8.516

*amount of molecules generated per mol RDX (mol/mol), according to Heilmann (1996)

Table 5.6: Calculation of the Expected OH⁻ consumption

The calculated and expected OH⁻ consumption is slightly larger than the measured one:

$$\text{a) } \frac{7.1 \text{ mmol OH}^-}{6.0 \text{ mmol OH}^-} = 1.2 \qquad \text{b) } \frac{8.5 \text{ mmol OH}^-}{6.0 \text{ mmol OH}^-} = 1.4$$

Measured OH ⁻ consumption (mol)	Calculation of the OH ⁻ consumption		Ratios	
	a (mol)	b (mol)	a (mol)	b (mol)
6.0	7.1	8.5	1.2	1.4

Table 5.7: Measured and Calculated OH⁻ Consumption in Regeneration Experiments RG6a, RG6b, and RG6c

The expected OH⁻ consumption is, respectively, 1.1 or 1.4 times of the measured OH⁻ consumption.

5.3.1.6. Comparison of the Regeneration Experiments

In Table 5.8 all regeneration experiments conducted are presented. In this table, the first four columns show the number, the parameters temperature, pH, and the flow rate of the experiments.

In column 5 the time and the bed volumes are shown when a ratio of 1.5 nitrite and formate per RDX in the Erlenmeyer-flask was reached. This time and BV is calculated: the largest ratio smaller than 1.5 and the smallest ratio larger than 1.5 were connected linear to form a straight line. The formula for this straight line was used to calculate the time and BV where the ratio of 1.5 for nitrite and formate was reached.

Column 6 shows the time and BV when the ratio became stable. Column 7 lists the time and BV when the experiments were stopped. Column 8 gives the concentration of nitrite and formate in the Erlenmeyer-flask at the end of the experiments.

The ratios for nitrite and formate at the end the regenerations were usually higher than observed by Heilmann (1996).

The time needed to generate ratios of 1.5 mol/mol for nitrite/RDX was most often less than 4 hours. Nine hours have been sufficient in most of the regenerations to generate a ratio of 1.5 mol/mol for formate/RDX. It also took longer for the formate ratio to become stable than it took for nitrite.

The flow rate did not have any marked influence on the velocity of the hydrolysis. If either the pH or the temperature was reduced to 11 or 70°C, respectively, or both, the ratios for both nitrite and formate was significantly lower than usual.

1	2	3	4	5				6				7		8		
				mol/mol ratio = 1.5				stable				Experiment stopped			final concentration	
				Nitrite		Formate		Nitrite		Formate		t	BV		Ni- trite	For- mate
t	BV	t	BV	t	BV	t	BV	t	BV							
RG1b	12	80	3.9	362	251	631	448	390	277	2800	1986	2790	2121	1.65	2.04	
2b	12	80	8.0	3259	2311	724	514	1380	2009	1380	2009	5760	8384	1.73	1.81	
3a	12	80	8.8	169	120	403	286	236	881	636	2373	3060	11418	1.66	1.83	
3b	12	80	8.5	911	67	221	157	580	2092	580	2092	2500	9019	1.95	2.17	
4a	12	80	5.2	202	143	427	303	539	1190	1398	3085	2851	6292	1.78	1.99	
4b	12	80	5.7	198	141	526	373	233	571	1342	3286	2791	6835	1.82	2.00	
5a	11	80	3.8									2778	4480	1.13	0.26	
5b	12	70	3.9			2778	1971	931	1529	2889	4745	5915	9716	1.10	1.64	
5c	11	70	3.7					1385	2193	4330	6855	5910	9356	0.77	0.05	
6a	12	80	3.3	152	108	296	210	287	414	825	1191	1419	2048	1.96	2.21	
6b	12	80	3.4	189	134	341	242	449	648	449	648	1358	1960	1.86	1.63	
6c	12	80	3.2	218	154	304	216	347	471	1645	2234	1943	2639	2.08	2.61	

Table 5.8: Data of the Conducted Regeneration Experiments (see explanation in text section)

5.3.2. Discussion

5.3.2.1. Errors

The sources of errors in these experiments are discussed in this section. No experiments have been performed to verify the source of errors. The following discussion is provided for those who may wish to continue this research, or make their own interpretations of the results.

The flow rate may have changed during an experiment due to a changing RPM of the pump and a plugging of screens and tubes. After changing the screens (see Chapter 5.2.2.1), the flow rate became significantly more stable. The slightly unstable flow rate that remained after changing the screens can be neglected because the flow rate in general did not have an detectable influence on the hydrolysis.

The water used to prepare the eluent for the IC (millipore water) had changing quality. Therefore, the base line changed and new standards had to be developed. Even though the error can not be neglected when small concentrations were measured. It may be greater than 20% when concentrations lower than 40 mg/L nitrite or formate were analyzed. The error was less than 10% for concentrations greater than 40 mg/L nitrite or formate. This is the concentration that was usually reached at the end of the experiments and therefore the most important concentration. However, this is the major source of error in the regeneration experiments.

The pH of the regeneration liquid was not exactly the same as the pH which was used to develop the IC standards, even though standards for pH 10, 11, and 12 were developed. This influenced the accuracy of the nitrite and formate measurement. Since the OH⁻ consumption and therefore the pH-drop was small during all experiments except of experiments RG5a, RG5c, RG6a, RG6b, and RG6c, the error was less then 10% for all other experiments. With the mentioned experiments either the initial pH was lowered down to 11, or the hydrolyzed amount of RDX was relatively great. Therefore, the pH-drop was larger and the error might be up to 30%.

The samples had to be diluted if the concentration of nitrite exceeded 50 mg/L. This was a minor error because accurate pipetts were used to prepare the dilution.

5.3.2.2. Findings

A nitrite/RDX (mol/mol) ratio of 1.6 and a formate/RDX (mol/mol) ratio of 1.7, or greater, were generated when a pH of 12 and a temperature of 80°C was used. Smaller ratios were generated when the pH and/or the temperature was reduced. This indicates that the alkaline hydrolysis will hydrolyze all RDX if pH 12 and T=80°C is used only, or an even higher pH and/or higher temperatures.

The ratios for both nitrite/RDX and formate/RDX usually exceeded the ratios Heilmann (1996) found in his research. This might be due to a higher HMX concentration on the activated carbon after adsorption. The HMX was hydrolyzed during the regeneration, generating additional nitrite and formate. The higher ratios might also be due to general experimental errors.

The generation of nitrite was very fast when pH 12 and $T=80^{\circ}\text{C}$ was used. At most of the experiments it took less than four hours to reach a nitrite/RDX ratio of 1.5 mol/mol.

The generation of formate was slower. Nevertheless, in most of the experiments it took less than 9 hours to generate a formate/RDX ratio of 1.5 mol/mol or more.

It may be sufficient to flush the columns for only four hours. Since nitrite is the first product hydrolyzed (see Chapter 2.9), a ratio of 1.6 mol nitrite/mol RDX proves that the RDX molecule itself is destroyed. It may also be desorbed from the activated carbon and all side products may be soluted in the regeneration liquid. The column may be used for the treatment of a new charge of RDX-laden water after four hours of regeneration. Further steps of the RDX hydrolysis, which lead to the harmless products such as nitrite and formate from the intermediate products, than happens in the Erlenmeyer-flask if the parameters are sufficient.

The significantly high ratio of nitrite/RDX and formate/RDX at experiment RG6c is most probably due to the regeneration RG5c. Regeneration RG5c, which was conducted in the same column directly before the adsorption/regeneration cycle number 6, did not generate the ratios as in most of the other regenerations. Some RDX might still have been adsorbed onto the activated carbon. This RDX was hydrolyzed in experiment RG6c, which leads to a higher ratio of nitrite/RDX and formate/RDX. The same might have occurred at RG6a and RG6b.

In the range between 3.2 and 8.8 mL/min the flow rate does not have a significant influence to the velocity or the quality of the hydrolysis. There might be an influence if the flow rate is smaller than 3.2 mL/min.

It was found in the adsorption experiments that the RDX adsorption capacity decreased with each adsorption/regeneration cycle. This might be due to the TOC adsorption onto the activated carbon. The large volume of RDX solution flushed through the fixed-beds lead to an adsorption of a significant amount of TOC. Approximately 1 mg TOC per liter RDX solution was adsorbed onto the carbon. The calculated TOC concentration in the regeneration liquid is approximately the three fold of the amount of TOC actually measured in the regeneration liquid. This is obviously a mistake. It can not be said whether the adsorbed TOC is desorbed during the regeneration or not. Therefore, it is unknown if the adsorbed TOC had an influence to the decreasing activated carbon adsorptive capacity.

Nevertheless, the activated carbon surface area decreased approximately 15% with 5 adsorption/ regeneration cycles. This indicates that either compounds such as TOC still adsorb onto the surface even after regeneration or that pores are plugged inside the activated carbon particles.

5.4. Additional Experiments

5.4.1. Results

5.4.1.1. Total Organic Carbon

Adsorbed total organic carbon (TOC) limits the RDX-adsorption capacity of activated carbon fixed-beds. In order to determine the amount of TOC adsorbed onto the carbon during an adsorption experiment, DI-water (without RDX) was flushed through the columns. The same DI-water was used to prepare the RDX-solution. Influent and effluent was analyzed for TOC.

During alkaline hydrolysis, the adsorbed TOC may desorb. Therefore, TOC was measured in the regeneration liquid after the regeneration experiments RG6a, RG6b, and RG6c. The data are presented in Table 5.9.

analysis of TOC in	mg TOC/g or mg TOC/L
DI-water	1.82
DI-water filtered using activated carbon fixed-beds	0.89
regeneration liquid after regenerations RG6a, RG6b, and RG6c	39.76

Table 5.9: TOC Data of Adsorption/Regeneration Cycle Number 6

0.93 mg TOC/L was adsorbed onto the activated carbon when DI-water was flushed through the fixed-beds. In experiments FB6a, FB6b, and FB6c, 67.44 L RDX-solution was flushed through the columns. The solution was prepared using DI-water (see Chapter 3.2.4). Therefore, 32.46 mg TOC/L was adsorbed onto the activated carbon after the three adsorptions experiments.

Before regeneration experiment RG6a was started, the initial TOC concentration in the regeneration liquid was 1.82 mg/L, because DI-water was used for its preparation. After RG6c, the TOC concentration was measured to be 39.76 mg/L.

A second source of TOC in the regeneration liquid are the end-products of the RDX hydrolysis (formate, acetate, and formaldehyde). The amount of TOC which is generated due to the RDX hydrolysis can be calculated using the mass balance presented in Chapter 2.9.

Endproduct of RDX hydrolysis	endproduct/RDX generated in the hydrolysis	carbon portion in endproduct	amount of end-product generated	carbon portion in endproduct
	(mol/mol)	(%)	(mg)	(mg)
HCOO ⁻	1.5	0.27	200	57.2
CH ₃ COO ⁻	0.2	0.41	26.7	11.1
HCHO	1.1	0.4	145	58.0
sum				122.3

Table 5.10: Calculation of the TOC Amount in the Regeneration Liquid due to the RDX Hydrolysis After Regeneration Experiments RG6a, RG6b, and RG6c.

According to this calculation, approximately three times of the measured TOC amount should be observed in the regeneration liquid.

5.4.1.2. Multipoint BET-Surface Area

The activated carbon surface area of both, the virgin carbon and of the carbon used for 5 adsorptions/regenerations is known through the product informations from Calgon Cooperation and the analysis conducted using a Gemini 2360 surface area analyzer, respectively, and shown in Table 5.11.

carbon	surface area (m ² /g)
virgin	950-1050
regenerated carbon	850

Table 5.11: Multipoint BET-surface area of Virgin and Regenerated Carbon

The surface area increases by approximately 15% due to the 5 adsorption/regeneration cycles.

5.4.2. Discussion

5.4.2.1. Errors

The TOC measured in the regeneration liquid after regeneration experiments RG6a, RG6b, and RG6c, is less than expected after calculating the mass balance. Evidently, these data are wrong. This may either be due to sampling error or the TOC analysis.

5.4.2.2. Findings

Total Organic Carbon

It was found in the adsorption experiments that the RDX adsorption capacity decreased with each adsorption/regeneration cycle. This might be due to the TOC adsorption onto the activated carbon. The large volume of RDX solution flushed through the fixed-beds led to an adsorption of a significant amount of TOC. Approximately 1 mg TOC per liter RDX solution was adsorbed onto the carbon.

The calculated TOC concentration in the regeneration liquid is approximately the threefold of the amount of TOC actually measured in the regeneration liquid. It can not be said whether the adsorbed TOC is desorbed during the regeneration or not because these results must be with error. Therefore, it is unknown whether the adsorbed TOC had an influence to the decreasing activated carbon adsorptive capacity or not.

BET-surface area measurements

Measurements done by Heilmann (1996) show that alkaline hydrolysis does not alter the surface area of virgin carbon. Therefore, the effect of the alkaline hydrolysis to laden carbon is due to desorption of previous adsorbed species only (see Chapter 3.3.4). This indicates, that a decreasing of the surface area during the adsorption/regeneration cycles is due to the adsorption of species which are not desorbed during the regeneration.

RDX could not be detected on regenerated activated carbon in Heilmann's (1996) study. In the present study, it was proved that all adsorbed RDX was hydrolysed and desorbed during the regeneration, using the indicators nitrite and formate. Therefore, other species, such as TOC, seem to adsorb onto the activated carbon without being desorbed by regeneration. This confirms the earlier described findings of decreasing RDX adsorption capacity with each adsorption/ regeneration cycle.

6. Conclusions

In this thesis experiments were conducted to investigate the RDX adsorption kinetics onto granular activated carbon. The objective of these experiments were to prove the feasibility of RDX adsorption onto activated carbon fixed-beds and regeneration of RDX-laden fixed-beds using alkaline hydrolysis. In all experiments the activated carbon Filtrasorb-400 was used. Columns with a height of 30 or 70 mm, respectively, and a diameter of 10 mm were used for the adsorption and regeneration experiments. Small columns were used to minimize the RDX mass needed.

The results indicate:

1. A surface diffusion coefficient D_s for RDX contaminated water adsorption onto granular activated carbon (F-400) of $9.11 \cdot 10^{-10} \text{ cm}^2/\text{s}$ was found. This number is very close to the earlier findings of Heilmann (1996). The standard deviation is $s=0.04$. According to Hand *et al.*'s criteria, this is a good to excellent model fit.
2. RDX-laden wastewater can successfully be treated using activated carbon fixed-beds.
 - Higher flow rates led to steeper slopes of the breakthrough curve.
 - The 30 mm tall columns were able to reduce RDX to the detection limit at flow rates of 0.6 mL/min for 364 bed volumes (dimensionless time units). The longest period in which no RDX could be measured in the beginning of an adsorption was 851 bed volumes when a virgin 70 mm tall column was used at a flow rate of 3.9 mL/min.
 - Regeneration only partially restored the adsorbent capacity of the columns. The activated carbon fixed-bed capacity to adsorb RDX dropped with each adsorption/regeneration step.
 - The TOC adsorbed onto the carbon was desorbed during the alkaline hydrolysis.
3. Regeneration of RDX-laden fixed-beds using alkaline hydrolysis is feasible at pH 12 and $T=80^\circ\text{C}$.
 - Complete regeneration was not achieved below pH 12 and $T=80^\circ\text{C}$.
 - Nitrite and formate were produced in molar rates of 1.7 and 1.6, respectively, which agrees well with previous aqueous homogeneous and batch regeneration experiments conducted by Heilmann (1996). In some cases these ratios were exceeded.
 - The generation of nitrite was much faster than the generation of formate. This indicates that the formation of nitrite is due to the first reaction step when nitrite is split off the RDX molecule. Formate is generated during both the mineralization of RDX h5 and the Cannizzaro reaction. This mechanism is consistent with Heilmann's (1996) proposed reaction mechanism.

- In the range between 3.2 and 8.8 mL/min the flow rate did not have significant influence on the reaction rate or the hydrolysis endpoint.
- The OH⁻ consumption during regeneration was measured. Additionally, the OH⁻ needed for the generation of nitrite, formate, and acetate during the regeneration was calculated. Both, the mol/mol ratios found by Heilmann (1996) and verified in this study and the amount of nitrite and formate detected in the regeneration liquid after the regeneration was used for the calculations.

The measured and calculated OH⁻ consumption meet within the experimental error. The calculated OH⁻ consumption is 1.2 times the measured consumption when Heilmann's (1996) ratios are used, and 1.4 times when the generated nitrite and formate is used for the calculation. Therefore, the amount of OH⁻ needed to balance the pH during a regeneration can be calculated.

It should be the objective of future research to determine the reason for decreasing RDX adsorption capacity of activated carbon fixed-beds with each adsorption/regeneration process. The decrease may be due to

- closed micropores which lead to a smaller surface area of the activated carbon
- adsorbed TOC which is not associated with RDX and HMX onto the activated carbon
- adsorbed by-products (e.g. formate, acetate) onto the activated carbon
- other adsorbed compounds onto the activated carbon

The regeneration may be improved through future research to develop additional procedures that restore the column capacity. The mentioned potential reasons for the decreasing adsorption capacity should be verified. In order to increase the available surface area, the regenerated carbon may be rinsed using hot water at a low pH of 3 or 4, thereby improving the regeneration.

Even though the carbon is not completely restored to its original capacity, the developed process is more favorable than existing technologies, which stockpile the waste HE-laden carbon.

7. Zusammenfassung

In der vorliegenden Arbeit sind Experimente zur Adsorptionskinetik von RDX auf granuliertem Aktivkoks beschrieben. Es war nachzuweisen, daß RDX auf Aktivkoks-Rohradsorbern adsorbiert werden kann und beladene Adsorber durch alkalische Hydrolyse regeneriert werden können. Alle Experimente wurden mit Filtrasorb-400 durchgeführt. Das Festbett der verwendeten Rohradsorber hatte einen Durchmesser von 10 mm und eine Länge von 30 bzw. 70 mm. Die kleineren Adsorber wurden verwendet, um den Verbrauch an RDX zu minimieren.

Ergebnisse der Untersuchungen sind:

1. Der Oberflächen-Diffusionskoeffizient D_s für die Adsorption von RDX-kontaminiertem Wasser auf granuliertem Aktivkoks (F-400) beträgt $9,11 \cdot 10^{-10} \text{ cm}^2/\text{s}$. Dieser Wert stimmt mit dem von Heilmann (1996) gefundenen Wert sehr gut überein. Die Standardabweichung von $s=0,04$ entspricht nach Hand *et al.* (1983) einer guten bis exzellenten Modellierung.
2. RDX-kontaminiertes Wasser kann mit Aktivkoks-Rohradsorbern gereinigt werden.
 - Mit steigenden Durchflußraten ergeben sich steilere Durchbruchkurven.
 - Bei Verwendung von einem 30 mm langen Rohradsorber und einem Durchfluß von 0,6 ml/min konnte RDX-kontaminiertes Wasser für 364 Leerbettverweilzeiten bis zur Nachweisgrenze gereinigt werden. Mit einem bislang unbenutztem 70 mm Rohradsorber und einem Durchfluß von 3,9 ml/min wurde eine Reinigung bis zur Nachweisgrenze für 851 Leerbettverweilzeiten erreicht.
 - Die untersuchte Regeneration führt nur zu einer teilweisen Wiederherstellung der ursprünglichen Adsorptionskapazität der Rohradsorber. Mit jeder Adsorptions-/Regenerationsstufe verringert sich deren Adsorptionskapazität.
 - Der auf dem Aktivkoks adsorbierte Gesamtkohlenstoff (TOC) wird bei der alkalischen Hydrolyse desorbiert.
3. Die Regeneration von RDX-beladenen Aktivkoks-Rohradsorbern kann mit alkalischer Hydrolyse durchgeführt werden.
 - Eine vollständige Regeneration wird bei einem pH unter 12 oder einer Temperatur unter 80°C nicht erreicht.
 - Nitrit und Formiat werden in Molverhältnissen von 1,7 bzw. 1,6 gebildet. Diese Ergebnisse stimmen mit den Ergebnissen aus Batchversuchen von Heilmann (1996) sehr gut überein. Teilweise werden die genannten Molverhältnisse überschritten.
 - Nitrit wird deutlich schneller gebildet als Formiat. Dies indiziert, daß die Bildung von Nitrit im ersten Reaktionsschritt der Hydrolyse, der Abspaltung des Nitritmoleküls von dem RDX-Molekül, stattfindet. Formiat wird sowohl durch die Mineralisierung von RDX h5, als auch durch die Cannizzaro Reaktion gebildet. Dieser Mechanismus stimmt mit dem von Heilmann (1996) angegebenen Mechanismus überein.

- Im Bereich zwischen 3,2 und 8,8 ml/min hat die Durchflußgeschwindigkeit keinen erkennbaren Einfluß auf die Reaktionsgeschwindigkeit oder den Endpunkt der Hydrolyse.
- Der Verbrauch von OH⁻-Ionen während der Regeneration wurde gemessen. Zusätzlich wurde berechnet, wieviele OH⁻-Ionen zur Bildung der Nitrit-, Formiat- und Acetat-Ionen benötigt wurden. Für diese Berechnung wurden sowohl die von Heilmann (1996) gefundenen und in dieser Arbeit bestätigten Molverhältnisse, als auch die Menge an Nitrit und Formiat, die in dem Regenerationsflüssigkeit am Ende der Regeneration gemessen wurde, verwendet.

Der gemessene OH⁻-Verbrauch unterscheidet sich von dem berechneten nur im Bereich der Meßungenauigkeiten. Auf der Grundlage der Molverhältnisse von Heilmann (1996) liegt der berechnete OH⁻-Verbrauch um das 1,2-fache über dem gemessenen Verbrauch. Werden die gemessenen Nitrit- und Formiatmengen verwendet, liegt die Abweichung bei Faktor 1,4. Die Menge von OH⁻-Ionen, die benötigt wird, um bei einer Regeneration den pH-Wert konstant zu halten, kann demgemäß berechnet werden.

Zukünftige Forschungen sollten Aufschluß geben darüber, warum die RDX-Adsorptionskapazität von Aktivkoks-Rohradsorbern mit jedem Adsorptions-/Regenerationsschritt geringer wird. Die geringere Adsorptionskapazität könnte bedingt sein durch:

- geschlossene Mikroporen, die zu einer geringeren Oberfläche des Aktivkoks führen,
- neben RDX und HMX auf dem Aktivkoks adsorbiertem TOC,
- auf dem Aktivkoks adsorbierte Nebenprodukte wie Formiat und Acetat und
- weitere auf dem Aktivkoks adsorbierte Stoffe.

Die Wiederherstellung der Rohradsorberkapazität kann durch die Entwicklung von zusätzlichen Regenerationstechniken verbessert werden. Die angeführten möglichen Gründe für die absinkende Adsorptionsfähigkeit der Rohradsorber sollten überprüft werden. Die zur Verfügung stehende Oberfläche von regeneriertem Aktivkoks könnte durch Spülung mit heißem Wasser bei pH 3 bis 4 erhöht werden. Dies würde zu einer vollständigeren Regeneration führen.

Die untersuchte Regeneration der beladenen Aktivkoks-Rohradsorber führt nicht zur ursprünglichen Adsorptionskapazität. Dennoch stellt der untersuchte Prozeß eine gute Alternative zu den existierenden Techniken dar, die erhebliche Mengen von mit Hochexplosivstoffen kontaminierten Aktivkoksabfällen produzieren.

Appendix I: References

- Almada, M.D.; Flory, G. (1993): End of Cold War Sprawns Flurry of Demilitarization Activities. The Radioactive Exchange. A Daily Conference News Bulletin. In: *Incineration '93*. Washington, D.C., 1993, p 1
- Andern, R.K.; Nystron, J.M.; McDonell, R.P.; Stevens, B.W. (1975): Explosives Removal From Munitions Wastewater. Proceedings of the 30th Industrial Waste Conference. p. 816-825
- Beccari, B.; Paolini, A.E.; Variali, G. (1977): Chemical Regeneration of Granular Activated Carbon. In: *Effluent and Water Treatment Journal*. 6/1977, p. 289-294
- Chiang, P.C.; Wu, J.S. (1989): Evaluation of Chemical and Thermal Regeneration of Activated Carbon. In: *Water Science and Technology*, Vol. 21, Brighton, 1989
- Dobratz, B.M. (1981): LLNL Explosives Handbook. Properties of Chemical Explosives Simultans. U.S. Department of Commerce. Nation Technical Information Service. Springfield, IL 1981
- Entsorga Magazin (1991): Tödliche Gefahr aus der Tiefe. In *Entsorga Magazin Entsorgungswirtschaft*, 9-91, p.181-184
- EPA (1986): Mobile Treatment Technoligies for Superfund Wastes. EPA/540/2-86/003 (f), U.S. Environmental Protection Agency. Waschington, D.C., 1986
- EPA (1991): Granular Activated Carbon Treatment. In: *Engineering Bulletin*. EPA/540/2-91/024, U.S. Environmental Protection Agency. Washington, D.C., October 1991
- Gibbs, T.R.; Popolato, A.; Eds. (1980): *LASL Explosive Property Data*. Universtiy of California Press: Berkeley, California
- Hand, D.W. (1982): User-Oriented Batch Solutions to the Homogeneous Surface Diffusion Model for Adsorption Processes Design Calculations: Batch Reactor Solutions. A Thesis Submittet in partial fulfillment of the requirements for the degree of Master of Sience in Civil Engineering, Michigan Technological University, 1982
- Hand, D.W.; Crittenden, J.C.; Asce, M.; Thacker, W.E. (1983): User-Oriented Batch Solutions to the Homogeneous Surface Diffusion Model. In: *Journal of Environmental Engineering*, Vol. 109, No.1, 1983, p.82-101
- Heilmann, H.M.; Stenstrom, M.K.; Hesselmann, R.X.P.; Wiesmann, U. (1994): Kinetics of the aqueous alkaline homogeneous hydrolysis of high explosives 1,3,5,7-tetraaza-1,3,5,7-tetranitrocyclooctane (HMX). In *Water Science and Technology*, Vol 30, No. 3 (1994), p. 53-61

- Heilmann, H.M. (1996): Physico-Chemical Treatment of Water Contaminated with the High Explosives RDX and HMX Using Activated Carbon Adsorption and Alkaline Hydrolysis. Doctor Thesis, Technical University of Berlin, 1996
- Heilmann, M.H.; Wiesmann, U.; Stenstrom, M.K. (1996a): Kinetics of the Alkaline Hydrolysis of High Explosives RDX and HMX in Aqueous Solution and Adsorbed to Activated Carbon. In *Environmental Science & Technology*, (in print)
- Hoffsommer, J.C.; Kubose, D.A.; Glover, D.J. (1977): Kinetic Isotope Effects and Intermediate Formation for the Aqueous Alkaline Homogeneous Hydrolysis of Hexahydro-1,3,5-tetranitro-1,3,5-triazine (RDX). In: *The Journal of Physical Chemistry*, Vol.81, No 5. 1977, p. 380-385
- Hutchinson, D.H.; Robinson, C.W. (1990): A Microbial Regeneration Process for Granular Activated Carbon I. Process Modelling. In: *Water Research*. Vol 24, No 10. 1990, p.1209-1214
- Jekel, M. (1992): Script zur Vorlesung Wasserreinigung II, Berlin 1992
- Johnson, Mc D.B.; Bacon, D.P. (1990): Developing a Testing System for Characterizing Emissions Produced During Open Burning/Open Detonation of Energetic Materials. U.S. Army Dugway Proving Ground. Dugway, 1990
- Linsley, R.K.; Kohler, M.A.; Paulhus, J.L.H. (1982): *Hydrology for Engineers* (3rd ed.), New York: McGraw-Hill Book Company, 1982.
- Martin, R.J.; Ng, W.J. (1985): Chemical Regeneration of Exhausted Activated Carbon-II. In: *Water Research*. Vol.19, No 12, 1985, p.1527-1535
- Masschelein, W.J. (1992): *Unit Processes in Drinking Water Treatment*, New York, 1992
- McCormick, N.G., Cornell, J.H., and Kaplan, A.M. (1981): Biodegradation of Hexahydro-1,3,5-Trinitro-1,3,5-Triazine. In: *Applied and Environmental Microbiology*, p. 949-958
- McLellan, W.; Hartley, W.R.; Brower, M. (1988): Health Adversory for Hexahydro-1,3,5-tetranitro-1,3,5-triazine. Technical Report No. PB90-273533; Office of Drinking Water, U.S. Environmental Protection Agency. Washington, D.C. 1988
- Metcalf and Eddy, Inc. (1991): *Wastewater Engineering, Treatment, Disposal, and Reuse* (3rd ed.). Revised by George Tchobanoglous and Franklin L. Burton. New York, 1991.
- Narbaiz, R.M.; Cen, J. (1994): Electrochemical Regeneration of Granular Activated Carbon. In: *Water Research*. Vol 28, No 8., 1994, p. 1771-1778
- Newcombe, G.; Drikas, M. (1993): Echemical Regeneration of Granular Activated Carbon from an Operating Water Treatment Plant. In: *Water Research*. Vol. 27, No 1., 1993, p.161-165

- Normann, S. (1987): Sorptionsverfahren. In: *DVGW-Schriftenreihe*, Wasser Nr. 206. DVGW-Fortbildungskurse. Wasserversorgungstechnik für Ingenieure und Naturwissenschaftler, Kurs 6: Wasseraufbereitungstechnik für Ingenieure, 3. Auflage. Eschborn, 1987
- Patterson, J; Shapira, N.I.; Brown, J. (1976): Pollution Abatement in the Military Explosives Industry. *Proceedings of the 31st Purdue Industrial Waste Conference*, Purdue University, West Lafayette, Indiana, p.385-394
- Ro, K.S. and Stenstrom, M.K. (1990): Aerobic Biological Degradation of RDX. In: *Progress Report No. 1, University of California Los Angeles, Civil and Environmental Engineering Department, 1990*
- Rosenblatt, D.H.; Burrows, E.P.; Mitchell, W.R.; Parmer, D.C. (1991): Organic Explosives and Related Compounds, *The Handbook of Environmental Chemistry*, Vol 3, Part 3. Berlin: Springer Verlag, 1991.
- Sontheimer, H.; Crittenden, J.C.; Summers, R.S. (1988): *Activated Carbon for Wastewater Treatment* (2nd ed.). Karlsruhe: Engler-Bunte Institut, 1988
- Spitzer, P; Gosse, I; Radke, K.H. (1993): *Adsorption und Hydrolyse von Methylparathion an Aktivkohle und Adsorberharz*. *Acta Hydrochimica et Hydrobiologica*. 21, No. 5. 1993, p.267-272
- Urbanski, T. (1977): *Chemistry and Technology of Explosives*. Programon Press, Oxford, p. 13-77
- Voice, T.C. (1989): Activated-Carbon Adsorption. In: *Standard Handbook of Hazardous Waste Treatment and Disposal*. New York: McGraw-Hill Book Company, 1989
- Wiesmann, U. (1992): Abwasserreinigung I, Script zur Vorlesung, Berlin, 1992
- Wiesmann, U. (1994): Bioverfahrenstechnik. Script zur Vorlesung. Berlin 1994
- Wiesmann, U. (1994a): Weiterführende Abwasserreinigung und Brauchwasseraufbereitung II. Script zur Vorlesung; Berlin 1994
- Wilkie, J. (1994): Biological Degradation of RDX. Masters Thesis, Chemical Engineering Department, UCLA, CA
- Wujcik, W.J.; Lowe, W.L.; Marks, P.J.; Sisk, W.E. (1992): Granular Activated Carbon Pilot Treatment Studies for Explosives Removal from Contaminated Groundwater. In: *Environmental Progress*, Vol.11, No.3, 1992, p178-189

Appendix II: Table of Abbreviations

AC	Activated carbon
beds fed	Dimensionless time for fixed-beds
BET-surface area	Internal surface, according to the adsorption theory of Brunauer, Emmett, and Teller
BV	Bed-volumns
CMBR	Completely-mixed batch reactor
DI-Water	Deionized water
DOD	U.S. Department of Defence
DOE	U.S. Department of Energy
EBCT	Empty bed contact time
F-400	Filtrisorb-400
FB	Fixed-bed
GAC	Granular activated carbon
HE	High explosives
HMX	Octahydro-1,3,5,7-Tetranitro-1,3,5,7-Tetrazocine, CAS 2691-41-0
HPLC	High Performance Liquid Chromatograph
HSDM	Homogeneous Surface Diffusion Model
IC	Ion Chromatograph
I.D.	Inner diameter
INF	Intermediate-Range Nuclear Forces Treaty
M	Mol
PAC	Powdered activated carbon
RDX	Hexahydro-1,3,5-Trinitro-1,3,5-Triazine (RDX), $C_3H_6N_6O_6$, CAS 121-82-4, Research Department, Royal Detonation, or Rapid Detonation Explosive
RPM	Revolutions per minute
START	Strategic Arms Reduction Treaties
TNT	2,4,6-trinitrotoluene
TOC	Total organic Carbon
UCLA	University of California Los Angeles
UV	Ultraviolet
w/w	Weight per weight

Chemical Abbreviations

CH_2O	Formaldehyde
CH_3COO^-	Acetate
CHOO^-	Formate
H_2	Hydrogen
H_3PO_4	Phosphoric acid
N_2	Nitrogen
NaHCO_3	Sodiumbicarbonate
Na_2CO_3	Sodiumcarbonate
NaOH	Sodiumhydroxide
N_2O	Nitrous Oxide
NH_3	Ammonia
NO_2^-	Nitrite
OH^-	Hydroxide-ion
ZnCl_2	Zinc Chlorine

Appendix III: Table of Tables:

Table 2.1	Typical Values for Granular Activated Carbon Adsorber Parameters
Table 2.2	Carbon and Nitrogen Mass Balance for the Hydrolysis of RDX
Table 3.1	Filtrisorb-400 Qualitys
Table 3.2	Results of the BET-Surface Area Measurements of Activated Carbon
Table 5.2	Data Analysis for the Kinetic of RDX Adsorption onto Activated Carbon (F-400), Conducted in order to Develop the Best Fit D_s
Table 5.3	List of Fixed-Bed Adsorption Experiments
Table 5.4	List of Fixed-Bed Regeneration Experiments
Table 5.5	Calculation of the OH^- Consumption in RG6a, RG6b, and RG6c
Table 5.6	Calculation of the Expected OH^- consumption
Table 5.7	Measured and Calculated OH^- Consumption in Regeneration Experiments RG6a, RG6b, and RG6c
Table 5.8	Data of the Conducted Regeneration Experiments
Table 5.9	TOC Data of Adsorption/Regeneration Cycle Number 6
Table 5.10	Calculation of the TOC Amount in the Regeneration Liquid due to the RDX Hydrolysis After Regeneration Experiments RG6a, RG6b, and RG6c.
Table 5.11	Surface area of Virgin and Regenerated Carbon
Appendix V	Fixed-Bed Adsorption Experiments Fixed-Bed Regeneration Experiments Fixed-Bed Kinetic Experiments

Appendix IV: Table of Figures:

Figure 2.1	Principle of Adsorption and Absorption
Figure 2.2	Concentration Profiles for a Single Particle Assuming no Internal Mass Transfer Resistance
Figure 2.3	Concentration Profiles According to the Film-Surface Diffusion Model
Figure 2.4	Principle of Surface Diffusion
Figure 2.5	Move of the Laden Area or Mass Transfer Zone of a Activated Carbon Fixed-Bed
Figure 2.6	Breakthrough Profile (Schematic) of Activated Carbon Filters
Figure 2.7	Loose of a Proton and a Nitrite as Supposed by Hoffsommer <i>et al.</i> (1977) and Heilmann (1996) and the Following Hydrolysis of RDX-h5
Figure 3.1	Hexahydro-1,3,5-Trinitro-1,3,5-Triazine (RDX), $C_3H_6N_6O_6$, CAS 121-82-4
Figure 3.2	Activated Carbon Fixed-Bed Adsorption Experiment, Experimental Setup
Figure 3.3	Activated Carbon Fixed-Bed Regeneration Experiment, Experimental Setup
Figure 4.1	Mechanisms and Assumptions that are Incorporated in the Homogeneous Surface Diffusion Model (after Hand <i>et al.</i> , 1983)
Figure 5.1	RDX Concentration in the Solution During the Kinetic Batch Experiment at Defined Elapsed Times
Figure 5.1	Comparison of Kinetic Experiments with Different Stirrer Experiments
Figure 5.2	Batch Rate Data and Model Calculations for the Adsorption of RDX Diluted in DI-Water onto Activated Carbon
Figure 5.3	Breakthrough Curves for Adsorption of RDX in Continuous Flow Activated Carbon Fixed-Beds, Experiments FB1b and FB2b
Figure 5.4	Breakthrough Curves for Adsorption of RDX in Continuous Flow Activated Carbon Fixed-Beds, Experiments BF2a, FB3b, and FB5c

- Figure 5.5** Breakthrough Curves for Adsorption of RDX in Continuous Flow Activated Carbon Fixed-Beds, Experiments FB5a, FB5b, FB4a, FB4b and FB5c
- Figure 5.6** Breakthrough Curves for Adsorption of RDX in Continuous Flow Activated Carbon Fixed-Beds, Experiments FB6b, FB6a, FB6c, FB3a and FB3b
- Figure 5.7** Breakthrough Curves for Adsorption of RDX in Continuous Flow Activated Carbon Fixed-Beds, Experiments FB5a, FB5b, and FB5c
- Figure 5.8** Mol End Product/Mol RDX Generated by Alkaline Hydrolysis of Laden Activated Carbon Fixed-Beds. Experiments RG1b and RG2b
- Figure 5.9** Mol End Product/Mol RDX Generated by Alkaline Hydrolysis of Laden Activated Carbon Fixed-Beds. Experiments RG3a and RG3b.
- Figure 5.10** Mol End Product/Mol RDX Generated by Alkaline Hydrolysis of Laden Activated Carbon Fixed-Beds. Experiments RG4a and RG4b.
- Figure 5.11** Mol End Product/Mol RDX Generated by Alkaline Hydrolysis of Laden Activated Carbon Fixed-Beds. Experiments RG5a, RG5b and RG5c.
- Figure 5.12** Mol End Product/Mol RDX Generated by Alkaline Hydrolysis of Laden Activated Carbon Fixed-Beds. Experiments RG5a
- Figure 5.13** Mol End Product/Mol RDX Generated by Alkaline Hydrolysis of Laden Activated Carbon Fixed-Beds. Experiments RG5c
- Figure 5.14** Mol End Product/Mol RDX Generated by Alkaline Hydrolysis of Laden Activated Carbon Fixed-Beds. Experiments RG6a, RG6b and RG6c
- Figure 5.15** Mol End Product/Mol RDX Generated by Alkaline Hydrolysis of Laden Activated Carbon Fixed-Beds. Experiments RG6a, RG6b and RG6c
- Appendix VI** Fixed-Bed Column Setup

Appendix V: Tables

Fixed Bed Adsorption onto AC Column					
Experiment #:			FB1b	Temperature (°C)	25-27
Date:			16.05.1995	Flow Rate (ml/min):	3,906
Column:			b	EBCT (min):	1,407
				Column Height (mm):	70
Mass AC (g):			2,4	Column Radius (mm):	5
Volume AC (ml):			5,50	Volume water treated (ml):	16580
Average Influent Concentration (mg/L):				17,77	HMX: 2,04
Average Effluent Concentration (mg/L):				1,11	HMX:
RDX on AC (mg)				276,19	
Exp stopped at (h):				70,75	
Regenerated:				virgin	
				INFLUENT	EFFLUENT
hours	min	elapsed time (min)	beds fed	content (mg/L)	content (mg/L)
0,00		0	0	17,65	0,00
20,00		1200	851	18,02	0,00
25,50		1530	1085	17,74	0,44
30,50		1830	1298	17,60	0,52
38,83		2330	1653	17,76	0,71
39,75		2385	1692		0,87
41,00		2460	1745		0,94
46,25		2775	1969		1,25
53,40		3204	2273		1,63
63,33		3800	2696	17,76	2,21
70,75		4245	3011	17,84	2,83
average (RDX)				17,30	7,13
average (HMX)					

Appendix V: Tables

Fixed Bed Adsorption onto AC Column					
Experiment #:			FB2b	Temperature (°C)	25,5-27,5
Date:			27.05.1995	Flow Rate (ml/min):	2,819
Column:			b	EBCT (min):	1,950
				Column Height (mm):	70
Mass AC (g):			2,4	Column Radius (mm):	5
Volume AC (ml):			5,50	Volume water treated (ml):	14800
Average Influent Concentration (mg/L):			17,47	HMX:	
Average Effluent Concentration (mg/L):			0,50	HMX:	
RDX on AC (mg)			251,18		
Exp stopped at (h):			87,50		
Regenerated:			once		
				INFLUENT	EFFLUENT
hours	min	elapsed time (min)	beds fed	content (mg/L)	content (mg/L)
0,00		0	0	17,53	0,00
13,50		810	575	17,20	0,07
20,00		1200	851	#DIV/0!	0,23
35,00		2100	1490	#DIV/0!	0,58
44,00		2640	1873	#DIV/0!	0,57
61,00		3660	2596	17,65	0,82
72,00		4320	3065	17,39	1,54
87,00		5220	3703	17,58	1,19
average (RDX)				17,47	0,50
average (HMX)					

Appendix V: Tables

Fixed Bed Adsorption onto AC Column					
Experiment #:			FB3a	Temperature (°C)	26-27
Date:			09.06.1995	Flow Rate (ml/min):	1,086
Column:			a	EBCT (min):	2,170
				Column Height (mm):	30
Mass AC (g):			1	Column Radius (mm):	5
Volume AC (ml):			2,36	Volume water treated (ml):	6900
Average Influent Concentration (mg/L):			17,83	HMX:	
Average Effluent Concentration (mg/L):			1,92	HMX:	
RDX on AC (mg)			109,79		
Exp stopped at (h):			105,92		
Regenerated:			1 times		
				INFLUENT	EFFLUENT
hours	min	elapsed time (min)	beds fed	content (mg/L)	content (mg/L)
0,00		0	0	17,82	0,00
0,25		15	8	#DIV/0!	0,24
0,58		35	18	#DIV/0!	0,10
2,58		155	79	17,84	0,24
5,58		335	171	#DIV/0!	0,23
10,75		645	329	#DIV/0!	0,21
18,16		1090	555	#DIV/0!	0,17
26,18		1571	800	#DIV/0!	4,00
31,08		1865	950	#DIV/0!	2,43
37,75		2265	1154	#DIV/0!	0,84
42,92		2575	1312	#DIV/0!	1,28
49,75		2985	1520	#DIV/0!	1,22
53,16		3190	1624	17,81	1,59
57,10		3426	1745	#DIV/0!	1,43
63,50		3810	1940	#DIV/0!	1,47
76,92		4615	2351	#DIV/0!	1,75
83,70		5022	2558	#DIV/0!	1,86
89,16		5350	2725	#DIV/0!	2,11
99,84		5990	3051	#DIV/0!	5,29
101,00		6060	3086	#DIV/0!	5,52
105,55		6333	3225	17,85	5,37
average (RDX)				17,83	1,92
average (HMX)					

Appendix V: Tables

Fixed Bed Adsorption onto AC Column					
Experiment #:			FB3b	Temperature (°C)	26-27
Date:			09.06.1995	Flow Rate (ml/min):	1,207
Column:			b	EBCT (min):	1,952
				Column Height (mm):	30
Mass AC (g):			1	Column Radius (mm):	5
Volume AC (ml):			2,36	Volume water treated (ml):	7600
Average Influent Concentration (mg/L):				17,83	HMX:
Average Effluent Concentration (mg/L):				1,68	HMX:
RDX on AC (mg)				122,74	
Exp stopped at (h):				104,92	
Regenerated:				virgin	
				INFLUENT	EFFLUENT
hours	min	elapsed time (min)	beds fed	content (mg/L)	content (mg/L)
0,00			0	17,82	0,00
1,42			47	17,84	0,23
4,58			152	#DIV/0!	0,26
9,75			323	#DIV/0!	0,36
16,75			555	#DIV/0!	0,48
24,32			805	#DIV/0!	0,68
36,75			1217	#DIV/0!	0,84
41,93			1388	#DIV/0!	0,85
48,75			1614	#DIV/0!	1,23
52,16			1727	17,81	1,30
56,18			1860	#DIV/0!	1,32
62,50			2069		1,62
75,98			2515		2,50
82,75			2739		2,93
88,16			2919		3,55
98,50			3261		4,35
104,92			3473	17,85	4,39
average (RDX)				17,83	1,68
average (HMX)					

Appendix V: Tables

Fixed Bed Adsorption onto AC Column					
Experiment #:			FB4a	Temperature (°C)	25,5-27
Date:			20.06.1990	Flow Rate (ml/min):	0,618
Column:			a	EBCT (min):	3,812
				Column Height (mm):	30
Mass AC (g):			1	Column Radius (mm):	5
Volume AC (ml):			2,36	Volume water treated (ml):	8070
Average Influent Concentration (mg/L):				17,91	HMX:
Average Effluent Concentration (mg/L):				1,51	HMX:
RDX on AC (mg)				132,33	
Exp stopped at (h):				217,60	
Regenerated:				2 times	
				INFLUENT	EFFLUENT
hours	min	elapsed time (min)	beds fed	content (mg/L)	content (mg/L)
		105	29	#DIV/0!	0,00
		552	152	#DIV/0!	0,00
		1320	364	17,91	0,00
		1730	477	#DIV/0!	0,11
		1965	542	#DIV/0!	0,09
		2730	753	#DIV/0!	0,22
		3045	840	#DIV/0!	0,27
		3585	989	#DIV/0!	0,32
		4110	1134	#DIV/0!	0,40
		4460	1230	#DIV/0!	0,48
		4900	1352	#DIV/0!	0,80
		5515	1521	#DIV/0!	0,75
		5740	1584	#DIV/0!	0,82
		6080	1677	#DIV/0!	1,03
		6420	1771	#DIV/0!	1,12
		6985	1927	#DIV/0!	1,34
		7307	2016	#DIV/0!	1,52
		7683	2120	#DIV/0!	1,68
		8415	2322	#DIV/0!	1,97
		8825	2435	#DIV/0!	2,13
		9785	2699	#DIV/0!	2,65
		11275	3111	#DIV/0!	3,21
		11635	3210	#DIV/0!	4,09
		12695	3502	#DIV/0!	3,90
		13055	3602	#DIV/0!	4,51
average (RDX)				17,91	1,51
average (HMX)					

Appendix V: Tables

Fixed Bed Adsorption onto AC Column					
Experiment #:			FB4b	Temperature (° C)	25.5-27.0
Date:			20.06.1995	Flow Rate (ml/min):	0,590
Column:			b	EBCT (min):	3,995
				Column Height (mm):	30
Mass AC (g):			1	Column Radius (mm):	5
Volume AC (ml):			2,36	Volume water treated (ml):	7700
Average Influent Concentration (mg/L):				17,91	HMX:
Average Effluent Concentration (mg/L):				1,25	HMX:
RDX on AC (mg)				128,26	
Exp stopped at (h):				217,60	
Regenerated:				once	
				INFLUENT	EFFLUENT
hours	min	elapsed time (min)	beds fed	content (mg/L)	content (mg/L)
		105	29	#DIV/0!	0,00
		552	152	#DIV/0!	0,00
		1320	364	17,91	0,14
		1730	477	#DIV/0!	0,19
		1965	542	#DIV/0!	0,15
		2730	753	#DIV/0!	0,26
		3045	840	#DIV/0!	0,35
		3585	989	#DIV/0!	0,31
		4110	1134	#DIV/0!	0,33
		4460	1230	#DIV/0!	1,39
		4900	1352	#DIV/0!	0,65
		5515	1521	#DIV/0!	0,68
		5740	1584	#DIV/0!	0,77
		6080	1677	#DIV/0!	0,89
		6420	1771	#DIV/0!	0,98
		6985	1927	#DIV/0!	1,03
		7303	2015	#DIV/0!	1,19
		7683	2120	#DIV/0!	1,16
		8415	2322	#DIV/0!	1,36
		8825	2435	#DIV/0!	1,68
		9785	2699	#DIV/0!	1,65
		10345	2854	#DIV/0!	1,76
		11635	3210	#DIV/0!	3,14
		12695	3502	#DIV/0!	3,42
		13055	3602	#DIV/0!	3,93
average (RDX)				17,91	1,25
average (HMX)					

Appendix V: Tables

Fixed Bed Adsorption onto AC Column					
Experiment #:		FB5a		Temperature (°C) 23-25	
Date:		01.08.1995		Real Flow Rate (ml/min): 0,605	
Column:		a		EBCT (min): 3,895	
Mass AC (g):		1		Column Height (mm): 30	
Volume AC (ml):		2,36		Column Radius (mm): 5	
				Volume water treated (ml): 19380	
Average Influent Concentration (mg/L):		17,30		HMX:	
Average Effluent Concentration (mg/L):		7,13		HMX:	
RDX on AC (mg)				197,09	
Exp stopped at (h):				534,10	
Regenerated:				3 times	
				INFLUENT	EFFLUENT
hours	min	elapsed time (min)	beds fed	content (mg/L)	content (mg/L)
	20	20	6	#DIV/0!	0,00
3	35	215	59	#DIV/0!	0,00
5	50	350	97	#DIV/0!	0,00
9	15	555	153	#DIV/0!	0,00
21	58	1318	364	#DIV/0!	0,11
29	10	1750	483	17,26	0,15
46	30	2790	770	17,18	0,36
69	50	4190	1156	#DIV/0!	0,48
81	50	4910	1355	#DIV/0!	0,67
95	46	5746	1585	17,27	0,86
106	12	6372	1758	#DIV/0!	1,05
120	44	7244	1998	17,28	1,48
129	30	7770	2144	#DIV/0!	1,77
142	45	8565	2363	#DIV/0!	1,90
149	40	8980	2477	17,19	2,21
164	47	9887	2728	#DIV/0!	2,42
173	40	10420	2875	#DIV/0!	3,36
189	47	11387	3141	#DIV/0!	3,80
198	2	11882	3278	17,37	4,65
212	42	12762	3521	17,25	4,93
220	50	13250	3655	#DIV/0!	5,92
225	20	13520	3730	#DIV/0!	6,15
236	55	14215	3922	#DIV/0!	6,62
246	15	14775	4076	17,33	7,19
264	20	15860	4375	#DIV/0!	8,05
274	40	16480	4546	#DIV/0!	8,19
290	5	17405	4802	17,31	8,54
296	45	17805	4912	#DIV/0!	9,58
310	10	18610	5134	#DIV/0!	9,12
322	0	19320	5330	#DIV/0!	10,16
332	35	19955	5505	#DIV/0!	10,08
382	35	22955	6333	17,52	11,68
404	0	24240	6687	#DIV/0!	11,89
417	15	25035	6907	17,45	12,71
440	50	26450	7297	#DIV/0!	13,66
455	8	27308	7534	#DIV/0!	13,68
462	55	27775	7662	#DIV/0!	14,14
473	30	28410	7838	#DIV/0!	13,98
488	45	29325	8090	#DIV/0!	15,36
504	40	30280	8354	17,37	16,20
509	40	30580	8436	#DIV/0!	16,66
528	20	31700	8745	#DIV/0!	16,69
534	10	32050	8842	#DIV/0!	17,22
average (RDX)				17,30	7,13
average (HMX)					

Appendix V: Tables

Fixed Bed Adsorption onto AC Column					
Experiment #:			FB5b	Temperature (°C)	23-25
Date:			01.08.1995	Flow Rate (ml/min):	0,552
Column:			b	EBCT (min):	4,269
Mass AC (g):			1	Column Height (mm):	30
Volume AC (ml):			2,36	Column Radius (mm):	5
				Volume water treated (ml):	17690
Average Influent Concentration (mg/L):				17,28	HMX:
Average Effluent Concentration (mg/L):				6,68	HMX:
RDX on AC (mg)				187,51	
Exp stopped at (h):				534,10	
Regenerated:				2 times	
				INFLUENT	EFFLUENT
hours	min	elapsed time (min)	beds fed	content (mg/L)	content (mg/L)
		20	6	#DIV/0!	0,00
3	40	220	61	#DIV/0!	0,00
5	55	355	98	#DIV/0!	0,00
9	20	560	154	#DIV/0!	0,00
21	58	1318	364	#DIV/0!	0,10
29	14	1754	484	17,26	0,16
46	33	2793	771	17,18	0,34
69	53	4193	1157	#DIV/0!	0,59
81	50	4910	1355	#DIV/0!	0,75
95	46	5746	1585	17,27	1,05
106	12	6372	1758	#DIV/0!	1,15
120	44	7244	1998	17,28	0,90
129	30	7770	2144	#DIV/0!	1,79
142	45	8565	2363	#DIV/0!	1,84
149	40	8980	2477	17,19	2,31
164	47	9887	2728	#DIV/0!	2,06
173	40	10420	2875	#DIV/0!	3,09
189	47	11387	3141	#DIV/0!	3,48
198	2	11882	3278	17,37	4,10
212	42	12762	3521	17,25	4,37
220	50	13250	3655	#DIV/0!	5,33
225	20	13520	3730	#DIV/0!	5,29
236	55	14215	3922	#DIV/0!	5,29
246	15	14775	4076	17,33	6,21
264	20	15860	4375	#DIV/0!	6,67
274	40	16480	4546	#DIV/0!	7,26
290	5	17405	4802	17,31	7,31
296	45	17805	4912	#DIV/0!	8,30
310	10	18610	5134	#DIV/0!	8,22
322	0	19320	5330	#DIV/0!	9,40
332	35	19955	5505	#DIV/0!	8,99
382	35	22955	6333	17,52	10,62
404	0	24240	6687	#DIV/0!	11,04
427	25	25645	7075	#DIV/0!	11,67
440	50	26450	7297	#DIV/0!	12,90
455	8	27308	7534	#DIV/0!	12,65
473	30	28410	7838	#DIV/0!	13,16
488	45	29325	8090	#DIV/0!	14,81
504	40	30280	8354	17,37	14,68
509	40	30580	8436	#DIV/0!	15,62
528	20	31700	8745	#DIV/0!	15,62
534	10	32050	8842	17,07	16,19
average (RDX)				17,28	6,68
average (HMX)					

Appendix V: Tables

Fixed Bed Adsorption onto AC Column						
Experiment #:			FB5c	Temperature (°C)	23-25	
Date:			01.08.1995	Flow Rate (ml/min):	0,594	
Column:			c	EBCT (min):	3,967	
Mass AC (g):			1	Column Height (mm):	30	
Volume AC (ml):			2,36	Column Radius (mm):	5	
				Volume water treated (ml):	19020	
Average Influent Concentration (mg/L):				17,32	HMX:	
Average Effluent Concentration (mg/L):				3,88	HMX:	
RDX on AC (mg)				255,54		
Exp stopped at (h):				534,10		
Regenerated:				virgin		
				INFLUENT	EFFLUENT	
hours	min	elapsed time (min)	beds fed	content (mg/L)	content (mg/L)	
		20	5	#DIV/0!	0,00	
3	45	225	57	#DIV/0!	0,00	
6	0	360	91	#DIV/0!	#DIV/0!	
9	25	565	142	#DIV/0!	0,00	
22	4	1324	334	#DIV/0!	0,13	
29	17	1757	443	17,26	0,13	
46	33	2793	704	17,18	0,34	
69	56	4196	1058	#DIV/0!	0,60	
81	50	4910	1238	#DIV/0!	0,76	
95	46	5746	1449	17,27	0,69	
106	12	6372	1606	#DIV/0!	0,64	
129	30	7770	1959	#DIV/0!	1,12	
142	45	8565	2159	#DIV/0!	1,11	
149	40	8980	2264	17,19	1,15	
165	38	9938	2505	#DIV/0!	1,07	
173	40	10420	2627	#DIV/0!	1,60	
189	47	11387	2871	#DIV/0!	2,29	
198	2	11882	2995	17,37	2,26	
212	42	12762	3217	17,25	2,34	
220	50	13250	3340	#DIV/0!	2,82	
225	20	13520	3408	#DIV/0!	2,96	
236	55	14215	3584	#DIV/0!	2,79	
246	15	14775	3725	17,33	3,43	
264	20	15860	3998	#DIV/0!	3,76	
274	40	16480	4155	#DIV/0!	4,37	
290	5	17405	4388	17,31	4,37	
296	45	17805	4489	#DIV/0!	4,80	
310	10	18610	4692	#DIV/0!	3,92	
322	0	19320	4871	#DIV/0!	3,65	
332	45	19965	5033	#DIV/0!	4,24	
344	45	20685	5215	#DIV/0!	4,63	
357	30	21450	5408	17,53	5,89	
367	40	22060	5561	#DIV/0!	6,45	
382	35	22955	5787	17,52	6,31	
404	0	24240	6111	#DIV/0!	7,01	
417	15	25035	6311	17,45	8,30	
427	25	25645	6465	#DIV/0!	8,21	
440	50	26450	6668	#DIV/0!	8,65	
455	8	27308	6884	#DIV/0!	9,20	
462	55	27775	7002	#DIV/0!	10,42	
473	30	28410	7162	#DIV/0!	9,78	
488	45	29325	7393	#DIV/0!	11,63	
504	40	30280	7634	17,37	12,14	
509	40	30580	7709	#DIV/0!	12,29	
528	20	31700	7992	#DIV/0!	13,08	
534	10	32050	8080	17,07	13,53	
average (RDX)				17,32	3,88	
average (HMX)						

Appendix V: Tables

Fixed Bed Adsorption onto AC Column					
Experiment #:			FB6b	Temperature (° C)	22-25
Date:			11.09.1995	Flow Rate (ml/min):	1,108
Column:			b	EBCT (min):	2,127
				Column Height (mm):	30
Mass AC (g):			1	Column Radius (mm):	5
Volume AC (ml):			2,36	Volume water treated (ml):	12640
Average Influent Concentration (mg/L):				18,09	HMX:
Average Effluent Concentration (mg/L):				7,35	HMX:
RDX on AC (mg)				135,79	
Exp stopped at (h):				190,20	
Regenerated:				3 times	
				INFLUENT	EFFLUENT
hours	min	elapsed time (min)	beds fed	content (mg/L)	content (mg/L)
	14	14	7	17,67	0,13
1	20	80	37	#DIV/0!	0,29
11	6	666	311	#DIV/0!	0,61
18	35	1115	521	18,13	1,19
36	3	2163	1010	#DIV/0!	1,86
46	42	2802	1308	#DIV/0!	3,13
59	10	3550	1657	18,35	3,92
71	32	4292	2004	#DIV/0!	4,93
83	44	5024	2346	#DIV/0!	5,76
91	10	5470	2554	#DIV/0!	6,76
108	10	6490	3030	#DIV/0!	8,05
117	50	7070	3301	#DIV/0!	8,94
132	50	7970	3721	18,20	9,36
143	45	8625	4027	#DIV/0!	10,54
155	20	9320	4351	#DIV/0!	10,51
166	30	9990	4664	#DIV/0!	12,65
180	11	10811	5047	#DIV/0!	12,76
190	10	11410	5327	#DIV/0!	13,60
average (RDX)				18,09	7,35
average (HMX)					

Appendix V: Tables

Fixed Bed Adsorption onto AC Column					
Experiment #:			FB6c	Temperature (° C)	22-25
Date:			11.09.1995	Flow Rate (ml/min):	1,11
Column:			c	EBCT (min):	2,121
				Column Height (mm):	30
Mass AC (g):			1	Column Radius (mm):	5
Volume AC (ml):			2,36	Volume water treated (ml):	12680
Average Influent Concentration (mg/L):				18,09	HMX:
Average Effluent Concentration (mg/L):				4,65	HMX:
RDX on AC (mg)				170,37	
Exp stopped at (h):				190,20	
Regenerated:				1 times	
				INFLUENT	EFFLUENT
hours	min	elapsed time (min)	beds fed	content (mg/L)	content (mg/L)
	15	15	7	17,67	0,00
1	21	81	38	#DIV/0!	0,08
11	7	667	311	#DIV/0!	0,10
18	35	1115	521	18,13	0,46
36	3	2163	1010	#DIV/0!	0,70
46	42	2802	1308	#DIV/0!	1,39
59	10	3550	1657	18,35	1,97
71	32	4292	2004	#DIV/0!	2,56
83	44	5024	2346	#DIV/0!	3,10
91	10	5470	2554	#DIV/0!	3,92
108	10	6490	3030	#DIV/0!	4,48
117	50	7070	3301	#DIV/0!	5,29
132	50	7970	3721	18,20	5,94
143	45	8625	4027	#DIV/0!	6,84
155	20	9320	4351	#DIV/0!	7,54
166	30	9990	4664	#DIV/0!	9,44
180	11	10811	5047	#DIV/0!	10,18
190	10	11410	5327	#DIV/0!	11,17
average (RDX)				18,09	4,65
average (HMX)					

Appendix V: Tables

Regeneration Experiment at Loaded Activated Carbon Column's						
Exp.:		RG1b		AC comes from experiment:		FB1b
Date:		06\05\95		RDX on AC (mg):		276,19
pH:		12		RDX on AC (mol)		1,244
Temperature (° C):		80		Mass of AC (g):		2,4
Flow rate (ml/min):		3,9		radius of bed (mm):		5
EBCT (min):		1,410		heigth of bed (mm):		70
V reg. water (mL):		1000		q-e (mg/g)		115,08
		Nitrite			Formate	
minutes	dimension-less time	concentration (mg/L)	NO ₂ ⁻ /RDX (mol/mol)	HCOO ⁻ /RDX (mol/mol)	concentration (mg/L)	remarks
0	0	0,00	0,00	0,00	0,00	
15	11	12,31	0,22	0,03	1,80	
30	21	22,54	0,39	0,10	5,64	
120	85	62,80	1,10	0,55	30,99	diluted 1:10
180	128	72,26	1,26	0,79	43,94	diluted 1:10
240	170	75,81	1,33	0,95	53,30	diluted 1:10, pH 11.8
300	213	75,78	1,32	1,03	57,50	diluted 1:10
390	277	90,39	1,58	1,39	77,98	diluted 1:10
520	369	86,41	1,51	1,45	81,26	diluted 1:10
1220	865	90,61	1,58	1,75	98,14	diluted 1:10, pH11.7
1720	1220	93,39	1,63	1,87	104,55	diluted 1:10
2800	1986	93,66	1,64	2,02	112,80	diluted 1:10
2970	2106	93,74	1,64	2,04	113,90	diluted 1:10
2990	2121	94,46	1,65	2,04	113,93	diluted 1:10
362	257		1,50			
631	448			1,50		

Appendix V: Tables

Regeneration Experiment at Loaded Activated Carbon Column's						
Exp.:		RG2b		AC comes from experiment:		FB2b
Date:		06\05\95		RDX on AC (mg):		251,18
pH:		12		RDX on AC (mol)		1,131
Temperature (°C):		80		Mass of AC (g):		2,4
Flow rate (ml/min):		8,0		radius of bed (mm):		10
EBCT (min):		0,687		height of bed (mm):		70
V reg. water (mL):		1000		q-e (mg/g)		104,66
		Nitrite			Formate	
minutes	dimension-less time	concentration (mg/L)	NO ₂ ⁻ /RDX (mol/mol)	HCOO ⁻ /RDX (mol/mol)	concentration (mg/L)	remarks
0	0	0,00	0,00	0,00	0,00	
150	218	9,54	0,18	0,44	22,65	diluted 1:10
210	306	26,72	0,51	1,22	61,90	diluted 1:10
240	349	32,89	0,63	1,32	67,06	diluted 1:10
1380	2009	74,34	1,43	1,75	88,91	diluted 1:10
3180	4629	77,58	1,49	1,76	89,68	diluted 1:10
4560	6638	85,61	1,65	1,85	94,33	diluted 1:10
5760	8384	89,88	1,73	1,81	91,92	diluted 1:10
3259	2311		1,50			
724	514			1,50		

Appendix V: Tables

Regeneration Experiment at Loaded Activated Carbon Column's						
Exp.:		RG3a		AC comes from experiment:		FB3a
Date:		15.06.1995		RDX on AC (mg):		123,21
pH:		12		RDX on AC (mol)		0,555
Temperature (° C):		80		Mass of AC (g):		1
Flow rate (ml/min):		8,8		radius of bed (mm):		5
EBCT (min):		0,268		height of bed (mm):		30
V reg. water (mL):		1000				
		Nitrite			Formate	
minutes	dimension-less time	concentration (mg/L)	NO ₂ ⁻ /RDX (mol/mol)	HCOO ⁻ /RDX (mol/mol)	concentration (mg/L)	remarks
0	0	0,00	0,00	0,00	0,00	
5	19	3,97	0,16	0,00	0,00	
15	56	11,00	0,43	0,00	0,00	
30	112	17,70	0,69	0,23	5,72	diluted 1:10
45	168	21,35	0,84	0,43	10,68	diluted 1:10
60	224	26,26	1,03	0,44	11,06	diluted 1:10
90	336	31,86	1,25	0,63	15,73	diluted 1:10
121	451	34,28	1,34	1,27	31,83	diluted 1:10
180	672	39,21	1,54	1,11	27,60	diluted 1:10
236	881	40,46	1,59	1,30	32,35	diluted 1:10
289	1078	39,89	1,56	1,37	34,20	diluted 1:10
388	1448	40,22	1,58	1,49	37,17	diluted 1:10
438	1634	40,08	1,57	1,53	38,09	diluted 1:10
636	2373	40,71	1,60	1,62	40,41	diluted 1:10
1560	5821	40,02	1,57	1,68	42,05	diluted 1:10
3060	11418	42,42	1,66	1,83	45,74	diluted 1:10
169	120		1,50			
403	286			1,50		

Appendix V: Tables

Regeneration Experiment at Loaded Activated Carbon Column's						
Exp.:		RG4a		AC comes from experiment:		FB4a
Date:		16.07.1995		RDX on AC (mg):		132,33
pH:		12		RDX on AC (mol)		0,596
Temperature (° C):		80		Mass of AC (g):		1
Flow rate (ml/min):		5,2		radius of bed (mm):		5
EBCT (min):		0,453		height of bed (mm):		30
V reg. water (mL):		1000				
		Nitrite			Formate	
minutes	dimension-less time	concentration (mg/L)	NO ₂ ⁻ /RDX (mol/mol)	HCOO ⁻ /RDX (mol/mol)	concentration (mg/L)	remarks
0	0	0,00	0,00	0,00	0,00	
5	11	1,16	0,04	0,21	5,64	
15	33	6,25	0,23	0,12	3,22	
30	66	13,69	0,50	0,15	4,11	
47	104	17,96	0,66	0,28	7,52	diluted 1:10
59	130	20,23	0,74	0,35	9,34	diluted 1:10
90	199	28,16	1,03	0,53	14,09	diluted 1:10
120	265	32,75	1,20	0,69	18,47	diluted 1:10
149	329	36,15	1,32	0,90	24,04	diluted 1:10
178	393	39,57	1,44	0,94	25,21	diluted 1:10
210	463	41,64	1,52	1,05	28,26	diluted 1:10
238	525	43,00	1,57	1,14	30,60	diluted 1:10
292	644	40,19	1,47	1,15	30,88	diluted 1:10
327	722	45,93	1,68	1,35	36,18	diluted 1:10
371	819	45,38	1,66	1,38	37,05	diluted 1:10
451	995	46,37	1,69	1,55	41,57	diluted 1:10
497	1097	46,50	1,70	1,53	41,13	diluted 1:10
539	1190	47,42	1,73	1,59	42,51	diluted 1:10
1398	3085	48,35	1,76	1,89	50,77	diluted 1:10
1779	3926	47,41	1,73	1,85	49,69	diluted 1:10
2851	6292	48,71	1,78	1,99	53,38	diluted 1:10
202	143		1,50			
427	303			1,50		

Appendix V: Tables

Regeneration Experiment at Loaded Activated Carbon Column's						
Exp.:		RG4b		AC comes from experiment:		FB4b
Date:		16.07.1995		RDX on AC (mg):		128,26
pH:		12		RDX on AC (mol)		0,577
Temperature (° C):		80		Mass of AC (g):		1
Flow rate (ml/min):		5,7		radius of bed (mm):		5
EBCT (min):		0,408		height of bed (mm):		30
V reg. water (mL):		1000				
		Nitrite			Formate	
minutes	dimension-less time	concentration (mg/L)	NO ₂ ⁻ /RDX (mol/mol)	HCOO ⁻ /RDX (mol/mol)	concentration (mg/L)	remarks
0	0	0,00	0,00	0,00	0,00	
5	12	1,36	0,05	0,21	5,39	
15	37	5,77	0,22	0,12	3,14	
30	73	12,68	0,48	0,15	3,87	
45	110	15,62	0,59	0,25	6,54	diluted 1:10
60	147	19,68	0,74	0,35	8,99	diluted 1:10
91	223	26,50	1,00	0,50	13,12	diluted 1:10
118	289	31,93	1,20	0,66	17,10	diluted 1:10
150	367	35,28	1,33	0,80	20,79	diluted 1:10
179	438	36,77	1,38	0,87	22,69	diluted 1:10
233	571	45,35	1,71	1,34	34,86	diluted 1:10
268	656	45,79	1,72	1,40	36,40	diluted 1:10
392	960	46,76	1,76	1,43	37,21	diluted 1:10
479	1173	44,91	1,69	1,47	38,23	diluted 1:10
1342	3286	51,48	1,94	2,00	51,90	diluted 1:10
1720	4212	46,44	1,75	1,85	48,16	diluted 1:10
2791	6835	48,21	1,82	2,00	52,03	diluted 1:10
198	141		1,50			
526	373			1,50		

Appendix V: Tables

Regeneration Experiment at Loaded Activated Carbon Column's						
Exp.:		RG5a		AC comes from experiment:	FB5a	
Date:		01.09.1995		RDX on AC (mg):	197,71	
pH:		11		RDX on AC (mol):	0,890	
Temperature (° C):		80		Mass of AC (g):	1	
Flow rate (ml/min):		3,8		radius of bed (mm):	5	
EBCT (min):		0,620		height of bed (mm):	30	
V reg. water (mL):		1000				
		Nitrite		Formate		
minutes	dimension-less time	concentration (mg/L)	NO ₂ ⁻ /RDX (mol/mol)	HCOO ⁻ /RDX (mol/mol)	concentration (mg/L)	remarks
0	0	0,00	0,00	0,00	0,00	
6	10	0,00	0,00	0,01	0,57	diluted 1:10
15	24	0,32	0,01	0,02	0,80	diluted 1:10
30	48	1,64	0,04	0,03	1,13	diluted 1:10
45	73	3,03	0,07	0,04	1,49	diluted 1:10
60	97	4,42	0,11	0,05	1,84	diluted 1:10
80	129	6,28	0,15	0,06	2,40	diluted 1:10
100	161	8,05	0,20	0,07	2,76	diluted 1:10
120	194	9,56	0,23	0,08	3,17	diluted 1:10
338	545	17,24	0,42	0,02	0,77	diluted 1:10
403	650	20,80	0,51	0,04	1,62	diluted 1:10
451	727	22,52	0,55	0,06	2,36	diluted 1:10
458	739	22,13	0,54	0,06	2,22	diluted 1:10
566	913	25,24	0,62	0,07	3,00	diluted 1:10
711	1147	29,93	0,73	0,10	4,14	diluted 1:10
815	1314	32,20	0,79	0,12	4,90	diluted 1:10
1347	2172	38,08	0,93	0,17	6,87	diluted 1:10
1491	2405	38,42	0,94	0,17	6,66	diluted 1:10
1770	2855	40,36	0,99	0,19	7,58	diluted 1:10
2001	3227	41,47	1,01	0,21	8,33	diluted 1:10
2238	3609	43,59	1,06	0,22	8,89	diluted 1:10
2778	4480	46,39	1,13	0,26	10,33	diluted 1:10; 2mL NaOH 10 Mol added
2798	4513	46,12	1,13	0,28	11,12	diluted 1:10
3003	4843	50,02	1,22	0,56	22,43	diluted 1:10
4007	6463	53,73	1,31	1,12	45,01	diluted 1:10
4153	6698	51,52	1,26	1,13	45,10	diluted 1:10
5406	8719	52,51	1,28	1,28	51,12	diluted 1:10
-	-		1,50			
-	-			1,50		

Appendix V: Tables

Regeneration Experiment at Loaded Activated Carbon Column's						
Exp.:		RG5b		AC comes from experiment:		FB5b
Date:		03.09.1995		RDX on AC (mg):		188,30
pH:		12		RDX on AC (mol)		0,848
Temperature (° C):		70		Mass of AC (g):		1
Flow rate (ml/min):		3,9		radius of bed (mm):		5
EBCT (min):		0,609		height of bed (mm):		30
V reg. water (mL):		1000				
		Nitrite			Formate	
minutes	dimension-less time	concentration (mg/L)	NO ₂ ⁻ /RDX (mol/mol)	HCOO ⁻ /RDX (mol/mol)	concentration (mg/L)	remarks
0	0	0,00	0,00	0,00	0,00	
6	10	0,00	0,00	0,00	0,00	
16	26	0,00	0,00	0,00	0,00	
30	49	3,27	0,08	0,03	1,07	
45	74	10,89	0,28	0,07	2,49	diluted 1:10
60	99	17,75	0,46	0,11	4,21	diluted 1:10
94	154	15,43	0,40	0,13	4,83	diluted 1:10
112	184	19,28	0,49	0,22	8,27	diluted 1:10
217	356	35,61	0,91	0,47	17,83	diluted 1:10
234	384	38,21	0,98	0,52	19,87	diluted 1:10
415	682	35,80	0,92	0,83	31,79	diluted 1:10
465	764	36,56	0,94	0,88	33,75	diluted 1:10
536	880	37,21	0,95	0,96	36,66	diluted 1:10
715	1174	39,25	1,01	1,12	42,90	diluted 1:10
931	1529	41,02	1,05	1,26	47,99	diluted 1:10
1441	2367	41,60	1,07	1,37	52,22	diluted 1:10
1597	2623	42,38	1,09	1,41	53,90	diluted 1:10
1762	2894	42,48	1,09	1,40	53,57	diluted 1:10
2889	4745	42,73	1,10	1,51	57,62	diluted 1:10
3428	5631	42,68	1,09	1,53	58,19	diluted 1:10
4388	7207	41,88	1,07	1,54	58,70	diluted 1:10
5915	9716	43,03	1,10	1,64	62,71	diluted 1:10
-	-		1,50			
2778	1971			1,50		

Appendix V: Tables

Regeneration Experiment at Loaded Activated Carbon Column's						
Exp.:		RG6a		AC comes from experiment:		FB6a
Date:		20.09.1995		RDX on AC (mg):		139,41
pH:		12		RDX on AC (mol)		0,628
Temperature (° C):		80		Mass of AC (g):		1
Flow rate (ml/min):		3,3		radius of bed (mm):		5
EBCT (min):		0,671		height of bed (mm):		30
V reg. water (mL):		1000				
		Nitrite			Formate	
minutes	dimension-less time	concentration (mg/L)	NO ₂ ⁻ /RDX (mol/mol)	HCOO ⁻ /RDX (mol/mol)	concentration (mg/L)	remarks
5	7	1,09	0,04	0,00	0,00	
17	25	7,20	0,25	0,00	0,00	
30	43	14,50	0,50	0,11	3,13	
45	65	20,99	0,73	0,17	4,71	
55	79	22,97	0,80	0,30	8,61	diluted 1:10
65	94	25,89	0,90	0,37	10,50	diluted 1:10
80	115	29,63	1,03	0,48	13,51	diluted 1:10
164	237	45,60	1,58	1,00	28,26	diluted 1:10
180	260	47,00	1,63	1,07	30,35	diluted 1:10
239	345	49,39	1,71	1,28	36,29	diluted 1:10
287	414	53,47	1,85	1,48	41,75	diluted 1:10
359	518	52,20	1,81	1,65	46,50	diluted 1:10
581	838	54,87	1,90	1,85	52,39	diluted 1:10
711	1026	53,52	1,85	1,90	53,59	diluted 1:10
825	1191	55,33	1,92	2,03	57,36	diluted 1:10
1366	1971	54,34	1,88	2,15	60,82	diluted 1:10
1419	2048	56,45	1,96	2,21	62,39	diluted 1:10
152	108		1,50			
296	210			1,50		

Appendix V: Tables

Regeneration Experiment at Loaded Activated Carbon Column's						
Exp.:		RG6b		AC comes from experiment:		FB6b
Date:		20.09.1995		RDX on AC (mg):		135,79
pH:		12		RDX on AC (mol)		0,611
Temperature (° C):		80		Mass of AC (g):		1
Flow rate (ml/min):		3,4		radius of bed (mm):		5
EBCT (min):		0,691		height of bed (mm):		30
V reg. water (mL):		1000				
		Nitrite			Formate	
minutes	dimension-less time	concentration (mg/L)	NO ₂ ⁻ /RDX (mol/mol)	HCOO ⁻ /RDX (mol/mol)	concentration (mg/L)	remarks
0	0	0,00	0,00	0,00	0,00	
5	7	1,83	0,07	0,00	0,00	
21	30	9,14	0,32	0,00	0,00	
124	179	37,99	1,35	0,73	20,03	
199	287	42,82	1,52	1,00	27,53	
288	416	48,40	1,72	1,27	34,92	diluted 1:10
305	440	50,93	1,81	1,36	37,43	diluted 1:10
449	648	53,95	1,92	1,92	52,94	diluted 1:10
585	844	54,57	1,94	1,89	52,07	diluted 1:10
782	1128	53,45	1,90	1,91	52,50	diluted 1:10
1358	1960	52,37	1,86	1,63	44,71	diluted 1:10
189	134		1,50			
341	242			1,50		

Appendix V: Tables

Regeneration Experiment at Loaded Activated Carbon Column's						
Exp.:		RG6c		AC comes from experiment:		FB6c
Date:		20.09.1995		RDX on AC (mg):		170,37
pH:		12		RDX on AC (mol)		0,767
Temperature (° C):		80		Mass of AC (g):		1
Flow rate (ml/min):		3,2		radius of bed (mm):		5
EBCT (min):		0,734		height of bed (mm):		30
V reg. water (mL):		1000				
		Nitrite			Formate	
minutes	dimension-less time	concentration (mg/L)	NO ₂ ⁻ /RDX (mol/mol)	HCOO ⁻ /RDX (mol/mol)	concentration (mg/L)	remarks
0	0	0,00	0,00	0,00	0,00	
14	19	7,94	0,22	0,40	13,97	diluted 1:10
30	41	13,37	0,38	0,46	15,90	diluted 1:10
44	60	24,11	0,68	0,75	25,82	diluted 1:10
66	90	32,68	0,93	0,74	25,71	diluted 1:10
85	115	39,72	1,13	0,87	30,03	diluted 1:10
198	269	47,31	1,34	1,04	35,73	diluted 1:10
240	326	59,30	1,68	1,24	42,66	dil 1:15
300	407	62,10	1,76	1,37	47,13	dil 1:15
347	471	69,35	1,97	1,63	56,17	dil 1:15
416	565	69,82	1,98	1,83	63,27	dil 1:15
451	613	70,21	1,99	1,80	62,00	dil 1:15
511	694	72,74	2,06	2,00	68,94	dil 1:15
570	774	69,52	1,97	1,99	68,53	dil 1:15
706	959	70,61	2,00	2,06	71,04	dil 1:15
1645	2234	75,43	2,14	2,74	94,63	dil 1:15
1943	2639	73,56	2,08	2,61	90,05	dil 1:15
218	154		1,50			
304	216			1,50		

Appendix V

Experiment from 06-07-95 - Adsorption of RDX and HMX onto activated carbon F-400						
HSDM-rate test		V=1L	T=23°C			
Standard	RDX					
Intercept	8421.136					
x1	159786.1					
Calculation for $C_e/C_0=0.5$			Freundlich-Isotherme from ad030294			
$C_0=$	36.35425		Intercept	4.574404	0.012069	
$C_e=$	18.17712		x1	0.354419	0.007071	
$D_0=$	0.067064 g ac		K=	96.97018 L/g		
X=	0.018177			0.09697 L/mg		
$Q_e=$	271.0428		n=	2.821519		
HSDM-model for HS060795						
data from Hand et al (1983):						
Parameter from table-1 (for 0.4)						
			A0	A1	A2	A3
K=	0.09697 L/mg		-1.14297	-9.14255	13.2803	-11.982
1/n=	0.354419 []		Parameter from table-3 (for 0.4)			
Radius:	0.0325 cm		-0.15229	-0.08166	0.035631	0.003788
\bar{C} permissible			D_s	S2	S	
0.899-0.012		75	7.35E-10	0.003122		
C_e/C_0 permissible		85	8.33E-10	0.001877		
0.43-0.59		90	8.82E-10	0.001641		
		93	9.11E-10	0.001602	0.04002	
		100	9.8E-10	0.001767		
		110	1.08E-09	0.00252		
		125	1.22E-09	0.004507		

Appendix V

D-s (90%)			D-s (110%)			D-s (125%)		
8.82E-10			1.08E-09			1.22E-09		
\bar{t}_m	C_m	error ²	\bar{t}_m	C_m	error ²	\bar{t}_m	C_m	error ²
0			0			0		
0.00025	0.815325	0.026939	0.000306	0.83481	0.020923	0.000348	0.844846	0.01812
0.001503	0.843787	0.002906	0.001837	0.829281	0.00468	0.002087	0.818518	0.006268
0.003006	0.781785	0.001982	0.003674	0.758056	0.004657	0.004175	0.74175	0.007149
0.004509	0.73151	0.001992	0.005511	0.703402	0.005291	0.006262	0.6845	0.008398
0.006012	0.690816	0.000947	0.007348	0.659856	0.003786	0.00835	0.639401	0.006722
0.007515	0.656307	0.000607	0.009185	0.623749	0.003271	0.010437	0.602256	0.006192
0.009018	0.626788	0.000316	0.011022	0.592931	0.002666	0.012525	0.570696	0.005456
0.010521	0.600898	0.000328	0.012859	0.56606	0.002803	0.014612	0.543274	0.005735
0.012124	0.576399	0.000164	0.014818	0.540754	0.002348	0.016839	0.517522	0.005139
0.013527	0.557084	1.14E-05	0.016533	0.520879	0.001567	0.018787	0.497343	0.003984
0.014829	0.540618	6.14E-08	0.018125	0.503985	0.001324	0.020596	0.48022	0.003618
0.016533	0.520879	2.97E-07	0.020207	0.48379	0.001336	0.022962	0.459785	0.003666
0.018036	0.504895	0.000106	0.022044	0.467479	0.000735	0.02505	0.443308	0.00263
0.019539	0.490057	0.0001	0.023881	0.452371	0.000766	0.027137	0.428066	0.002701
0.021042	0.476215	7.07E-07	0.025718	0.438305	0.001374	0.029225	0.413893	0.00378
0.022545	0.463247	4.98E-05	0.027555	0.425151	0.000964	0.031312	0.400654	0.003085
0.024198	0.449871	0.000154	0.029575	0.411607	0.000669	0.033608	0.387037	0.002543
0.025551	0.439544	6.11E-05	0.031229	0.401167	0.000934	0.035487	0.37655	0.003045
0.027104	0.428302	0.000122	0.033127	0.389816	0.000752	0.037644	0.365159	0.002712
0.028557	0.418321	0.00046	0.034903	0.379754	0.000293	0.039662	0.355069	0.001748
0.03006	0.408492	0.000166	0.03674	0.369856	0.000663	0.04175	0.345152	0.002546
0.031563	0.399123	0.000316	0.038577	0.360432	0.000437	0.043837	0.335716	0.002081
0.033066	0.390173	0.000614	0.040414	0.35144	0.000195	0.045924	0.32672	0.001496
0.034569	0.381608	0.000447	0.042251	0.342845	0.000311	0.048012	0.318127	0.001793
0.036222	0.372596	0.000521	0.044271	0.33381	0.000255	0.050308	0.3091	0.001654
0.075049	0.232353	0.001716	0.091727	0.194506	1.28E-05	0.104235	0.170741	0.000408
	SUM	0.041026		SUM	0.063011		SUM	0.112669
	S2	0.001641		S2	0.00252		S2	0.004507
	S	0.04051		S	0.050204		S	0.067133

Appendix VI: Figures

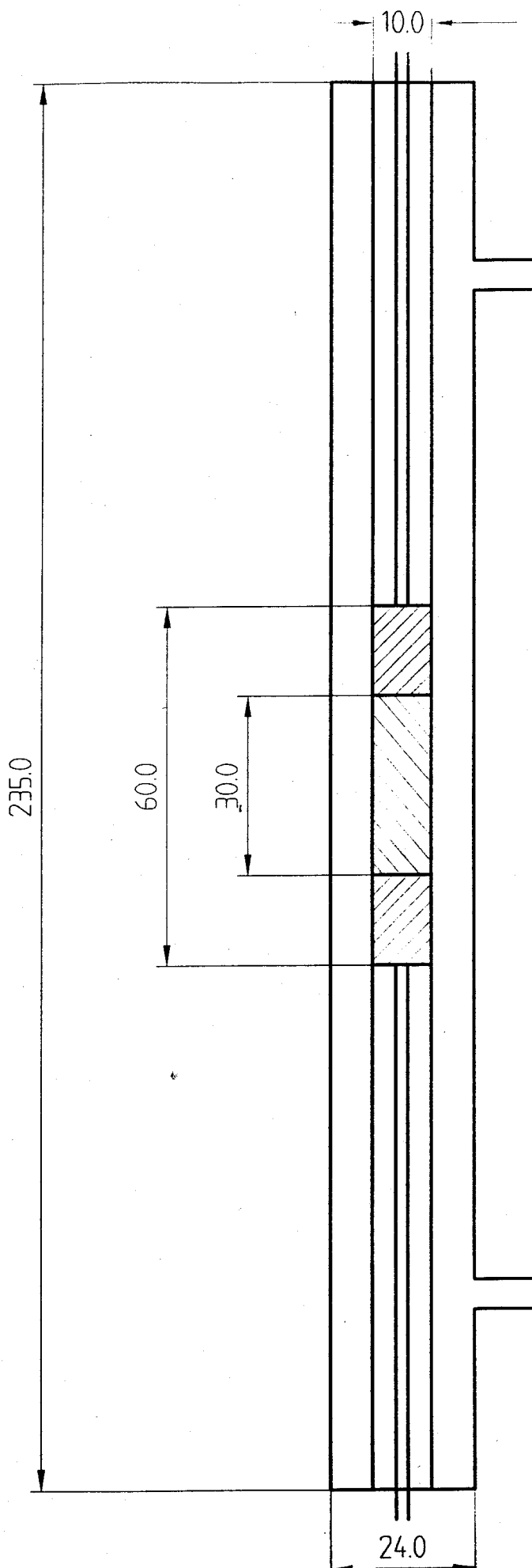


Figure A.1:
Fixed-Bed Column Setup

Appendix VII: Derivation of the Homogeneous Surface Diffusion Model (HSDM)

Chapter 1

The development of the model equations which describe the concentration of an adsorbate within the liquid and adsorbent-phases as functions of time are presented here. The equations are developed with dimensional variables in Chapter 1 and converted into dimensionless variables in Chapter 2 of this appendix. The batch reactor is assumed to be completely-mixed; consequently, the liquid-phase concentration is assumed to be the same regardless of position in the reactor. Additional assumptions and mechanisms which are incorporated into the model are discussed in the text section, Chapter 4.1.

The sequence of this development will be to derive (a) the overall mass balance for a completely-mixed batch reactor (CMBR), (b) the liquid-phase mass balance and its initial condition, (c) the intraparticle mass balance and its initial and boundary conditions, and (d) an expression which couples the liquid and adsorbent-phase mass balances.

a) To derive the overall mass balance, we equate the mass of adsorbate in the CMBR at time, t , to the mass of adsorbate in the time initially:

$$\varepsilon VC(t) + Mq_{ave}(t) = \varepsilon VC_0 \quad (A.1)$$

mass of ad- sorbate in the liquid at time t	+	mass of the adsor- bent-phase at time t	=	mass of ad- sorbate in the CMBR initially
--	---	--	---	--

In order to describe the overall mass balance the particle radius r is used:

$$\text{Mass of Adsorbate in Shell as } \Delta r \rightarrow 0 = q(r, t) \rho_a 4 \pi r^2 dr \quad (A.2)$$

$$\text{Mass of Adsorbate in Particle} = q_{ave}(t) \rho_a \frac{4 \pi R^3}{3} = \int_0^R q(r, t) \rho_a 4 \pi r^2 dr \quad (A.3)$$

Therefore, the final form of the overall mass balance can be written as

$$C_0 = C(t) + \frac{3M}{\varepsilon VR^3} \int_0^R q(r, t) r^2 dr \quad (A.4)$$

b) In the following equations, the liquid and adsorbent-phases are treated separately. The liquid-phase mass balance in its differential form is

$$-\Delta t k_f A_p [C(t) - C_s(t)] = \varepsilon V [C(t + \Delta t) - C(t)] \quad (A.5)$$

- Mass of Adsorbate in the Liquid-Phase Adsorbed by the Adsorbent Phase	=	Mass of Adsorbate Accumulated in the Liquid-Phase
--	---	---

Dividing (A.5) by Δt and taking the limit as Δt goes to zero, the following expression is obtained:

$$\varepsilon v \frac{\partial C(t)}{\partial t} = -k_f A_p [C(t) - C_s(t)] \quad (\text{A.6})$$

A_p is defined with

$$A_p = \left[\frac{3M}{4\pi R^3 \rho_a} \right] \left[4\pi R^2 \right] \left[\frac{1}{\phi} \right] \quad (\text{A.7})$$

A_p = Number of Adsorbent Particles * Surface Area of a Spherical Particle * Actual Surface Area of the Particle / Surface Area of a Sphere

When substituting A.7 into A.6, A.8 may be obtained after some algebraic manipulations:

$$\frac{\partial C(t)}{\partial t} = \frac{k_f 3M}{\rho_a R \varepsilon V \phi} [C(t) - C_s(t)] \quad (\text{A.8})$$

The dosage of the adsorbent may be written in terms of ε and ρ_a :

$$\frac{M}{V} = D_0 = \rho_a (1 - \varepsilon) \quad (\text{A.9})$$

$\frac{M}{V} = D_0 =$ Mass of Adsorbent / Volume of Adsorbent * Volume of Total CMBR / Volume

The final form of the liquid-phase mass balance is

$$\frac{\partial C(t)}{\partial t} = \frac{3k_f (1 - \varepsilon)}{R \varepsilon \phi} [C(t) - C_s(t)] \quad (\text{A.10})$$

with the initial condition

$$C(t=0) = C_0 \quad (\text{A.11})$$

c) The intraparticle mass balance in its differential form is

$$\begin{aligned} & (-D_s \rho_a \frac{\partial q(r,t)}{\partial r} 4\pi r^2 \Delta r) - (-D_s \rho_a \frac{\partial q(r+\Delta r,t)}{\partial r} 4\pi r^2 \Delta r) \\ & = [4\pi r^2 \Delta r \rho_a q(r,t+\Delta t) - 4\pi r^2 \Delta r \rho_a q(r,t)] \end{aligned} \quad (\text{A.12})$$

Mass of Adsorbate Entering at r - Mass of Adsorbate at $r+\Delta r$ = Mass of Adsorbate Accumulating in Spherical Shell

The final form of the intraparticle mass balance is

$$\frac{\partial q(r,t)}{\partial t} = \frac{D_s}{r^2} \frac{\partial}{\partial r} \left[r^2 \frac{\partial q(r,t)}{\partial r} \right] \quad (\text{A.13})$$

with the initial condition

$$q(0 \leq r \leq R, t=0) = 0 \quad (\text{A.14})$$

and the boundary conditions

$$\frac{\partial q(r=0, t \geq 0)}{\partial r} = 0 \quad (\text{A.15})$$

d) The boundary condition at the external particle surface is derived by performing a mass balance on the external surface of the adsorbent. Since the mass flux from the liquid-phase must equal the mass in the particle we may write the following equation:

$$\frac{k_f}{\phi} [C(t) - C_s(t)] \frac{4\pi R^2}{\phi} = \rho_a D_s \frac{\partial q(r=R, t)}{\partial r} \frac{4\pi R^2}{\phi} \quad (\text{A.16})$$

Mass of Adsorbate Transferred through the Liquid-Phase Boundary Layer = Mass of Adsorbate Transferred away from the Exterior Surface by Surface Diffusion

Dividing by the external surface area, we obtain the final form of the boundary condition:

$$\frac{\partial q(r=R, t)}{\partial r} = \frac{k_f}{\rho_a D_s} [C(t) - C_s(t)] \quad (\text{A.17})$$

In order to solve Equations (A.10) (liquid-phase mass balance) and (A.13) (intraparticle mass balance), we need to express the surface concentration of the adsorbate in the liquid-phase, $C_s(t)$, in terms of the surface concentration of adsorbate in the adsorbate-phase, $q(r=R, t)$. This is known as the coupling equation. The Freundlich isotherm equation is used to describe the adsorption equilibrium conditions:

$$q(r=R, t) = K C_s(t)^{\frac{1}{n}} \quad (\text{A.18})$$

This completes the derivation of the equations for Homogeneous Surface Diffusion Model.

Chapter 2

In this chapter, the equations presented in Chapter 1 of this appendix are transferred into dimensionless form using the following dimensionless parameters:

$$\bar{C}(\bar{t}) = \frac{C(t) - C_e}{C_0 - C_e} \quad (\text{A.19})$$

$$\bar{r} = \frac{r}{R} \quad (\text{A.20})$$

$$\bar{q}(\bar{r}, \bar{t}) = \frac{q(r, t)}{q_e} \quad (\text{A.21})$$

$$\bar{t} = \frac{D_s t}{R^2} \quad (\text{A.22})$$

$$D_g = \frac{M q_e}{C_0 V \varepsilon} = \frac{\rho_a q_e (1 - \varepsilon)}{C_0 \varepsilon} \quad (\text{A.23})$$

$$Bi = \frac{k_f R (1 - \varepsilon)}{D_g D_s \varepsilon \phi} \left(1 - \frac{C_e}{C_0}\right) \quad (\text{A.24})$$

a) The overall mass balance in dimensionless form is written

$$C_0 = (C_0 - C_e) \bar{C}(\bar{t}) + C_e + \frac{3M}{\varepsilon V R^3} \int_0^1 q_e \bar{q}(\bar{r}, \bar{t}) \bar{r}^2 R^2 R d\bar{r} \quad (\text{A.25})$$

with the initial condition

$$\frac{dr}{d\bar{r}} = R \quad (\text{A.26})$$

The final dimensionless overall mass balance is given with

$$0 = \left(1 - \frac{C_e}{C_0}\right) \frac{\partial \bar{C}(\bar{t})}{\partial \bar{t}} + 3D_g \frac{\partial}{\partial \bar{t}} \int_0^1 \bar{q}(\bar{r}, \bar{t}) \bar{r}^2 d\bar{r} \quad (\text{A.27})$$

and the initial conditions

$$\bar{C}(\bar{t} = 0) = 1 \quad (\text{A.28})$$

$$\bar{q}(0 \leq \bar{r} \leq 1, \bar{t} = 0) = 0 \quad (\text{A.29})$$

b) The final dimensionless liquid-phase mass balance is

$$\frac{\partial \bar{C}(\bar{t})}{\partial \bar{t}} = \frac{-3BiD_g}{\left(1 - \frac{C_e}{C_0}\right)} \left[\bar{C}(\bar{t}) - \bar{C}_s(\bar{t}) \right] \quad (\text{A.30})$$

with the initial condition

$$\bar{C}(\bar{t}=0) = 1 \quad (\text{A.28})$$

c) The final dimensionless intraparticle mass balance is

$$\frac{\partial \bar{q}(\bar{r}, \bar{t})}{\partial \bar{t}} = \frac{1}{\bar{r}^2} \frac{\partial}{\partial \bar{r}} \left[\bar{r}^2 \frac{\partial \bar{q}(\bar{r}, \bar{t})}{\partial \bar{r}} \right] \quad (\text{A.31})$$

with the initial condition

$$\bar{q}(\bar{r} \leq 1, \bar{t}=0) = 0 \quad (\text{A.29})$$

and the boundary conditions

$$\frac{\partial \bar{q}(\bar{r}=0, \bar{t} \geq 0)}{\partial \bar{r}} = 0 \quad (\text{A.32})$$

$$\frac{\partial}{\partial \bar{t}} \int_0^1 \bar{q}(\bar{r}, \bar{t}) \bar{r}^2 d\bar{r} = Bi \left[\bar{C}(\bar{t}) - \bar{C}_s(\bar{t}) \right] \quad (\text{A.33})$$

d) The final dimensionless form of the non-linear coupling equation is

$$\bar{q}(\bar{r}=1, \bar{t}) = \left[\left(1 - \frac{C_e}{C_0}\right) \bar{C}_s(\bar{t}) + \frac{C_e}{C_0} \right]^{\frac{1}{n}} \quad (\text{A.34})$$

Appendix VIII: Symbols

A_F	cross-sectional area	L^2
A_p	total external surface area of the adsorbent which is available for the mass transfer	L^2
A_0, A_1, A_2, A_3	coefficients for polynomial equation which fits model prediction curves	
Bi	Biot number based on surface diffusion coefficient	(dimensionless)
BV	bed volumes	(dimensionless)
C	concentration of the adsorbate	M/L^3
\bar{C}	fluid-phase concentration	(dimensionless)
C_{AC}	activated carbon concentration	M/L^3
$\bar{C}_{data,i}$	individual concentration	(dimensionless)
C_e	liquid-phase equilibrium concentration or effluent concentration	M/L^3
c_i	adsorbate concentration in the bulk solution	M/L^3
c_i^*	adsorbate concentration on the external surface of the adsorbent	M/L^3
\bar{C}_{mod}	modelled concentration	(dimensionless)
$\bar{C}_{model,calculated,i}$	modelled concentration	(dimensionless)
C_s	liquid-phase concentration at the adsorbent surface	(dimensionless)
C_0	concentration of adsorbate in the liquid-phase initially	M/L^3
D_g	solute distribution parameter	(dimensionless)
d_p	particle diameter	L
D_s	surface diffusion coefficient	L^2/t
EBCT	empty bed contact time	t
K	Freundlich isotherm capacity coefficient	$L^3/M^{1/n}$
k_2	second order rate constant	$L \text{ mol} / \text{mol}$
k_f	liquid-phase mass transfer coefficient	L/t
l	length	L
M	mass of adsorbent in the reactor	M

$n_{L,i}$	mass transfer rate per unit of surface area	M/L^2t
$n_{s,j}$	mass flux in the adsorbed phase	
$1/n$	Freundlich isotherm intensity constant	(dimensionless)
\bar{q}	reduced adsorbent-phase concentration	(dimensionless)
q_{ave}	average concentration in the adsorbent	M/M
q_e	adsorbent-phase concentration in equilibrium with the initial fluid-phase concentration	M/M
q_i	solid-phase concentration	M/L^3
\bar{q}_i	mean solid-phase concentration	M/L^3
r	radial coordinate	L
R	particle radius (geometric mean) or Reynolds number	L (dimensionless)
\bar{r}	reduced radial coordinate	(dimensionless)
s^2	square of standard error	
t	elapsed time	t
\bar{t}	elapsed time	(dimensionless)
T	temperature	
t_A	empty bed contact time	t
t_{Ft}	operation time	t
V	volume of the reactor including the volume occupied by the adsorbent and liquid-phase	L^3
\dot{V}	volumetric flow rate	L/t
V_{bed}	volume of fixed-bed	L^3
V_F	bed volume	L^3
v_F	void fraction	(dimensionless)
V_L	throughput volume	L^3
V_{sp}	specific throughput	L^3/M

δ	thickness of the boundary layer	L
ε	volume fraction of the reactor occupied by the liquid-phase or filter velocity	(dimensionless) L/t
ϕ	sphericity, ratio of the surface area of the equivalent-volume sphere to the actual surface area of the particle	(dimensionless)
ρ_a	adsorbent density which includes pore volume	M/L ³
ρ_F	filter density	M/L ³
τ	effective contact time	t